

INSIG-MEDIATED REGULATION OF MAMMALIAN HMG COA REDUCTASE
UBIQUITINATION AND DEGRADATION

APPROVED BY SUPERVISORY COMMITTEE

Michael S. Brown, M.D.

Joseph L. Goldstein, M.D.

Xiaodong Wang, Ph.D.

Richard G.W. Anderson, Ph.D.

Hongtao Yu, Ph.D.

INSIG-MEDIATED REGULATION OF MAMMALIAN HMG COA REDUCTASE
UBIQUITINATION AND DEGRADATION

by

NAVDAR SEVER

DISSERTATION

Presented to the Faculty of the Graduate School of Biomedical Sciences

The University of Texas Southwestern Medical Center at Dallas

In Partial Fulfillment of the Requirements

For the Degree of

DOCTOR OF PHILOSOPHY

The University of Texas Southwestern Medical Center at Dallas

Dallas, Texas

December, 2004

Copyright

by

Navdar Sever, 2004

All Rights Reserved

ACKNOWLEDGEMENTS

“What kind of mentor is he? Is he patient, loving and kind like Joe and me? Will he worry himself to death when your experiments aren’t going well, like Joe and I do? Does he have a positive, encouraging attitude and a great sense of humor, like Joe’s and mine?”

Michael S. Brown

I could not describe what to look for in a mentor in a better way than Mike’s words. He has been supportive at multiple critical points during my time in the lab. I thank both Mike Brown and Joe Goldstein for giving me the opportunity to work in their lab on technically challenging questions and trusting me with such a relatively big and important project as genetic selection. I will miss a lot of things about them, including Mike’s humor, Joe’s art collection, and their excitement and sudden spark of ideas in the lab meetings, but most important things I hope to be able to take with me are their amazing energy and unique approach to science. I would also like to thank the members of my Graduate Committee, Xiaodong Wang, Dick Anderson, and Hongtao Yu, for spending their time in meetings for my scientific progress and education. I have to thank members of Brown and Goldstein lab, each of whom helped me at one time or another. Russell DeBose-Boyd and Dai Yabe taught me everything I know about how to design and carry out an experiment; Russell also contributed a lot to this work and more on HMG CoA reductase degradation. Rob Rawson openly shared his experience with somatic cell genetics and provided helpful suggestions. Yi Gong taught me how to do blue native gels and generously provided probes and other reagents. Luke Engelking showed me how to do Northern and Southern blots. I thank Peter

Lee for working with me on characterizing some of the mutant cells; with him, I know all the cells are in good hands and look forward to hearing great discoveries. On behalf of tissue culture staff, I thank Lisa Beatty, who subcloned every single cell line generated in the course of this work in addition to their daily work of setting up the cultures for routine experiments. Their excellent technical assistance is what makes the efficiency of the department possible and is another thing I will sorely miss.

Parts of this study have been reprinted from Molecular Cell, Vol 11, Sever et al: "Accelerated Degradation of HMG CoA Reductase Mediated by Binding of Insig-1 to Its Sterol-Sensing Domain", pp.25-33, Copyright (2003), with permission from Elsevier; Journal of Biological Chemistry, Vol 278, Sever et al: "Insig-dependent Ubiquitination and Degradation of Mammalian 3-Hydroxy-3-methylglutaryl-CoA Reductase Stimulated by Sterols and Geranylgeraniol", pp.52479-52490, Copyright (2003), and Vol 279, Sever et al: "Isolation of Mutant Cells Lacking Insig-1 through Selection with SR-12813, an Agent That Stimulates Degradation of 3-Hydroxy-3-methylglutaryl-Coenzyme A Reductase", pp.43136-43147, Copyright (2004), with permission from American Society for Biochemistry and Molecular Biology.

This work is dedicated to my father, Dr. M. Emin Sever, who encouraged me to study genetics in college; to my mother, Sadiye Sever, who never went to school but will still be happy it is done; and to my people, Kurds, who have suffered incredibly under oppression and poverty, and whose fate, once again, is being determined by others, with the hope that, one day, high cholesterol will be the only thing to worry about.

INSIG-MEDIATED REGULATION OF MAMMALIAN HMG COA REDUCTASE
UBIQUITINATION AND DEGRADATION

Publication No. _____

Navdar Sever, Ph.D.

The University of Texas Southwestern Medical Center at Dallas, 2004

Supervising Professors: Michael S. Brown, M.D. and Joseph L. Goldstein, M.D.

3-hydroxy-3-methylglutaryl coenzyme A (HMG CoA) reductase (HMGR) catalyzes the conversion of HMG CoA to mevalonate, which is the rate limiting step in the production of cholesterol and numerous nonsterol isoprenoid products. Mammalian HMGR is regulated by transcriptional and post-transcriptional feedback mechanisms. The transcriptional regulation is mediated by sterol regulatory element binding proteins (SREBPs), which are synthesized as inactive precursors in the endoplasmic reticulum (ER) membrane. In the absence of sterols, SREBP cleavage activating protein (SCAP) escorts SREBPs from ER to the Golgi apparatus, where SREBPs are cleaved by site 1 and site 2 proteases so as to release their

amino terminal transcription factor domains to the nucleus. Sterols inhibit the exit of SCAP-SREBP complex from the ER by promoting the binding of two related polytopic ER membrane proteins, Insig-1 and Insig-2, to the membrane domain of SCAP. Insig-1, but not Insig-2, is an SREBP target gene, causing Insig-1 levels to drop in the presence of sterols, when it is expected to exert its action. The degradation of HMGR requires both sterols and a nonsterol product of the mevalonate pathway and the eight membrane spanning segments in its amino terminus. The membrane domains of HMGR and SCAP bear sequence similarity prompting the investigation of whether Insig proteins can also bind to HMGR. Indeed, Insig-1 and Insig-2 were found to interact with HMGR in a regulated manner and mediate its proteasomal degradation. This effect can be specifically inhibited by overexpressing the membrane domain of SCAP. Insigs were shown to promote the ubiquitination of HMGR on lysine 248 in the cytoplasmic loop between transmembrane segments 6 and 7. In an attempt to achieve a better understanding of the mechanism by which HMGR is degraded, a genetic approach was developed to select mutant somatic cells that cannot degrade HMGR in the presence of sterols. The isolation and characterization of Chinese hamster ovary cells deficient in Insig-1 confirmed the endogenous requirement of Insig-1 for HMGR degradation and revealed the role of differential regulation of Insig-1 and Insig-2 in terms of SREBP processing. These studies revealed a complex feedback regulatory system governing cholesterol homeostasis.

TABLE OF CONTENTS

CHAPTER ONE Introduction	1
Global regulation of cholesterol homeostasis	1
Two Sources of Cellular Cholesterol.....	1
Regulation of the Mevalonate Pathway	4
CHAPTER TWO Review of the Literature	10
ER-associated degradation.....	10
Quality Control in the ER	10
Mechanism of HMGR Degradation.....	13
CHAPTER THREE Methodology	21
Experimental procedures	21
Materials	21
Methods.....	25
CHAPTER FOUR Results.....	36
Ubiquitination and degradation of HMGR mediated by binding of Insig to its sterol- sensing domain.....	36
The Regulated Degradation of HMGR Occurs in the ER.....	36
Insig-Mediated Degradation of HMGR.....	42
Insig-Dependent Ubiquitination of HMGR	48
gp78 As A Candidate E3 Ubiquitin Ligase for HMGR.....	61
Isolation of mutant cells through selection with SR-12813, an agent that stimulates degradation of HMGR	65

SR-12813 As A Selecting Agent to Isolate Mutant Cells Incapable of Accelerating HMGR Degradation.....	65
Insig-1 Mutants	72
CHAPTER FIVE Conclusions and Recommendations	88
Central role of Insig-1 and Insig-2 in the control of cholesterol homeostasis	88
Regulated Degradation of Mammalian HMGR Requires Insig Proteins.....	88
Selection of SR-12813-Resistant Cells	91
Perspectives for the Future.....	96
Bibliography	100
Vitae	111

PRIOR PUBLICATIONS

Sever, N., Yang, T., Brown, M.S., Goldstein, J.L., and DeBose-Boyd, R.A. (2003).

Accelerated degradation of HMG CoA reductase mediated by binding of insig-1 to its sterol sensing domain. *Mol. Cell* 11, 25-33.

Sever, N., Song, B.L., Yabe, D., Goldstein, J.L., Brown, M.S., and DeBose-Boyd, R.A.

(2003). Insig-dependent ubiquitination and degradation of mammalian 3-hydroxy-3-methylglutaryl-CoA reductase stimulated by sterols and geranylgeraniol. *J. Biol. Chem.* 278, 52479-52490.

Sever, N., Lee, P.C.W., Song, B.L., Rawson, R.B., and DeBose-Boyd, R.A. (2004). Isolation of cells lacking Insig-1 through selection with SR-12813, an agent that stimulates degradation of 3-hydroxy-3-methylglutaryl coenzyme A reductase. *J. Biol. Chem.* 279, 43136-43147.

LIST OF FIGURES

FIGURE 1-1	2
FIGURE 1-2	6
FIGURE 2-1	12
FIGURE 2-2	15
FIGURE 4-1	37
FIGURE 4-2	38
FIGURE 4-3	40
FIGURE 4-4	41
FIGURE 4-5	43
FIGURE 4-6	44
FIGURE 4-7	45
FIGURE 4-8	47
FIGURE 4-9	49
FIGURE 4-10	50-51
FIGURE 4-11	52
FIGURE 4-12	53
FIGURE 4-13	57
FIGURE 4-14	58
FIGURE 4-15	60
FIGURE 4-16	62
FIGURE 4-17	64

FIGURE 4-18	66
FIGURE 4-19	68
FIGURE 4-20	70
FIGURE 4-21	71
FIGURE 4-22	73
FIGURE 4-23	75
FIGURE 4-24	77
FIGURE 4-25	79
FIGURE 4-26	81-82
FIGURE 4-27	83
FIGURE 4-28	85
FIGURE 4-29	86
FIGURE 5-1	94
FIGURE 5-2	98

LIST OF TABLES

TABLE ONE	3
TABLE TWO	34

LIST OF ABBREVIATIONS

LDL – low density lipoprotein

HMGR – 3-hydroxy-3-methylglutaryl coenzyme A reductase

ER – endoplasmic reticulum

SREBP – SRE-binding protein

SCAP – SREBP cleavage-activating protein

S1P – site 1 protease

S2P – site 2 protease

bHLH-Zip – basic helix-loop-helix leucine zipper

COP – coat protein

TM – transmembrane

SSD – sterol sensing domain

NPC1 – Niemann-Pick C1

INSIG-1 – insulin induced gene-1

25-HC – 25-hydroxycholesterol

SRD – sterol regulatory defective

ERAD – ER-associated degradation

Ub – ubiquitin

E1 – ubiquitin-activating enzyme

E2 – ubiquitin-conjugating enzyme

E3 – ubiquitin ligase

HECT – homologous to E6-AP carboxyl-terminus

FPP – farnesol pyrophosphate

HRD – HMG CoA reductase degradation

CUE – coupling of ubiquitin conjugation to ER degradation

COD – control of degradation

GG-OH – geranylgeraniol

ALLN – N-acetyl-leucinal-leucinal-norleucinal

PNGase F – peptide N-glycosidase F

HPCD – hydroxypropyl- β -cyclodextrin

LPDS – lipoprotein-deficient serum

mAb – monoclonal antibody

CMV – cytomegalovirus

CHO – Chinese hamster ovary

FCS – fetal calf serum

PBS – phosphate-buffered saline

SDS – sodium dodecyl sulfate

PAGE – polyacrylamide gel electrophoresis

GAPDH – glyceraldehyde-3-phosphate dehydrogenase

ORF – open reading frame

RNAi – RNA interference

NF- κ B – nuclear factor κ B

I κ B – inhibitor of NF- κ B

TNF – tumor necrosis factor

CHAPTER ONE

Introduction

GLOBAL REGULATION OF CHOLESTEROL HOMEOSTASIS

Two Sources of Cellular Cholesterol

Cholesterol is an essential molecule for animal cells. It has long been known to modulate the fluidity and phase transitions in the plasma membrane, as well as produce lipoproteins, bile acids, vitamin D and steroid hormones. More recently, it was shown to be involved in the formation of membrane microdomains called rafts or caveolae, which have roles in signal transduction (Simons and Ikonen, 1997; 2000; Anderson, 1998). In addition, it is covalently attached to Hedgehog (Hh), a morphogen essential for embryonic patterning (Mann and Beachy, 2004). On the other hand, excess cholesterol is toxic because it forms solid crystals that kill cells. Excess cholesterol in the blood must also be avoided because it deposits in arteries, initiating atherosclerosis (Libby et al., 2000). Therefore, cellular cholesterol levels are tightly regulated.

There are two sources of cellular cholesterol: *de novo* synthesis and uptake from the plasma low density lipoprotein (LDL) via LDL receptor-mediated endocytosis. Endogenous synthesis of cholesterol takes place in more than 20 steps starting with the condensation of acetyl coenzyme A (CoA) and acetoacetyl CoA to produce 3-hydroxy-3-methylglutaryl (HMG) CoA, which is catalyzed by HMG CoA synthase. HMG CoA is then converted into mevalonate by HMG CoA reductase (HMGR), which is the rate limiting step in the so called mevalonate pathway (Goldstein and Brown, 1990). In addition to cholesterol, mevalonate is

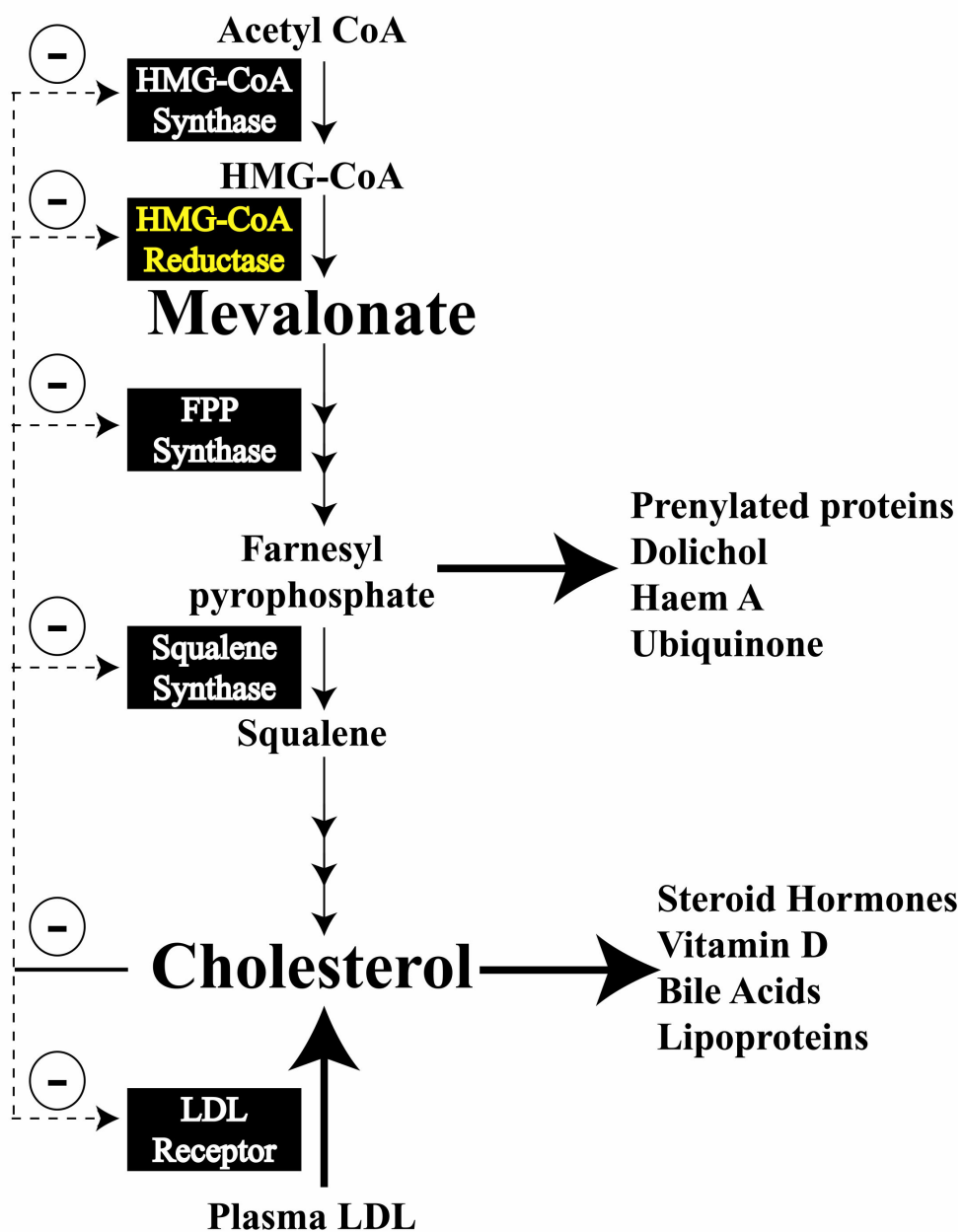


Figure 1-1. The mevalonate pathway. Adapted from Goldstein and Brown (1990).

used to produce numerous nonsterol isoprenoids, including ubiquinone, haem A, dolichol and prenyl groups that are attached to several proteins (Figure 1-1). The synthesis and uptake of cholesterol are coordinately regulated such that excess cellular cholesterol can decrease the levels of most cholesterol biosynthetic enzymes and the LDL receptor. This forms the basis of the cholesterol lowering effects of statins, which inhibit HMGR. Since they inhibit endogenous cholesterol synthesis, the resulting drop in the cholesterol levels relieves the negative feedback repression giving rise to an increase in the LDL receptor levels. Increased LDL receptor levels lead to a decrease in the LDL cholesterol levels in the blood and to a reduction in the occurrence of heart attacks (Brown and Goldstein, 1996). However, the levels of all the cholesterol biosynthetic enzymes also go up in response to statins, creating a resistance to the drug. Finding a way to prevent the buildup of HMGR protein could potentially improve the effectiveness of the statins.

Level of control	Mevalonate-derived product		Proposed target for regulation	Amplitude of change
	Sterol	Nonsterol		
Transcriptional	+	-	SRE-1 sequence in promoter	8-fold
Translation of mRNA	-	+	Complex 5' untranslated region	5-fold
Degradation of protein	+	+	Eight membrane-spanning regions in N-terminal domain	5-fold
Inactivation of enzyme	-	-	C-terminal domain phosphorylated by AMP-dependent kinase	?

Table 1. Multivalent feedback regulation of HMGR. Adapted from Goldstein and Brown (1990).

Regulation of the Mevalonate Pathway

Because the mevalonate pathway produces essential molecules with diverse functions, it is under complex negative feedback regulation (Table 1; Goldstein and Brown, 1990). The coordinate regulation of cholesterol biosynthetic enzymes and LDL receptor is mediated by sterol-regulated transcription. HMGR is also regulated at the level of its translation and its half-life (Nakanishi et al., 1988). The translational regulation of HMGR is mediated by nonsterol products of mevalonate pathway through an unknown mechanism but it requires the complex 5' untranslated region of HMGR mRNA. The half-life of HMGR is regulated by both sterol and nonsterol products and requires the eight membrane-spanning regions in its NH₂-terminal domain that anchors the protein to the endoplasmic reticulum (ER) membrane. Altogether, these modes of regulation give rise to a practically all-or-none change in HMGR activity. An additional control mechanism is the reversible phosphorylation of HMGR COOH-terminal catalytic domain that projects into the cytosol by AMP-dependent kinase, which inactivates HMGR. AMP-dependent kinase senses the cellular energy levels and inhibits cholesterol synthesis under conditions of low ATP levels. This phosphorylation event is not part of the end-product mediated negative feedback regulation and does not affect the half-life of HMGR under any condition (Sato et al., 1993).

Transcriptional Regulation Mediated by SREBPs

The transcriptional regulation of HMGR is mediated by sterol regulatory element-binding proteins (SREBPs), a small family of transcription factors that are synthesized as inactive

precursors in the ER membrane (Brown and Goldstein 1997; 1999). SREBP-1a and SREBP-1c isoforms are produced from a single gene by alternative splicing whereas SREBP-2 is produced from a separate gene. While SREBP-2 preferentially activates the genes involved in cholesterol biosynthesis and uptake, SREBP-1c activates genes involved in fatty acid biosynthesis. SREBP-1a is a more potent transactivator than SREBP-1c and activates the complete program of cholesterol, fatty acid and triglyceride biosynthesis (Horton et al., 2003). In most cultured cells, SREBP-1a and SREBP-2 are the predominant isoforms whereas SREBP-1c and SREBP-2 are predominant in the liver.

In the absence of sterols, SREBP cleavage-activating protein (SCAP) escorts SREBPs from the ER to the Golgi apparatus, where SREBPs are cleaved by site 1 and site 2 proteases (S1P and S2P, respectively) in a process termed regulated intramembrane proteolysis (Brown et al., 2000). Site 2 cleavage can occur only after site 1 cleavage. The resulting NH₂-terminal basic helix-loop-helix leucine zipper (bHLH-Zip) transcription factor domains are now free to translocate to the nucleus, where they bind the sterol regulatory elements (SREs) found in the promoters of genes including HMGR and LDL receptor (Figure 1-2). Sterols inhibit this process by preventing the entry of SCAP-SREBP complex into COPII vesicles so that SREBP is retained in the ER separated from S1P (Nohturfft et al., 2000; Espenshade et al., 2002). In addition to the regulation of its proteolytic processing, hepatic transcription of SREBP-1c is enhanced by insulin and liver X receptor (Horton et al., 2002). Unsaturated fatty acids, on the other hand, suppress SREBP-1 isoforms transcriptionally and posttranscriptionally (Hannah et al., 2001; Ou et al., 2001). Whether fatty acids also regulate the movement of SCAP similar to the sterol mediated regulation is not known.

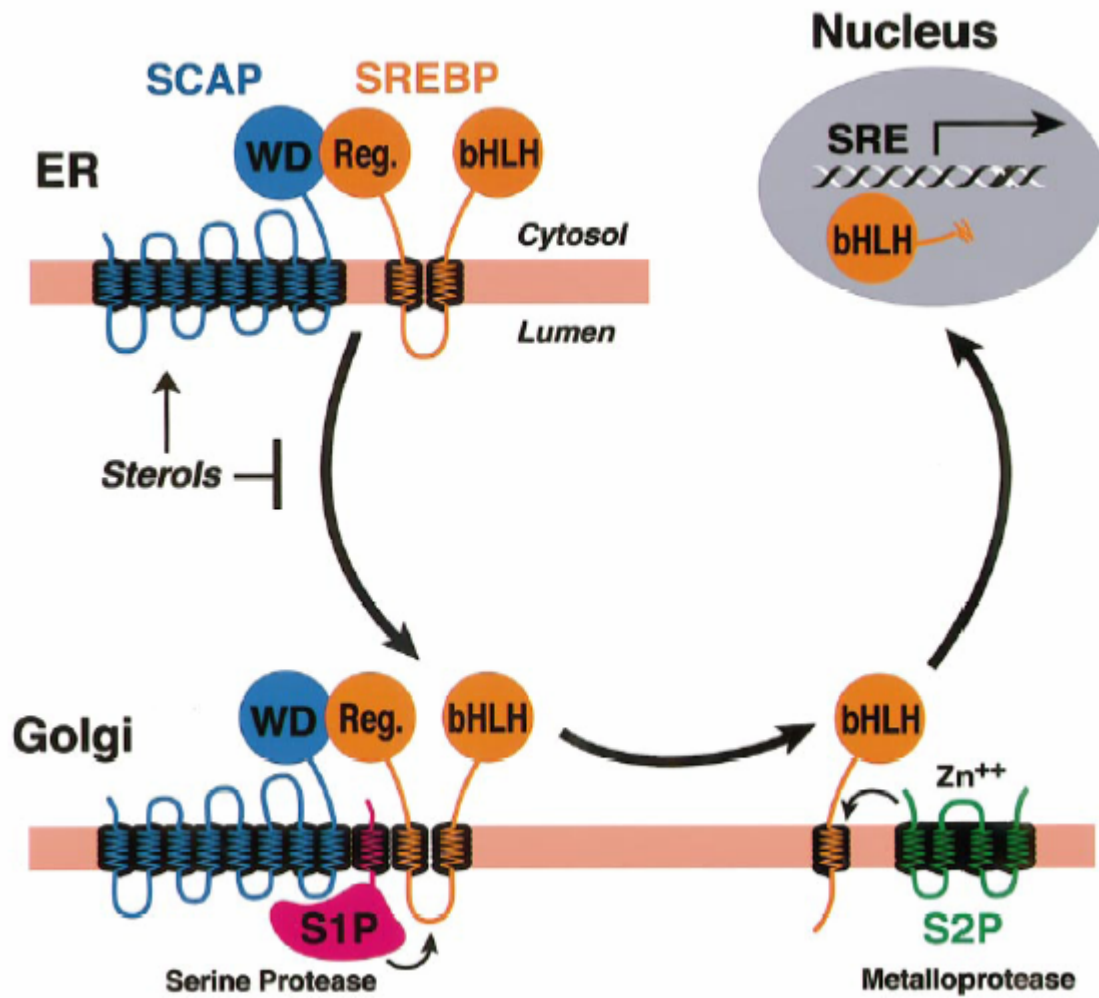


Figure 1-2. The SREBP pathway. Reprinted from Goldstein et al., Copyright (2002), with permission from Elsevier.

SCAP is a polytopic protein that contains eight transmembrane segments (TMs) in its NH₂-terminal domain and a WD-repeat containing domain in its COOH-terminus. The COOH-terminal WD domain of SCAP binds tightly to the COOH-terminal domain of SREBPs; this interaction is required for SREBP processing. The TM2-6 region of SCAP is termed the sterol sensing domain (SSD) because it shows sequence similarity to HMGR and other proteins that have functions related to cholesterol, including the lipid transport protein Niemann-Pick C1 (NPC1); the Hh receptor Patched; the membrane protein Dispatched that facilitates the secretion of Hh from cells producing it; the penultimate enzyme in the cholesterol biosynthetic pathway, 7-dehydrocholesterol reductase; and the transport protein NPC1L1 that facilitates the intestinal absorption of dietary cholesterol (Nohturfft et al., 1998b; Kuwabara and Labouesse, 2002; Altmann et al., 2004). So far, cholesterol has only been shown to directly bind SCAP and NPC1 (Radhakrishnan et al., 2004; Ohgami et al., 2004). Whether any of the other SSD-containing proteins bind directly to a sterol is not known. Interestingly, the covalently attached cholesterol moiety of Hh is dispensable for its binding to Patched receptor (Mann and Beachy, 2004).

Recently, it was found that cholesterol induces a conformational change in SCAP SSD that allows it to bind Insig-1 or Insig-2, two related ER proteins, and this interaction prevents the budding of SCAP-SREBP complex from the ER (Brown et al., 2002; Yang et al., 2002; Yabe et al., 2002a; Rawson, 2003). Insig-1 and Insig-2 are homologous polytopic membrane proteins that contain six TMs (Feramisco et al., 2004). Even though they seem functionally redundant in transfection studies, they are differentially regulated. *INSIG-1* (insulin induced gene-1) is an SREBP target gene giving rise to an apparent paradox, where

Insig-1 is suppressed by sterols, exactly when it is supposed to exert its action. Insig-2 has two alternative splice forms, Insig-2a and Insig-2b, which produce identical proteins (Yabe et al., 2003). Insig-2a is the liver-specific isoform and is repressed by insulin whereas Insig-2b is constitutive and the only form expressed in cultured cells.

25-hydroxycholesterol (25-HC), a more potent inhibitor of SREBP processing, neither binds SCAP directly nor has an effect on SCAP conformation (Brown et al., 2002; Radhakrishnan et al., 2004). However, it also requires Insig-SCAP interaction to exert its inhibitory action, suggesting that oxysterols act in intact cells by translocating cholesterol from plasma membrane to ER. Alternatively, they interact with some unidentified regulatory protein that enhances Insig-SCAP binding without a detectable change in SCAP conformation.

Somatic Cell Genetics

Somatic cell genetics has been invaluable in unraveling the SREBP pathway (Goldstein et al., 2002). Two classes of sterol regulatory defective (SRD) cells have been described. Cells in the first class are cholesterol auxotrophs and isolated by the use of amphotericin B, which is a polyene antibiotic that kills the cell by binding to cholesterol and forming pores in the plasma membrane. SCAP, S1P and S2P deficient cells are in this category. These cells cannot process SREBP; therefore, they do not express the cholesterol biosynthetic enzymes, explaining their survival against a transient treatment with amphotericin B. The other class consists of sterol-resistant cells, which fail to properly regulate the processing of SREBP in response to sterols. They were isolated using 25-HC, which can suppress SREBP processing

but cannot replace cholesterol in the plasma membrane. Wild type cells die in the continual presence of 25-HC due to cholesterol starvation. Two types of mutations have been observed in sterol-resistant cells. Type 1 mutations occur in the SREBP-2 gene, producing truncated SREBP-2 that terminates before the first transmembrane segment and does not need the proteolytic events to move to the nucleus. Type 2 mutations are point mutations, Y298C, L315F and D443N, which are in the SSD of SCAP and render SCAP insensitive to sterols. These SCAP mutants cannot bind to Insig-1 or Insig-2; thus, they escort SREBP to the Golgi even in the presence of sterols explaining the constitutive processing of SREBPs in cells expressing these mutants (Yabe et al., 2002b).

CHAPTER TWO
Review of the Literature
ER-ASSOCIATED DEGRADATION

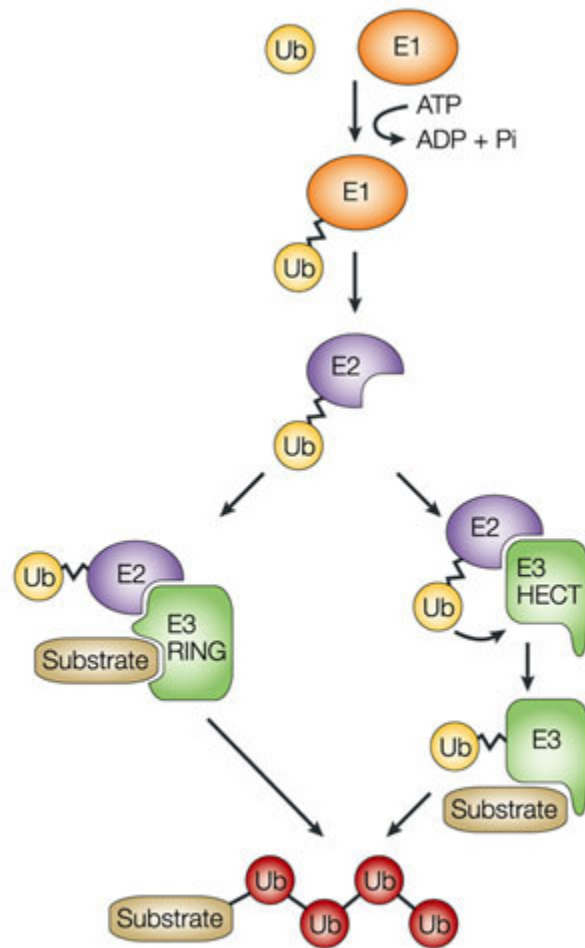
Quality Control in the ER

Endoplasmic reticulum (ER) is the site of entry for the secretory pathway. Secreted proteins and the resident proteins of ER as well as those of the Golgi apparatus, the endosomal system, lysosome and the plasma membrane are first synthesized on ribosomes attached to the surface of the rough ER and cotranslationally translocated through the Sec61 translocon into the ER lumen or inserted into the ER membrane (Matlack et al., 1998). Once the synthesis of the nascent polypeptide chain is complete, the final protein product is assembled into its native tertiary structure followed by oligomeric assembly. Some proteins are also modified at this stage by disulphide bond formation and N-linked glycosylation (Ellgaard and Helenius, 2003). All these folding steps are assisted by chaperones that reside in the ER lumen and prevent proteins to leave the ER before they are properly folded. When unfolded or misfolded proteins accumulate in the ER, they trigger the unfolded protein response, which upregulates the expression of chaperones (Zhang and Kaufman, 2004). If the folding problem persists, however, several additional genes are upregulated that are components of the ER-associated degradation (ERAD) machinery (Friedlander et al., 2000; Travers et al., 2000).

The Ubiquitin-Proteasome Pathway

Misfolded or unassembled ER proteins are believed to retro-translocate to the cytosol where they are degraded by the 26S proteasome (Bonifacino and Weissman, 1998; Tsai et al., 2002). Proteasome is a large multi-catalytic protease that is abundant in the cytosol and the nucleus and that is responsible for most of the non-lysosomal degradation in the cell. It consists of the 20S catalytic particle and the 19S regulatory cap. The 20S complex forms a cylinder with the active sites inside and two 19S particles on each opening. The 19S particle recognizes proteins tagged for proteasomal degradation (usually by polyubiquitination), unfolds them by its associated ATPase activity and feeds them into the interior of the 20S particle where the actual breakdown of the protein into small peptides takes place (DeMartino and Slaughter, 1999; Voges et al., 1999).

Ubiquitin (Ub) is a 76-amino acid polypeptide that is attached to the ϵ -amino group of a lysine residue on a target protein in a cascade of enzymatic reactions (Figure 2-1; Weissman, 2001). First, Ub is attached via a thiol-ester bond to a cysteine in the ubiquitin-activating enzyme (E1) in an ATP-dependent reaction. In the second step, Ub is transferred to the active site cysteine of one of more than twenty ubiquitin-conjugating enzymes (E2s). In the final step, a ubiquitin ligase (E3) transfers the Ub to its substrate via an isopeptide bond. There are two main classes of E3s. HECT domain containing E3s form thiol-ester intermediates with Ub before transferring it to the substrate whereas RING finger domain containing E3s directly transfer Ub from the E2 to the substrate without an intermediate. There are many more E3s than there are E2s; so, the substrate specificity is mainly determined by E3s. Ub can also be attached to lysine 48 (K48) residue of another Ub moiety



Nature Reviews | Molecular Cell Biology

Figure 2-1. The ubiquitin pathway. Reprinted from Di Fiore et al. (2003) with permission.

that is already attached to a protein. Most proteins must be polyubiquitinated in this manner in order to be recognized as a proteasome substrate. The polyubiquitin chain is removed by Ub-specific isopeptidases from the substrate before its destruction so that the Ub moieties can be recycled to the cytosol. However, monoubiquitination has been increasingly recognized as a reversible signal for binding to Ub receptors that serve a variety of functions, including membrane transport (Hicke, 2001; Di Fiore et al., 2003). Polyubiquitin chains linked through K63 have also been described as a non-proteolytic signal (Sun and Chen, 2004).

Mechanism of HMGR Degradation

There are two HMG CoA reductase isozymes in the yeast *Saccharomyces cerevisiae*, Hmg1p and Hmg2p, which are similar in overall structure to each other and to mammalian HMGR (Basson et al., 1986; 1988). They both have eight membrane-spanning regions in their NH₂-terminal domains that localize them to the ER membrane and a catalytic COOH-terminal domain exposed to the cytosol. Whereas their catalytic domains are homologous to their mammalian counterpart, the membrane domains are ~50% identical to each other but do not show significant sequence similarity to the mammalian HMGR. Interestingly, only Hmg2p isozyme undergoes regulated degradation (Hampton, 2002b). Although the relevance of this model system to the mammalian HMGR degradation is not certain, I will first introduce the components involved in yeast Hmg2p degradation and then give a critical review of studies in mammalian cells.

Degradation of Yeast Hmg2p by the Ubiquitin-Proteasome Pathway

Regulated degradation of Hmg2p requires its membrane domain similar to mammalian HMGR and occurs in the ER. When the flux through the mevalonate pathway is low, Hmg2p is stable with a half-life of 6 h compared to 5-10 min in the presence of mevalonate-derived signals (Hampton, 2002b). The rapid degradation obtained with zaragozic acid, an inhibitor of squalene synthase, points to farnesol pyrophosphate (FPP) or a metabolite derived from it, as the signal for Hmg2p degradation and genetic manipulation of squalene synthase expression is consistent with this model (Gardner and Hampton, 1999). A partial effect of oxysterols has also been suggested for maximal response to the FPP-derived signal (Gardner et al., 2001).

The ease of genetic manipulation in *S. cerevisiae* prompted Hampton and colleagues to set out to isolate mutants deficient in regulated degradation of Hmg2p. A parent strain expressing a constitutively degraded Hmg2p variant was used to select mutants resistant to the HMGR inhibitor lovastatin (Hampton et al., 1996). One of the mutations obtained, *HRD2* (for HMG CoA reductase degradation), was in the gene encoding a known proteasome subunit, RPN1, suggesting the involvement of proteasome in the regulated degradation of yeast Hmg2p. This is consistent with the ubiquitination of Hmg2p observed under conditions of high flux through the mevalonate pathway (Hampton and Bhakta, 1997).

The characterization of two other *HRD* mutants led to the identification of a membrane-bound ubiquitin ligase complex that consists of Hrd1p and Hrd3p (Figure 2-2*top*; Hampton et al., 1996). Hrd1p is predicted to span the ER membrane several times and has a cytosolic RING finger domain. Together with the E2 enzyme, Ubc7p (or to a lesser extent,

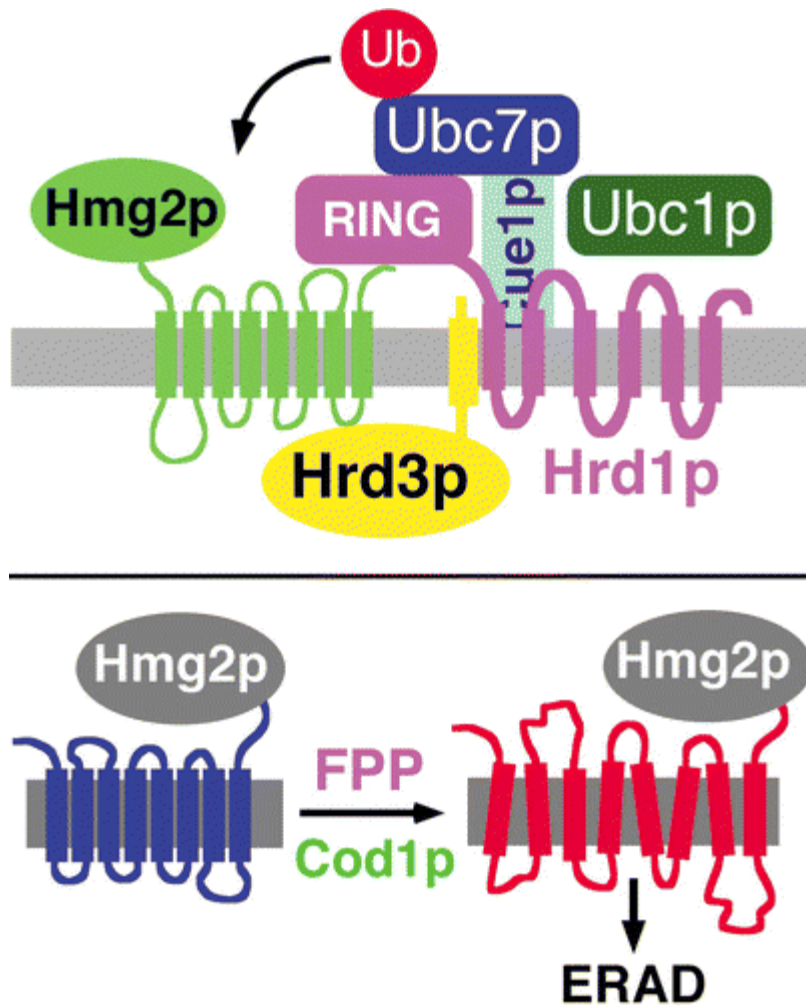


Figure 2-2. (Top) ER-associated Hrd1p/Hrd3p ubiquitin ligase complex of *S. cerevisiae*. (Bottom) The structural transition model for regulated degradation of Hmg2p. Reprinted, with permission, from the Annual Review of Cell and Developmental Biology, Volume 18 © 2002 by Annual Reviews www.annualreviews.org (Hampton et al., 2002b).

Ubc1p), Hrd1p/Hrd3p complex is required for the ubiquitination and the subsequent proteasomal degradation of Hmg2p (Bays et al., 2001a). The cytosolic Ubc7p requires Cue1p (for coupling of ubiquitin conjugation to ER degradation) as an ER membrane anchor. The isolation of yet another gene from the HRD selection, HRD4, revealed a previously poorly understood step in the degradation of ER proteins by the proteasome. In *HRD4/NPL4* mutants, Hmg2p is ubiquitinated but fails to be degraded which led to the suggestion that Npl4p, which is found in a complex with Cdc48p and Ufd1p, is required for the extraction of Hmg2p from the ER membrane (Bays et al., 2001b).

The HRD genes described above are not specific for Hmg2p since they are also involved in degradation of many other ER proteins (Hampton et al., 1996). Therefore, they are the components of ERAD, the quality control mechanism of the ER that targets unfolded proteins for proteasomal degradation. These findings could be explained with a model where the presence of excess mevalonate pathway products signals Hmg2p to undergo a structural transition towards a conformation that is recognized by the ER quality control apparatus as “unfolded” or “misfolded” (Figure 2-2bottom; Shearer and Hampton, 2004; Hampton, 2002a). To identify the genes that are involved in regulating this structural transition Hampton et al. looked for mutants that constitutively degrade Hmg2p. Consequently, these *COD* (control of degradation) mutants show higher sensitivity to lovastatin. The first gene obtained from this selection, COD1, encodes a P-type ATPase that is involved in calcium homeostasis in the ER (Cronin et al., 2000; 2002). The mechanism by which Cod1p regulates Hmg2p degradation is entirely unknown.

Regulated Degradation of Mammalian HMGR

Mammalian HMGR was long known to be rapidly degraded in the presence of excess sterols or mevalonate (Edwards et al., 1983). When the COOH-terminal domain was expressed in HMGR-deficient cells, it completely restored the growth in the absence of exogenously supplied cholesterol, suggesting that this domain is necessary and sufficient for the catalytic activity (Gil et al., 1985). However, this truncated protein no longer exhibits regulated turnover, indicating that the NH₂-terminal membrane domain is necessary for the regulated degradation (Gil et al., 1985). Further, the membrane domain of HMGR was shown to confer regulated degradation on β -galactosidase fused to its COOH-terminus demonstrating that the membrane domain is not only necessary but also sufficient for the sterol-accelerated degradation (Skalnik et al., 1988).

There have been controversial reports regarding the identity of the nonsterol isoprenoid required for full HMGR degradation. Several studies suggested FPP as the nonsterol signal for mammalian HMGR degradation similar to yeast Hmg2p (Correll et al., 1994; Meigs et al., 1996; Meigs and Simoni, 1997). However, geranylgeraniol (GG-OH) but not farnesol, can replace the mevalonate requirement when added exogenously, suggesting the involvement of a geranylgeranylated protein (Sever et al., 2003). Nevertheless, the mammalian HMGR degradation depends more on the sterol signal as opposed to the dependence of yeast Hmg2p degradation on FPP.

The mechanism by which mammalian HMGR is degraded has been subject to a number of equally conflicting reports. Early studies implicated the involvement of a putative membrane-bound cathepsin-L type cysteine protease in the degradation of HMGR in the ER

(Inoue et al., 1991; McGee et al., 1996; Moriyama et al., 1998; 2001). More recently, the ubiquitin-proteasome pathway was suggested to be mediating this process, consistent with studies in yeast (Ravid et al., 2000). The most likely explanation of this discrepancy is the possible artifacts of *in vitro* experimentation utilized in the early studies. It is conceivable that sterols cause a conformational change in HMGR making it susceptible to *in vitro* cleavage by a protease that has no physiological relevance.

There are predicted mammalian homologues of all the HRD genes including HRD1, which encodes the ubiquitin ligase (Ponting, 2000). Human Hrd1 (hHrd1) was indeed shown to have ubiquitin ligase activity and was upregulated by ER stress; however, it was not involved in the degradation of HMGR, at least not in the sterol-regulated degradation (Kaneko et al., 2002; Nadav et al., 2003; Kikkert et al., 2004). These data raise the question of whether there is an E3 that is specific for HMGR in mammals. Interestingly, the tumor autocrine motility factor receptor, gp78, was shown to ubiquitinate the unassembled T cell receptor subunit CD3- δ and apolipoprotein B100 in the ER (Fang et al., 2001; Liang et al., 2003). gp78 is structurally similar to Hrd1p in that it also has multiple membrane-spanning segments in its NH₂-terminus and a RING finger domain in its COOH-terminus. In addition, gp78 contains a domain found in the yeast Cue1p, which is also involved in Hmg2p degradation; this domain is called the CUE domain. It is not known whether gp78 is involved in HMGR degradation.

Unfortunately, attempts to delineate the mechanism of the regulated degradation of HMGR by a genetic approach have not been successful in mammalian cells. Analogous to selection of *HRD* mutants by lovastatin, cells resistant to compactin, another HMGR

inhibitor, have been isolated but the cause of the resistance is the massive overproduction of HMGR protein due to amplification and enhanced transcription of the gene encoding the enzyme (Chin et al., 1982; Luskey et al., 1983). These cells, called UT-1 cells, still exhibit accelerated degradation in response to sterols indicating that the degradation machinery is intact (Faust et al., 1982). Another statin-resistant cell line has been reported to lack the regulated degradation but the underlying defect has not been found (Ravid et al., 1999). On the other hand, UT-2 cells, which are mevalonate auxotrophs, lack detectable HMGR mRNA and protein (Mosley et al., 1983). Mammalian cells that have constitutively degraded HMGR have not been reported to date.

Even though 25-HC degrades HMGR and kills wild-type cells, all the 25-HC-resistant cells isolated so far show defects in regulation of SREBP processing rather than HMGR degradation presumably because 25-HC also suppresses SREBP cleavage (Dawson et al., 1991; Goldstein et al., 2002; see Chapter 1). Therefore, a reagent that promotes degradation of HMGR without suppressing SREBP cleavage would be of enormous use. The cholesterol-lowering drugs, SR-12813 and Apomine, seem to fulfill these criteria. While SR-12813 reduced the half-life of HMGR, the mRNAs for HMGR and LDL receptor were upregulated (Berkhout et al., 1996). Similarly, Apomine was shown to degrade HMGR and stimulate SREBP processing (Roitelman et al., 2004). The stimulation of SREBP cleavage and subsequent upregulation of its target genes are probably secondary effects of the decrease in cellular cholesterol levels due to degradation of HMGR, which are also seen by statins. Importantly, these results suggest that SR-12813 does not directly affect SCAP.

Since HMGR SSD show sequence similarity to the SSD of SCAP, the first hypothesis tested in this study is whether Insig-1 and Insig-2 bind to the SSD of HMGR and whether this binding event is involved in the regulated degradation of HMGR. The second hypothesis is that there is a specific lysine residue that is the ubiquitination site required for the proteasomal degradation of HMGR. Finally, a genetic approach was developed to select SR-12813-resistant cells that cannot degrade HMGR in the presence of sterols.

CHAPTER THREE

Methodology

EXPERIMENTAL PROCEDURES

Materials

Reagents

The following reagents were obtained from the indicated sources: SR-12813 from Dr. Timothy M. Willson, GlaxoSmithKline (Research Triangle Park, NC) or Sandhya Kulkarni of the Core Medicinal Chemistry Laboratory, Department of Biochemistry, University of Texas Southwestern Medical Center; sterols (cholesterol and 25-HC) from Steraloids, Inc. (Newport, RI); MG-132, N-acetyl-leucinal-leucinal-norleucinal (ALLN), Nonidet P-40 (NP-40), digitonin, and hexyl- β -D-glucopyranoside from Calbiochem; endo H and peptide N-glycosidase F (PNGase F) from New England Biolabs; 6-amino-n-hexanoic acid, aprotinin and phenylmethylsulfonyl fluoride (PMSF) from Sigma Chemical Company; Pefabloc (4-[2-aminoethyl]benzenesulfonylfluoride), leupeptin, and pepstatin A from Boehringer Mannheim; N-ethylmaleimide from Pierce; hydroxypropyl- β -cyclodextrin (HPCD) from Cyclodextrin Technologies, Inc. (Gainesville, FL); Megaprime DNA Labeling System from Amersham Pharmacia Biotech; ExpressHyb Hybridization Solution from CLONTECH; and horseradish peroxidase-conjugated, affinity purified donkey anti-mouse, and anti-rabbit IgGs from Jackson ImmunoResearch Laboratories. Stock solutions of digitonin were prepared by dissolving 1 g of solid in 10 ml of boiling H₂O. After cooling to room temperature, the solutions were filtered, aliquoted, and stored in -20°C until use. Lipoprotein-deficient

newborn calf serum (LPDS, $d > 1.215$ g/ml), sodium mevalonate, sodium oleate, and sodium compactin was prepared as described (Brown et al., 1978; Goldstein et al., 1983).

Antibodies

The primary antibodies used for immunoblotting were as follows: 1:1000 dilution of mouse monoclonal anti-T7-Tag (IgG2b; Novagen); 1-5 μ g/ml of mouse monoclonal anti-myc (IgG fraction) from the culture medium of hybridoma clone 9E10 (American Type Culture Collection); 5 μ g/ml of IgG-A9, a mouse monoclonal antibody (mAb) against the catalytic domain of hamster HMGR (amino acids 450-887; Liscum et al., 1983b); 5 μ g/ml of IgG-R139, a rabbit polyclonal antibody against hamster SCAP (amino acids 54-277 and 540-707; Sakai et al., 1997); 5 μ g/ml of IgG-7D4, a mouse mAb against the NH₂ terminus of hamster SREBP-2 (Yang et al., 1995); 1:1000 dilution of anti-Insig-1, a rabbit polyclonal antibody against full-length mouse Insig-1 (Engelking et al. 2004); 2 μ g/ml of IgG-P4D1, a mouse mAb against bovine ubiquitin (Santa Cruz Biotechnology); and 1:1000 dilution of HA-11 (raw ascites fluid), a mAb against the HA epitope tag (Covance Inc., Princeton, NJ).

Construction of Plasmids

The following recombinant expression plasmids were previously described: pCMV-Insig-1-Myc and pCMV-Insig-2-Myc, encoding human Insig-1 or Insig-2, respectively, followed by six tandem copies of a c-myc epitope tag under control of the cytomegalovirus (CMV) promoter (Yang et al., 2002; Yabe et al., 2002); and pCMV-CBP-Flag-SCAP(TM1-6)-Myc, encoding the first six transmembrane domains (aa 1-448) of hamster SCAP followed by three

tandem copies of a Myc epitope under control of the CMV promoter (Yang et al., 2002). The Y298C mutant version of the latter plasmid, designated pCMV-CBP-Flag-SCAP(TM1-6;Y298C)-Myc; and pCMV-HMG-Red-T7(TM1-8), encoding the eight transmembrane domains (aa 1-346) of hamster HMGR, followed by three tandem copies of the T7 epitope tag (MASMTGGQMG), was obtained from Tong Yang; pCMV-HMG-Red, encoding full-length hamster HMGR, was obtained from Voe Hannah; pCMV-HMG-Red-T7, which encodes full-length hamster HMGR (aa 1-887) followed by three tandem copies of the T7-epitope tag; pCMV-HMG-Red-Myc(TM1-8), which encodes the eight transmembrane domains of hamster HMGR, followed by three tandem copies of the Myc epitope tag, and the SSD mutant versions (YIYF-(75-78) to AAAA) of pCMV-HMG-Red-T7 and pCMV-HMG-Red-T7(TM1-8) were obtained from Russell DeBose-Boyd; pCMV-Insig-1-T7, encoding human Insig-1 followed by three tandem copies of the T7 epitope tag under control of the CMV promoter was obtained from Daisuke Yabe; pCIneo-gp78, encoding full-length human gp78, was provided by Dr. Alan Weissman (National Cancer Institute, Bethesda, MD); and pEF1a-HA-Ub, encoding human ubiquitin preceded by an epitope tag derived from the influenza hemagglutinin (HA) protein (YPYDVDPDY) under the control of the EF1a promoter, was provided by Dr. Zhijian Chen (University of Texas Southwestern Medical Center).

pNS3, encoding full-length hamster HMGR in which two tandem copies of the T7-epitope tag are inserted between amino acids 294 and 295, was constructed using pCMV-HMG-Red as the parental vector as follows: a BspDI site was inserted into pCMV-HMG-Red by a two-step PCR-based approach. In the first PCR reaction, a portion of pCMV-HMG-

Red was amplified using primer I (5'-TCTCCTTGGAATCGATGAAGATGTGT-3', corresponding to aa 290-297 with Leu293 changed to Ile) and primer II (5'-TGGACTCTGTCTCTGCTTGTTC AAAGA-3', corresponding to aa 339-346). The resulting 174 bp PCR product was utilized as a “mega-primer” together with primer III (5'-AACTAGAGAACCCACTGCTTACTGGCTTAT-3', corresponding to a vector sequence 5' to the site of insertion) in a second round of PCR amplification from pCMV-HMG-Red. The resulting product was subjected to BamHI/BstEII digestion and inserted into the corresponding region of pCMV-HMG-Red, generating pCMV-HMG-Red/BspDI. In the final step, a complementary pair of 5'-phosphorylated oligonucleotides (5'-CGATATGGCTAGCATGATGGTGGACAGCAAATGGGTGGCGCGCCTATGGCTAGCATGACTGGTGGACAGCAAATGGGTAT-3' and 5'-CGATACCCATTTGCTGTCCACCAGTCATGCTAGCCATAGGCGCGCCACCCATTTGCTGTCCACCAGTCATGCTAGCCATAT-3') containing two tandem T7 epitopes flanked by BspDI sites were annealed and ligated with BspDI-digested pCMV-HMG-Red/BspDI, resulting in pNS3.

pCMV-HMG-Red-Myc, which encodes full-length hamster HMGR followed by six tandem copies of the Myc epitope tag; and pCMV-gp78-Myc, which encodes full-length human gp78 followed by five tandem copies of the Myc epitope tag, were constructed by standard methods. Lysine mutations (K89R, K248R, and K89R/K248R) of HMGR and C356G mutation of gp78 were generated with the QuikChange XL site-directed mutagenesis kit (Statagene). The integrity of all plasmids was confirmed by DNA sequencing of their open reading frames and ligation joints.

Methods

Cell Culture

Monolayers of Chinese hamster ovary cells (CHO-K1); CHO-7 cells, a subline of CHO-K1 cells selected for growth in LPDS (Metherall et al., 1989); UT-2 cells, a line of mutant CHO cells that lacks HMGR (Mosley et al., 1983); and SRD-13A cells, a line of mutant CHO cells that lacks SCAP (Rawson et al., 1999), were maintained in tissue culture at 37°C in 8-9% CO₂. Stock cultures of CHO-K1 cells were maintained in medium A (1:1 mixture of Ham's F12 medium and Dulbecco's modified Eagle medium containing 100 U/ml penicillin and 100 µg/ml streptomycin sulfate) supplemented with 5% (v/v) fetal calf serum (FCS). CHO-7 cells were maintained in medium B (medium A supplemented with 5% LPDS). Stock cultures of UT-2 cells were maintained in medium C (medium A supplemented with 5% FCS) containing 200µM mevalonate. SRD-13A cells were cultured in medium C supplemented with 5 µg/ml cholesterol, 1 mM sodium mevalonate, and 20 µM sodium oleate.

Transient Transfection

Cells were transfected using the Fugene 6 reagent (Roche Molecular Biochemicals) as previously described with minor modifications (Rawson et al., 1999). On day 0, CHO-K1 or CHO-7 cells were set up at 5×10^5 cells/60-mm dish. On day 1, the cells were transfected with up to 3 µg of DNA/dish using a ratio of 3 µl of Fugene/µg of DNA in medium A in a final volume of 0.2 ml. SRD-13A cells were set up on day 0 at 8×10^5 cells/100-mm dish. On day 2, the cells were transfected with 5 µg of DNA/dish using a ratio of 3 µl of

Fugene/ μ g of DNA in medium A in a final volume of 0.4 ml. The total amount of DNA in each transient transfection experiment was adjusted by addition of pcDNA3 mock vector (Invitrogen). Fugene was diluted in medium A and incubated for 5 min at room temperature prior to being added dropwise to the DNA solution. This mixture was then further incubated for 15 min at room temperature. Plates were refed with fresh medium. The Fugene/DNA mixture was then added to each dish.

Cell Fractionation and Immunoblot Analysis

Monolayers of CHO cells at 80%-90% confluency were scraped into the medium, and pooled suspensions were centrifuged at $10^3 \times g$ for 5 min at 4°C. Each cell pellet was then resuspended in 1 ml of PBS, transferred to microcentrifuge tubes, and centrifuged again at $10^3 \times g$ for 5 min at 4°C. Following aspiration of the supernatants, the cell pellets were resuspended in 0.5 ml buffer A (10 mM HEPES-KOH [pH 7.4], 10 mM KCl, 1.5 mM $MgCl_2$, 5 mM sodium EDTA, 5 mM sodium EGTA, and 250 mM sucrose) supplemented with protease inhibitor cocktail consisting of 1 mM dithiothreitol (DTT), 1 mM PMSF, 0.5 mM Pefabloc, 10 μ g/ml leupeptin, 5 μ g/ml pepstatin A, 50 μ g/ml ALLN, and 10 μ g/ml aprotinin. For HMGR immunoblots, the concentrations of DTT and leupeptin were increased to 5 mM and 0.1 mM, respectively. The cell suspension was passed through a 22.5 gauge needle 25 times and centrifuged at $10^3 \times g$ for 7 min at 4°C. The $10^3 \times g$ pellet was resuspended in 0.3 ml of buffer (20 mM HEPES-KOH [pH 7.6], 25% (v/v) glycerol, 0.42 M NaCl, 1.5 mM $MgCl_2$, 1 mM EDTA, 1 mM EGTA, and protease inhibitor cocktail), rotated at 4°C for 1 h, and centrifuged at $10^5 \times g$ for 30 min at 4°C in a Beckman TLA 100.2 rotor.

The supernatant from this spin was designated as the nuclear extract fraction and precipitated with 1.5 ml acetone for 16 h at -20°C. Precipitated material and the supernatant from the original spin were collected by centrifugation at 20,000 X g for 15 min and solubilized in 100 µl of buffer containing 10 mM Tris-HCl (pH 6.8), 1% (w/v) sodium dodecyl sulfate (SDS), 100 mM NaCl, 1 mM EDTA, and 1 mM EGTA. Protein concentrations of nuclear extract and membrane fractions were measured using the BCA Kit (Pierce). For HMGR immunoblots, an equal volume of Buffer B containing 62.5 mM Tris-HCl [pH 6.8], 15% (w/v) SDS, 8 M urea, 10% (v/v) glycerol, and 100 mM DTT was added to the membrane fractions obtained after centrifugation of the supernatant from the original spin. Aliquots of the membrane and nuclear extract fractions were mixed with 5X SDS loading buffer (Bollag and Edelstein, 1991) to achieve a final concentration of 1X, and boiled for 5 min except for HMGR immunoblots in which case membrane fractions were incubated at 37°C for 30 min prior to SDS-PAGE.

After SDS-PAGE on 8% or 10% gels, proteins were transferred to Hybond C-Extra nitrocellulose filters (Amersham). The filters were incubated with the antibodies described above and bound antibodies were visualized with peroxidase-conjugated, affinity-purified donkey anti-mouse or anti-rabbit IgG using the SuperSignal CL-HRP substrate system (Pierce) according to the manufacturer's instructions. Gels were calibrated with prestained molecular mass markers (Bio-Rad or Amersham). Filters were exposed to X-Omat Blue XB-1 film (Kodak) at room temperature for the indicated times.

Trypsin and Glycosidase Treatments

A 20,000 X g pellet was prepared as described above except that no protease inhibitors were added. The resulting membrane pellets were resuspended in 50 μ l of buffer C (buffer A containing 100 mM NaCl). Aliquots (2 μ l) were added to 2 μ l of a solution of 20% (w/v) hexyl- β -D-glucopyranoside to determine the protein concentration by using Coomassie Plus Protein Assay Reagent (Pierce). Equal amounts of protein were then incubated in the presence of indicated amount of trypsin in a total volume of 50 μ l for 30 min at 30°C. Reactions were stopped by addition of 2 μ l of soybean trypsin inhibitor (400 units). For subsequent glycosidase treatments, individual samples received 6 μ l of solution containing 3.5% (w/v) SDS and 7% (v/v) 2-mercaptoethanol. After heating at 100°C for 5-10 min, each sample received sequential additions of either 7.5 μ l of 0.5 M sodium citrate (pH 5.5), 7.5 μ l of solution containing 10X protease inhibitors (a concentration of 1X corresponding to 10 μ g/ml leupeptin, 5 μ g/ml pepstatin A, and 2 μ g/ml aprotinin), followed by 1 μ l of endo H (0.05 units); or 7.5 μ l of 0.5 M sodium phosphate (pH 7.5), 7.5 μ l of solution containing 10% (v/v) NP-40 and 10X protease inhibitors, followed by 1 μ l of PNGase F (7.7×10^{-3} units). All reactions were carried out overnight at 37°C. An aliquot of 27 μ l was mixed with 9 μ l of 4X SDS loading buffer and boiled for 5 min for SCAP immunoblot. The remaining 48 μ l were mixed with 48 μ l of buffer B and 32 μ l of 4X SDS loading buffer and incubated at 37°C for 30 min for HMGR immunoblot. The samples were subjected to SDS-PAGE on 5-12% gradient gels.

Immunoprecipitation

The cells were harvested into the medium by scraping, washed with PBS and lysed in 0.5 ml of Buffer D (50 mM HEPES-KOH (pH 7.4), 100 mM NaCl, 1.5 mM MgCl₂, 0.1% NP-40) for coimmunoprecipitation experiments, buffer E (PBS containing 1% NP-40, 1% (w/v) deoxycholate, 5 mM EDTA and 5 mM EGTA) for detecting endogenous HMGR ubiquitination, or RIPA buffer (50 mM Tris-HCl (pH 8.0), 150 mM NaCl, 0.1% SDS, 1.5% NP-40, 0.5% deoxycholate, 2 mM MgCl₂) for detecting ubiquitination of transfected constructs, supplemented with 50 µg/ml leupeptin, 50 µg/ml ALLN, 1mM PMSF, 0.5 mM Pefabloc, 5 µg/ml pepstatin A, and 10 µg/ml aprotinin. In some experiments, 10 mM N-ethylmaleimide was also added for detection of ubiquitinated proteins. The lysates were passed through a 22.5 gauge needle 5-10 times, rotated for 0.5-1 hr at 4°C and clarified by centrifugation at 10⁵ X g for 15 min at 4°C. An aliquot was removed for measuring protein concentrations using the BCA Kit (Pierce) and the remainder of the supernatant was adjusted to equal concentration in 1 ml lysis buffer and precleared by rotation for 1 hr at 4°C with 20 µg of an irrelevant IgG and 50 µl protein A/G agarose (Santa Cruz Biotechnology). After centrifugation at 1000 X g for 1-3 min at 4°C, the supernatant was transferred to a fresh tube, and immunoprecipitations from detergent lysates were carried out with either 30 µl of monoclonal anti-T7 IgG-coupled agarose beads (Novagen); or, first 30 µg of a polyclonal antibody against the 60-kDa COOH-terminal domain of human HMGR, or 5 µg of polyclonal anti-Myc IgG (Upstate), and then 30-50 µl protein A/G agarose for 16 hr at 4°C. In some experiments, the resulting supernatant was transferred to a new tube and precipitated with five volumes of acetone for 10 min at -20°C, followed by centrifugation at 3000 X g

for 15 min. The pellet was resuspended in 0.1 ml of Buffer B and SDS loading buffer, boiled for 5 min, and designated as the supernatant fraction of the immunoprecipitate (IP). The pelleted beads were washed three times (15 min each), resuspended in 80 μ l of Buffer B and 20 μ l 5X SDS loading buffer, and boiled for 5 min. After centrifugation at 1000 X g for 1-3 min at room temperature, the supernatant was transferred to a fresh tube and designated as the pellet fraction of the IP. Aliquots of the IP pellet and supernatant were subjected to SDS-PAGE, transferred to nylon membranes, and subjected to immunoblot analysis.

Blue Native-PAGE for Detection of HMGR-Insig Complex

Blue native-PAGE (BN-PAGE) was carried out as described by Schagger et al. (1994) and Yang et al. (2002). SRD-13A cells were transfected in medium B or C. Twelve h after transfection, cells were washed once with PBS and incubated for 1 h at 37°C with medium B containing 50 μ M compactin, and 1% HPCD. The cells were then washed twice with PBS and switched to medium B containing 50 μ M compactin and the indicated additions. After incubation for 2 h at 37°C, cells were pooled and resuspended in 0.5 ml of buffer (10 mM HEPES-KOH [pH 7.2], 250 mM sorbitol, 10 mM KOAc, and 0.5 mM $\text{Mg}(\text{OAc})_2$) supplemented with protease inhibitor cocktail. The cell suspension was passed through a 22.5 gauge needle 30 times and centrifuged at 1000 X g for 5 min at 4°C. A 16,000 X g membrane pellet isolated from the supernatant by centrifugation for 3 min at 4°C was resuspended in 0.5 ml Buffer F containing 50 mM HEPES-KOH [pH 7.2], 250 mM sorbitol, 70 mM KOAc, 5 mM EGTA, 1.5 mM $\text{Mg}(\text{OAc})_2$ and protease inhibitor cocktail, centrifuged again at 16,000 X g for 3 min at 4°C, and resuspended in 50-100 μ l of Buffer F as described

(Nohturfft et al., 2000). Aliquots of the membranes were mixed with an equal volume of buffer containing 40 mM HEPES-KOH [pH 7.0], 2 mM Mg(OAc)₂, and 2% (w/v) digitonin. After incubation at 4°C for 30 min, detergent insoluble material was removed by centrifugation at 20,000 X g for 2 min at 4°C. One aliquot of the supernatant was mixed with 10X buffer containing 50 mM Bis-Tris-HCl [pH 7.0], 0.75 M 6-amino-n-hexanoic acid, 5% (w/v) Coomassie G250, and 10% (v/v) glycerol; loaded onto a 4-16% BN gel; and subjected to PAGE (Schagger et al., 1994). After electrophoresis, proteins were transferred electrophoretically to a PVDF membrane (Millipore Corp.), destained with methanol, and subjected to immunoblot analysis with 5 µg/ml of monoclonal anti-Myc IgG directed against epitope-tagged Insig-1 or 1:1000 dilution of monoclonal anti-T7 IgG directed against HMGR(TM1-8). A separate aliquot of the digitonin-containing supernatant was mixed with 5X SDS loading buffer and subjected to SDS-PAGE on 10% gels for immunoblot analysis of epitope-tagged HMGR(TM1-8) and Insig-1.

For antibody supershift assays, a 50 µl aliquot of membranes was added to 50 µl of the above digitonin-containing buffer together with the indicated amount of monoclonal antibody (control IgG-2001, anti-Myc IgG-9E10 or anti-T7). The mixture was incubated at 4°C for 30 min, processed for BN-PAGE, and subjected to immunoblot analysis with 0.66 µg/ml of polyclonal anti-Myc IgG directed against epitope-tagged Insig-1.

Mutagenesis and Isolation of SR-12813-resistant Cells

On day 0, CHO-7 cells were harvested from stock cultures by trypsinization, centrifuged, washed, and resuspended in PBS. The cell suspension was divided into five aliquots of 1 X

10^7 cells/ml per aliquot, which were exposed to 750 rads of γ -irradiation from a ^{137}Cs source using a Mark I irradiator (J. L. Shepherd Co., San Fernando, CA) as previously described (Rawson et al., 1998). The cells were immediately plated at 5×10^5 cells/100-mm dish in medium B. On day 1, the medium was replaced with medium B containing 5-10 μM SR-12813. Fresh medium was added to the cells every 2 days until colonies formed. Of the 50 original dishes treated with 10 μM SR-12813, 14 contained colonies. On day 29, the surviving colonies were recovered with cloning cylinders, replated, and cloned by limiting dilution. One of the 8 colonies that lacked expression of Insig-1 mRNA was designated SRD-14 cells.

2.5×10^7 SRD-14 cells were further mutagenized the same way and selected in medium B containing 10 μM SR-12813 and 0.5 $\mu\text{g/ml}$ 25-HC. Of the 50 original dishes, 19 contained colonies. The surviving colonies were cloned as above.

Stable Cell Lines

SRD-14/pInsig-1 and SRD-14/pInsig-2 cells, derivatives of SRD-14 cells stably expressing Insig-1-Myc or Insig-2-Myc, respectively, were generated as follows. On day 0, SRD-14 cells were set up at 5×10^5 cells/60-mm dish in medium B. On day 1, the cells were transfected with 1 μg of pCMV-Insig-1-Myc or pCMV-Insig-2-Myc using the Fugene 6 transfection reagent as described above. On day 2, cells were switched to medium B supplemented with 700 $\mu\text{g/ml}$ G418. Fresh medium was added every 2-3 days until colonies formed. Individual colonies were isolated with cloning cylinders, and Insig-1 or Insig-2 expression was assessed by immunoblot analysis with anti-Myc. Cells from the colonies that

express the highest level of Insig-1 and Insig-2 were cloned by limiting dilution and maintained in medium B containing 500 µg/ml G418 at 37°C, 8-9% CO₂.

UT-2/pNS3 cells, derivatives of UT-2 cells stably expressing pNS3 were generated as follows. On day 0, UT-2 cells were set up at 7×10^5 cells/100-mm dish in medium D (medium C containing 200 µM mevalonate). On day 1, the cells were transfected with up to 3 µg of pNS3. On day 2, cells were switched to medium E (medium D supplemented with 700 µg/ml G418). Individual colonies were isolated as above and the expression and regulation of pNS3 was assessed by immunoblot analysis with IgG-A9 against HMGR. Cells from a single colony were cloned by limiting dilution and maintained in medium F (medium D containing 500 µg/ml G418) at 37°C, 8-9% CO₂.

Quantitative Real-Time PCR, Northern and Southern Blot Analysis

The protocol for real-time PCR was identical to that described by Liang et al. (2002). Total RNA was isolated from CHO-7 and SRD-14 cells using the RNeasy Kit and RNase-free DNase set (Qiagen) according to the manufacturer's instructions. First strand cDNA was synthesized from 2 µg of DNase-I treated total RNA with random hexamer primers using the ABI cDNA synthesis kit (catalog no. N808-0234; Applied Biosystems). Specific primers for each gene (Table 2) were designed using Primer Express software (Applied Biosystems). The real time PCR contained, in a final volume of 20 µl, 20 ng of reverse transcribed total RNA, 167 nM forward and reverse primers, and 10 µl of 2X SYBR Green PCR Master Mix (catalog no. 4312704; PerkinElmer Life Sciences). PCR was carried out in 384-well plates

using the ABI PRISM 7900HT Sequence Detection System (Applied Biosystems). All reactions were done in triplicate. Relative amounts of mRNAs were calculated using the comparative C_T method. GAPDH mRNA was used as the invariant control for all studies.

Hamster Insig-1 cDNA probe for Northern and Southern Blot analysis prepared by PCR amplification of reverse-transcribed total RNA isolated from wild type CHO-7 cells was obtained from Yi Gong. The PCR products, encoding the entire coding region of Insig-1, were radiolabeled with [α - 32 P]dCTP using the Megaprime DNA Labeling System. Total RNA and restriction enzyme-digested genomic DNA was subjected to electrophoresis and transferred to Hybond N⁺ membranes (Amersham Pharmacia Biotech) using standard molecular biology techniques, and filters were hybridized at 60-68°C with radiolabeled probe (2 X 10⁶ cpm/ml and 4 X 10⁶ cpm/ml for Northern and Southern blots, respectively) using the ExpressHyb Hybridization Solution according to the manufacturer's instructions. Filters were exposed to film with intensifying screens for the indicated time at -80°C.

mRNA	Sequences of forward and reverse primers (5' to 3')	GenBank accession no.
Insig-1	GGCTTGTTGGTGGACATTCTG GGCGATGGTGATCCCAAGT	AF527628
Insig-2	GGGTGGTGCTCTTCTTCATTG CAGGTGGAAAAAGTGTCACGTTT	AF527629
HMG CoA reductase	AGATACTGGAGAGTGCCGAGAAA TTGTAGGCTGGGATGTGCTT	X00494
HMG CoA synthase	CCTGGGTCACTTCCTTTGAATG GATCTCAAGGGCAACGATTCC	AH001829
LDL receptor	AGACACATGCGACAGGAATGAG GACCCACTTGCTGGCGATA	M13877
GAPDH	GCAAGTTCAAAGGCACAGTCAA CGCTCCTGGAAGATGGTGAT	X52123

Table 2. Nucleotide sequences of gene-specific primers used for quantitative real-time PCR.

Sequencing of Insig-1 from Parental and Mutant Cells

PCRs were performed using the Advantage-GC 2 PCR kit (CLONTECH) with 5 µl of the first-strand product per 50-µl PCR. The following primer pair was employed to amplify hamster Insig-1 transcript: 5'-GCTACGTGCGGTGTCGTG-3' and 5'-CCATGTGAACACTTCTTCAGGA-3'. PCR products were cloned using the pGEM-T Easy Vector System (Promega) according to the manufacturer's protocol, and multiple clones from each PCR reaction were sequenced in their entirety.

PCR on high molecular weight genomic DNA from parental CHO-7 cells and mutant cells was performed in 50-µl reactions using the following primer pair: 5'-GTTTCTTGTGTATAATGGTGTCTA-3' or 5'-GAACGAATATAAAGGAAATCTGG-3'. The PCR products were cloned and sequenced as described above.

CHAPTER FOUR

Results

UBIQUITINATION AND DEGRADATION OF HMGR MEDIATED BY BINDING OF INSIG TO ITS STEROL-SENSING DOMAIN

The Regulated Degradation of HMGR Occurs in the ER

To study the turnover of HMG CoA reductase (HMGR), I constructed a plasmid, designated pNS3, encoding the full-length enzyme with two tandem copies of an 11 amino acid epitope tag inserted between amino acids 294 and 295. This tag, derived from the major capsid protein of T7 bacteriophage, is inserted into the long loop between transmembrane (TM) helices 7 and 8 of HMGR that projects into the lumen of the ER. Expression of the plasmid is driven by the strong CMV promoter, and the construct does not contain any untranslated regions of HMGR mRNA required for translational regulation. HMGR-deficient UT-2 cells were transfected with pNS3 and an HMGR-expressing clone was isolated. To determine whether HMGR degradation is regulated in these cells, I depleted the cells of sterols by incubating them in lipoprotein-deficient serum (LPDS) in the presence of an HMGR inhibitor (compactin) plus a low concentration of mevalonate (50 μ M) to maintain viability. Some of the dishes were repleted with sterols by the addition of a mixture of 1 μ g/ml of 25-hydroxycholesterol (25-HC) and 10 μ g/ml cholesterol added in ethanol and with increasing concentrations of mevalonate. After overnight incubation, HMGR stability was assessed by SDS-PAGE and immunoblotting with monoclonal anti-HMGR antibody. In sterol-depleted cells, I observed a band of full-length HMGR that migrated with an apparent molecular mass

of ~97 kDa (Figure 4-1, lane 1). This protein did not change in amount when sterols alone were present (lane 2). The complete degradation of HMGR required sterols and at least 1 mM mevalonate (lanes 3-10). Concentrations of mevalonate above 10 mM caused HMGR degradation even in the absence of sterols, suggesting that these concentrations give rise to both sterol and nonsterol isoprenoid products (lanes 11 and 12). Although the absolute concentrations of mevalonate that cause these effects depend on the cell line and the experimental conditions, this experiment illustrates the requirement of both sterols and at least one nonsterol mevalonate product to completely degrade HMGR (Nakanishi et al., 1988; Roitelman and Simoni, 1992). Further, the epitope tag in the pNS3 construct does not interfere with the ability of HMGR to respond to the regulatory signals that modulate its half-

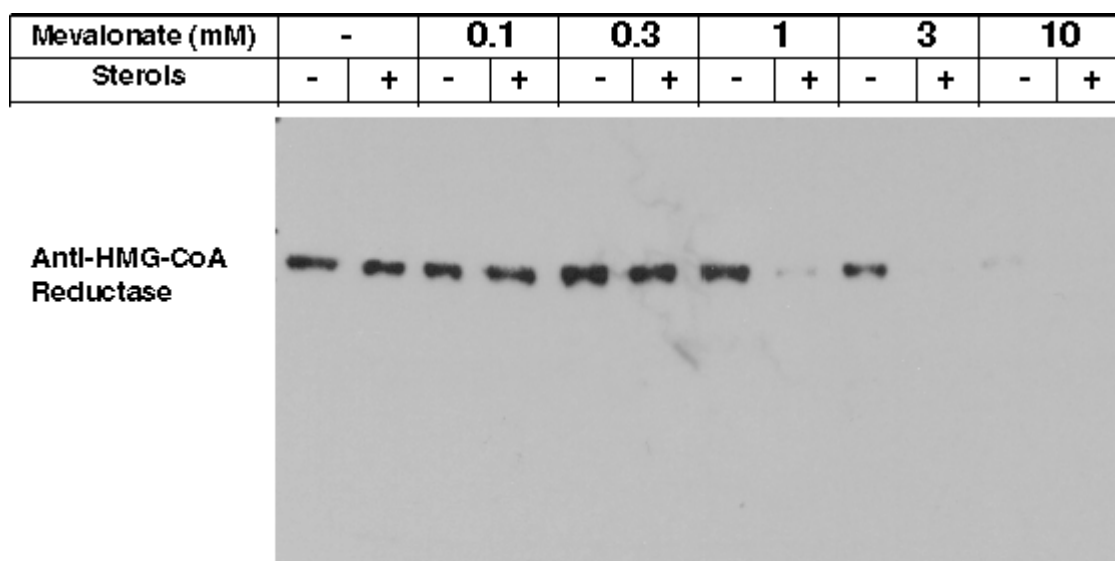


Figure 4-1. Regulated degradation of HMGR requires sterols and a nonsterol mevalonate derivative. UT-2/pNS3 cells were set up on day 0 in medium F at 5×10^5 cells per 100 mm dish. On day 2, cells were switched to medium B containing 50 μ M compactin in the absence (-) or presence (+) of sterols and the indicated concentration of mevalonate. After incubation for 16 h, cells were harvested, membrane fractions were prepared and an aliquot (10 μ g protein) were subjected to immunoblotting with IgG-A9 (against HMGR), and exposed to film for 1 min.

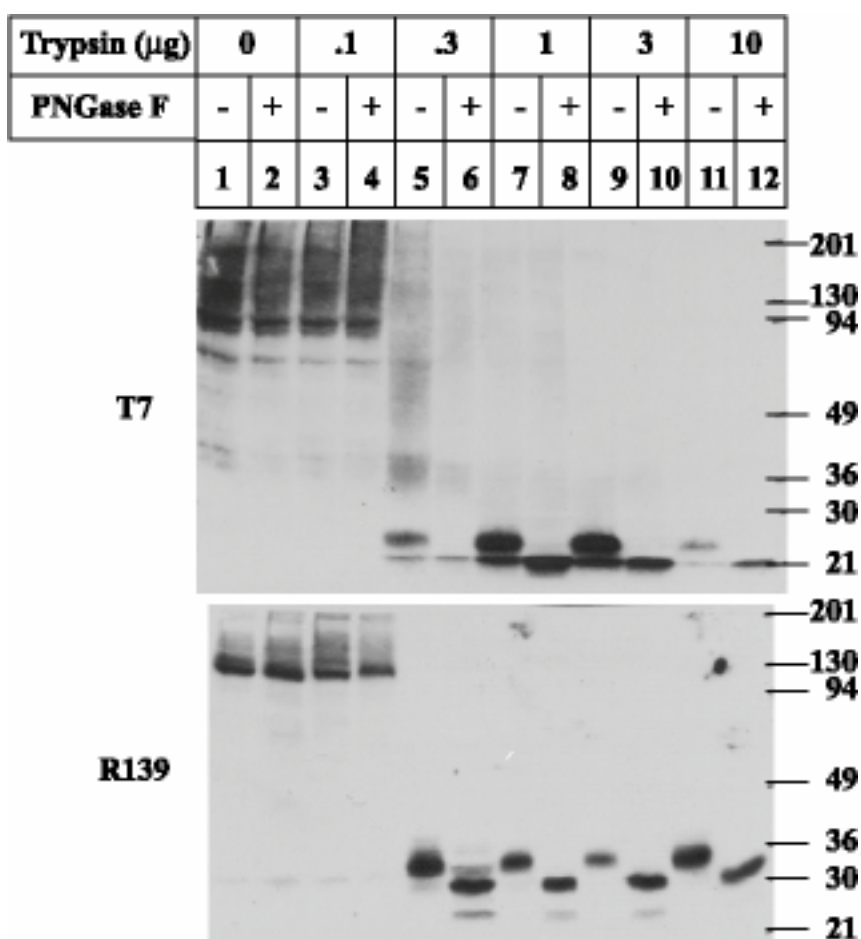


Figure 4-2. Insertion of the T7 tag preserves the topology of the loop between the TMs 7 and 8. UT-2/pNS3 cells were set up on day 0 as in Figure 4-1. On day 2, cells were switched to medium B containing 50 μ M compactin and 50 μ M mevalonate. On day 3, cells were harvested, and membrane fractions were prepared as described in Chapter 3. Aliquots of membrane fractions were incubated in the presence of indicated amount of trypsin. Proteolysis was stopped, the samples were incubated in the absence (-) or presence (+) of PNGase F, subjected to immunoblotting with anti-T7 IgG (against HMGR) or R139 IgG (against SCAP), and exposed to film for 5 s.

life, suggesting that the protein is correctly folded and validating the use of this construct for the study of regulated degradation of HMGR.

To further confirm that pNS3 encodes a correctly folded protein, I determined whether insertion of the T7 epitope tag between TMs 7 and 8 preserves the intraluminal topology of this loop. As shown in Figure 4-2, the epitope tag is protected from digestion when sealed membrane vesicles are digested with trypsin *in vitro*, suggesting that the tag is projected into the lumen of the ER. Further, PNGase F treatment increases the mobility of the protected fragment consistent with the fact that there is an N-linked glycosylation site in this loop (Liscum et al., 1983a; 1985). As a positive control, I used R139, a polyclonal antibody against SCAP, to verify that the epitope recognized by this antibody is also protected from digestion and has N-linked glycosylation sites as expected (Nohturfft et al., 1998a; b).

Next, I utilized the pNS3 construct to determine whether HMGR stability is modulated by transport between ER and Golgi compartments analogous to the sterol inhibited movement of SCAP from ER to Golgi (Nohturfft et al., 1999). N-linked oligosaccharides of proteins residing in the ER have a configuration that is sensitive to endo H digestion. As glycoproteins are transported to the Golgi, their sugars are modified such that the resulting oligosaccharide structure is resistant to digestion by endo H (Maley et al., 1989). If HMGR were transported to the Golgi, it should be resistant to endo H. However, as shown in Figure 4-3, HMGR was sensitive to endo H under all conditions tested whereas SCAP was endo H-resistant in the absence of sterols. Addition of 1 mM mevalonate did not affect either of the two proteins. ALLN, an inhibitor of the 26S proteasome, was added 5 h prior to harvest in lanes 5 and 10 to prevent the degradation of HMGR in the presence of

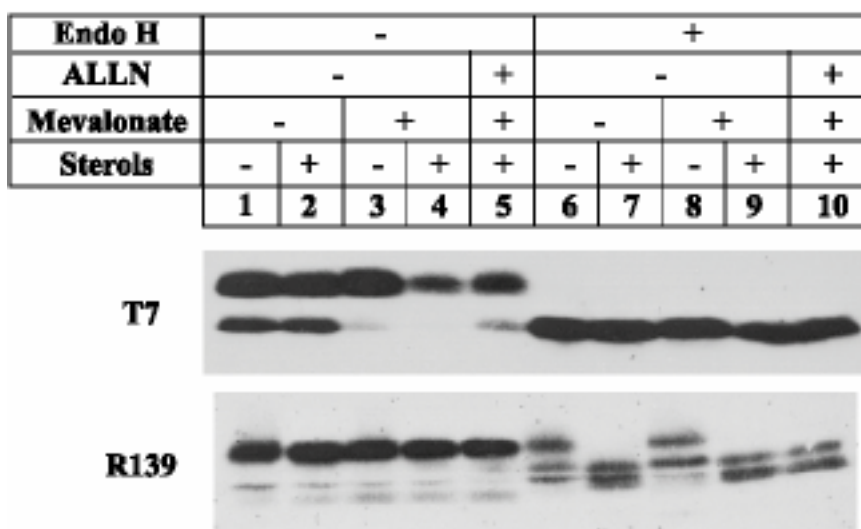


Figure 4-3. Sterols and mevalonate do not affect the endo H sensitivity of HMGR. On day 0, UT-2/pNS3 cells were set up as in Figure 4-1. On day 2, cells were switched to medium B containing 50 μ M compactin and 50 μ M mevalonate in the absence or presence of sterols and 1mM mevalonate as indicated. On day 3, each dish received 25 μ g/ml ALLN (lanes 5 and 10) or DMSO (dimethyl sulfoxide). After incubation for 5 h, cells were harvested, and membrane fractions were prepared as described in Chapter 3. Aliquots of membrane fractions (164 μ g protein) were incubated in the presence of 1 μ g trypsin. Proteolysis was stopped, and the samples were incubated for 16 h at 37°C in the absence (lanes 1-5) or presence (lanes 6-10) of endo H, subjected to immunoblotting with anti-T7 IgG (against HMGR) or R139 IgG (against SCAP), and exposed to film for 30 s.

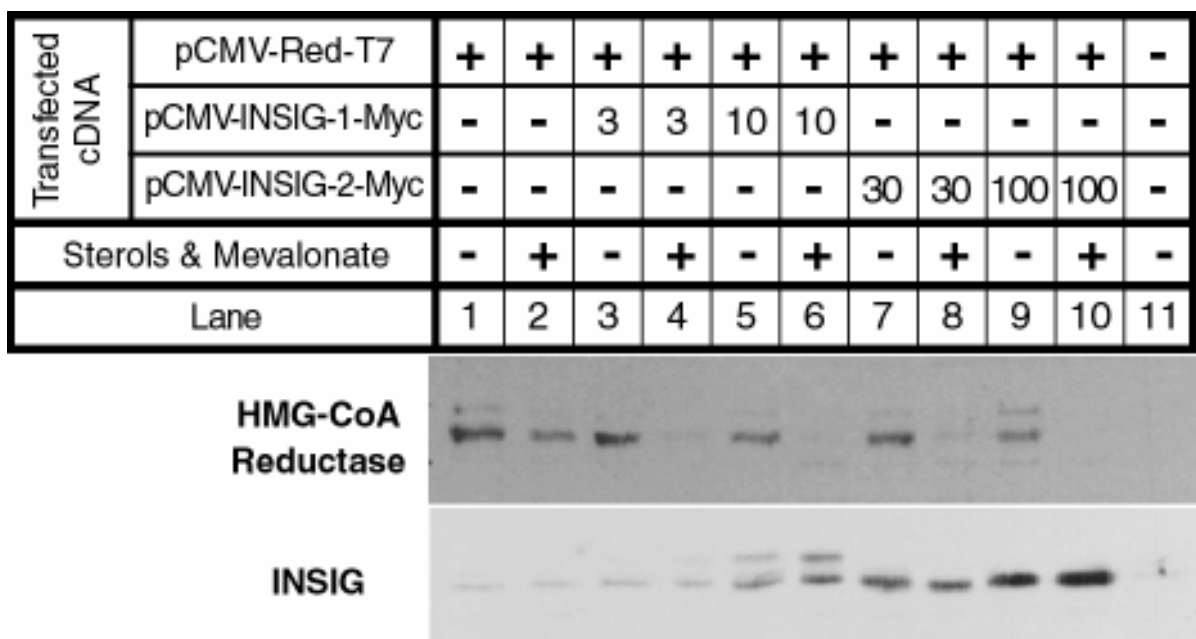


Figure 4-4. Insig-1 and Insig-2 confer sterol-mediated degradation upon HMGR in transfected CHO-K1 cells. On day 1, cells were transfected in 2 ml of medium B with 3 μ g pNS3 and the indicated amount of pCMV-Insig-1-Myc or pCMV-Insig-2-Myc. Three to six hours after transfection, cells received a direct addition of 2 ml of medium B containing (final concentration) 50 μ M compactin, 50 μ M mevalonate, and sterols plus 10 mM mevalonate as indicated. After 16 h, cells were harvested, membrane fractions were prepared, and aliquots (25 μ g) were subjected to immunoblot analysis with anti-T7 IgG (against HMGR) and anti-Myc IgG (against Insig-1 and Insig-2). Filters were exposed to film for 10-30 s.

sterols and mevalonate. These results are consistent with previous immunofluorescence and subcellular fractionation studies which indicate that HMGR degradation occurs in the ER (Lecureux and Wattenberg, 1994).

Insig-Mediated Degradation of HMGR

I tested the hypothesis that Insig-1 or Insig-2 plays a role in the sterol-regulated degradation of HMGR. For this purpose, pNS3 was introduced into wild-type CHO-K1 cells by transient transfection, and the protein was visualized by SDS-PAGE and immunoblotting with monoclonal anti-T7 antibody (Figure 4-4). When HMGR was overexpressed to this degree, the enzyme no longer showed rapid degradation when sterols and mevalonate were added (lanes 1 and 2). I attribute this to a saturation of some component of the degradative machinery that interacts with HMGR in a stoichiometric manner. When Myc-tagged Insig-1 was overexpressed by cotransfection, the HMGR band was still visualized in the sterol-depleted cells (lanes 3 and 5). HMGR decreased when sterols and mevalonate were added (lanes 4 and 6). When a cDNA encoding Insig-2 was cotransfected with HMGR cDNA, sterol-regulated degradation was also restored (lanes 7-10).

To demonstrate directly that Insig was restoring sterol-mediated degradation, I tested to see if ALLN can prevent the effect of Insig-1 on HMGR (Figure 4-5). In the absence of Insig-1, the amount of HMGR slightly increased when the culture medium contained ALLN, and there was no effect of sterols plus mevalonate (lanes 2-5). When cells were transfected with 100 ng of Insig-1, the amount of HMGR declined markedly, but only in the presence of

sterols plus mevalonate (lanes 10 and 11). This disappearance was blocked in the presence of ALLN (lanes 12 and 13).

The ability of Insig to restore sterol-dependent degradation of HMGR in overexpressing cells resembles its ability to restore sterol-dependent ER retention of the SCAP-SREBP complex in cells overexpressing SCAP (Yang et al., 2002). In HMGR and SCAP, sterol-dependent regulation requires the membrane anchor, which contains the sterol-sensing domain (SSD). To determine whether the membrane anchor domains of HMGR and SCAP interact with the same site on Insig, I performed a competition experiment (Figure 4-6). Cells were transfected with pNS3, Insig-1 or Insig-2, and a plasmid encoding a portion of the membrane anchor domain of SCAP (TM1-6), which contains the SSD. As a control, I used a plasmid encoding the same portion of SCAP with a substitution of a cysteine for a

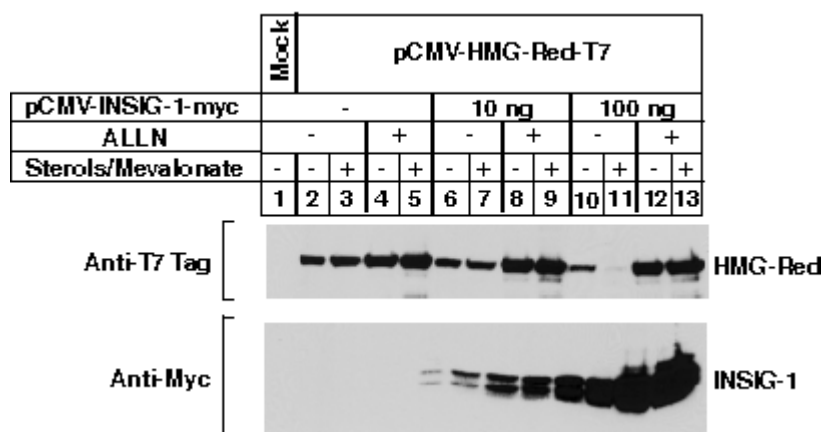


Figure 4-5. Effect of Insig-1 on HMGR can be inhibited by ALLN. On day 1, CHO-K1 cells were transfected in medium C with 3 μ g pNS3 and the indicated amount of pCMV-Insig-1-Myc. Three to six hours after transfection, cells were refed with medium B containing 50 μ M compactin, 50 μ M mevalonate, and sterols plus 10 mM mevalonate as indicated. On day 2, the cells were refed the same medium with or without 25 μ g/ml ALLN as indicated. After incubation for 4 h, cells were harvested, membrane fractions were prepared, and aliquots (33 μ g) were subjected to immunoblot analysis with anti-T7 IgG (against HMGR) and anti-Myc IgG (against Insig-1). Filters were exposed to film for 10-30 s.

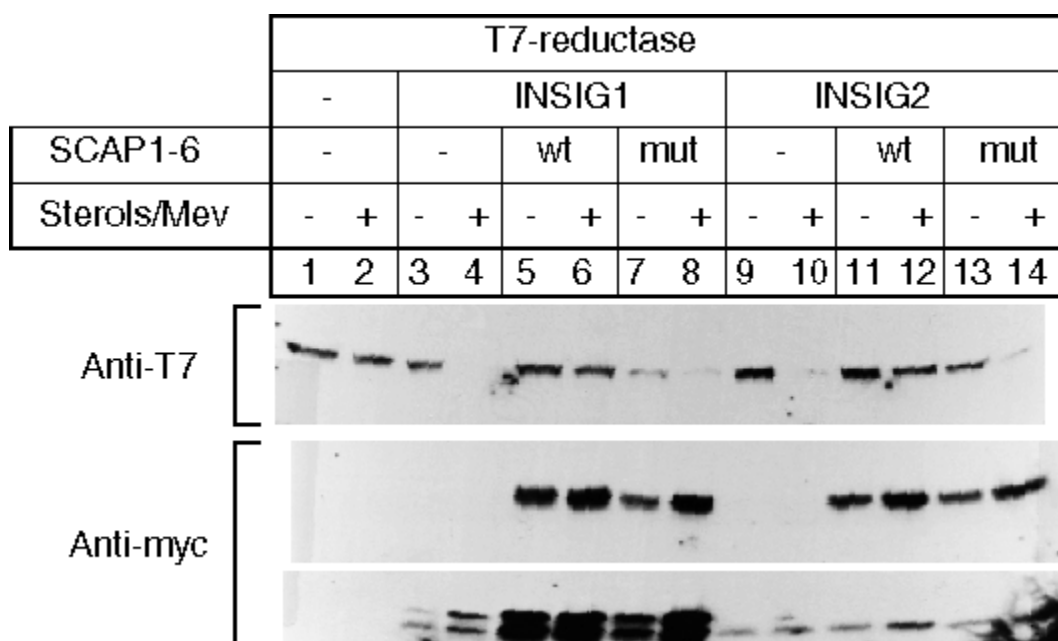


Figure 4-6. Overexpression of wild-type, but not mutant, SCAP(TM1-6) prevents Insig-mediated degradation of transfected HMGR in CHO-K1 cells. On day 1, cells were transfected in 2 ml of medium B with 3 μ g pNS3, 10 ng of either pCMV-Insig-1-Myc (lanes 3-8) or pCMV-Insig-2-Myc (lanes 9-14), and 30 ng of either wild-type (lanes 5, 6, 11, and 12) or mutant Y298C (lanes 7, 8, 13, and 14) versions of pCMV-CBP-Flag-SCAP(TM1-6)-Myc. Three to six hours after transfection, cells received a direct addition of 2 ml of medium B containing 50 μ M compactin, 50 μ M mevalonate in the absence (-) or presence (+) of sterols plus 10 mM mevalonate. On day 2, cells were harvested, membrane fractions were prepared, and aliquots (32 μ g) were subjected to immunoblot analysis with anti-T7 IgG (against HMGR) and anti-Myc IgG (against SCAP(TM1-6) and Insig). Filters were exposed to film for 5-30 s.

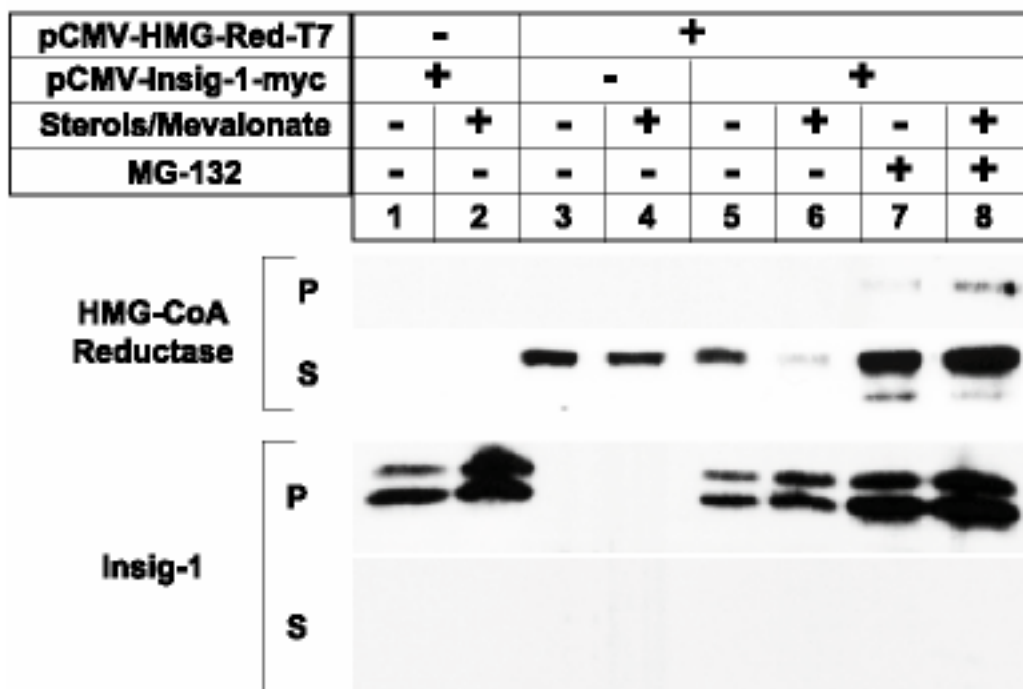


Figure 4-7. Sterol-dependent binding of HMGR to Insig-1. On day 1, CHO-K1 cells were transfected in medium C with 3 μ g pNS3 (lanes 3-8) and 10 ng pCMV-Insig-1-Myc (lanes 1, 2, and 5-8). Six hours after transfection, cells were refed with medium B containing 50 μ M compactin, 50 μ M mevalonate, and sterols plus 10 mM mevalonate as indicated. On day 3, each dish received a direct addition of 3 μ l of DMSO (lanes 1-6) or 10 μ M MG-132 (lanes 7 and 8). After incubation for 4 h, cells were harvested, lysed in Buffer D, and subjected to IP with polyclonal anti-Myc IgG as described in Experimental Procedures. Fractions of resuspended pellet and supernatant solutions were subjected to immunoblotting with anti-Myc IgG (against Insig-1) and anti-T7 IgG (against HMGR). Filters were exposed to film for 1-10 s.

tyrosine in the SSD (Y298C). This mutation renders SCAP resistant to sterol-mediated ER retention (Nohurfft et al., 1998a). Previous studies showed that wild-type SCAP binds Insig, whereas the Y298C mutant protein does not (Yang et al., 2002; Yabe et al., 2002a; b). In the absence of Insig, sterols plus mevalonate had no effect on the amount of HMGR (lanes 1 and 2). When I cotransfected the Insig-1 or Insig-2 plasmid, sterols and mevalonate reduced the amount of HMGR (lanes 3, 4, 9 and 10). The sterol effect was abolished when I overexpressed the TM1-6 portion of wild-type SCAP (lanes 5, 6, 11 and 12), but not the Y298C mutant (lanes 7, 8, 13, and 14). The middle and bottom panels of Figure 4-6 show immunoblots for the TM1-6 portion of SCAP and Insig, respectively.

HMGR-Insig-1 Interaction

To demonstrate directly the sterol-mediated interaction of HMGR and Insig-1, I used coimmunoprecipitation (Figure 4-7). CHO-K1 cells were transfected with pNS3 with or without pCMV-Insig-1-Myc and incubated in sterol-depleted or sterol-repleted conditions. Detergent-solubilized extracts were immunoprecipitated with the anti-Myc antibody, which precipitates the transfected Insig-1. Immunoprecipitation (IP) was essentially complete, as revealed by immunoblotting of the supernatant and pellet fractions (Figure 4-7, bottom two panels). When cells were cotransfected with HMGR and Insig-1, sterols and mevalonate degraded HMGR (Figure 4-7, lanes 5 and 6). When the cells received MG-132 to block sterol-induced degradation four hours prior to harvest, the pellet fraction contained HMGR, but only when the cells were incubated with sterols and mevalonate (lanes 7 and 8). This finding suggests that sterols plus mevalonate induce the binding of HMGR to Insig-1.

To determine whether the binding of HMGR to Insig-1 is mediated by the membrane domain of HMGR, I transfected cells with a plasmid encoding a truncated version of HMGR containing the entire membrane anchor domain (TM1-8), but lacking the catalytic domain (Figure 4-8). The COOH-terminus of this protein is composed of three copies of the T7 epitope tag. I cotransfected pCMV-Insig-1-Myc, incubated the cells with or without sterols plus mevalonate, and added ALLN 4 h prior to harvest in order to prevent degradation of the HMGR membrane domain. The anti-myc antibody brought down the membrane domain of HMGR only in the presence of sterols (lane 6).

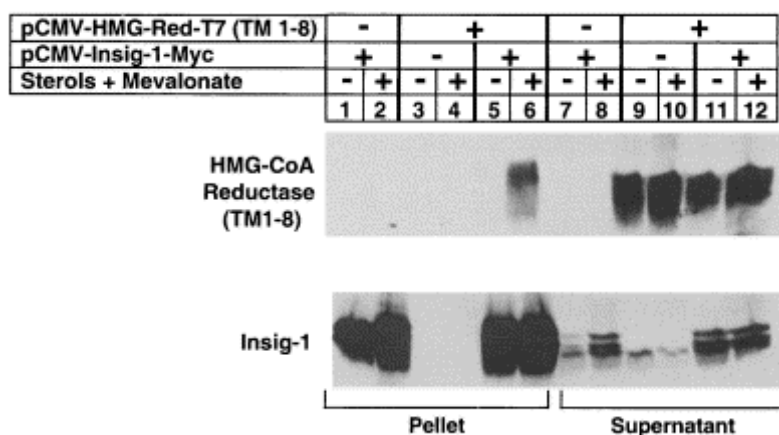


Figure 4-8. Insig-1 binds to the membrane domain of HMGR. On day 1, CHO-K1 cells were transfected in medium C with 1 μ g pCMV-HMG-Red-T7(TM1-8), and 10 ng pCMV-Insig-1-Myc. Six hours after transfection, cells were incubated for 16 h in medium B containing 50 μ M compactin, 50 μ M mevalonate, and sterols plus 10 mM mevalonate as indicated. Four hours prior to harvest, each dish received a direct addition of 3 μ l of ALLN to give a final concentration of 25 μ g/ml. Cells were harvested, lysed in Buffer D, and subjected to IP with polyclonal anti-Myc IgG as described in Experimental Procedures. Equal fractions of resuspended pellet (lanes 1-6) and acetone-precipitated supernatant (lanes 7-12) solutions were subjected to immunoblotting with anti-T7 IgG (against HMGR) and anti-Myc IgG (against Insig-1). Filters were exposed to film for 1-10 s.

Insig-Dependent Ubiquitination of HMGR

Ubiquitination of proteins is a multistep process, culminating in the covalent attachment of Ub to the ϵ -amino group of a lysine residue in the target protein. The topology of the ubiquitination machinery makes it likely that potential sites of ubiquitination are accessible to the cytosol. The membrane domain of HMGR is not only necessary, but sufficient for regulated degradation, and I have determined in transfection experiments that the membrane domain (aa 1-346 corresponding to TM1-8) of HMGR retains the ability to undergo Insig-dependent, sterol-regulated degradation (Gil et al., 1985; Skalnik et al., 1988; Figure 4-10A, lanes 1-4). As shown in Figure 4-9, aa 1-346 of HMGR contain only two lysines that are exposed to the cytosol (positions 89 and 248). To ascertain their participation in regulated degradation of HMGR, I changed the lysine codons at positions 89 and 248 to arginine in pCMV-HMG-Red-Myc(TM1-8) or pCMV-HMG-Red-Myc, expression plasmids encoding truncated or full-length HMGR with three or six tandem copies of the Myc epitope tag at the COOH terminus of the protein, respectively. In the experiments shown in Figures 4-10A and B, CHO cells were transfected with wild-type (lanes 1-4) or mutant versions (lanes 5-16) of HMGR in the absence or presence of Insig-1 and incubated with or without sterols plus mevalonate for 5 h (Figure 4-10A) or 16 h (Figure 4-10B). Mutating K89 to arginine had no effect on degradation (lanes 5-8). However, mutating K248 to arginine individually or in combination with the K89R mutation eliminated the regulated degradation of HMGR (lanes 11-12 and 15-16).

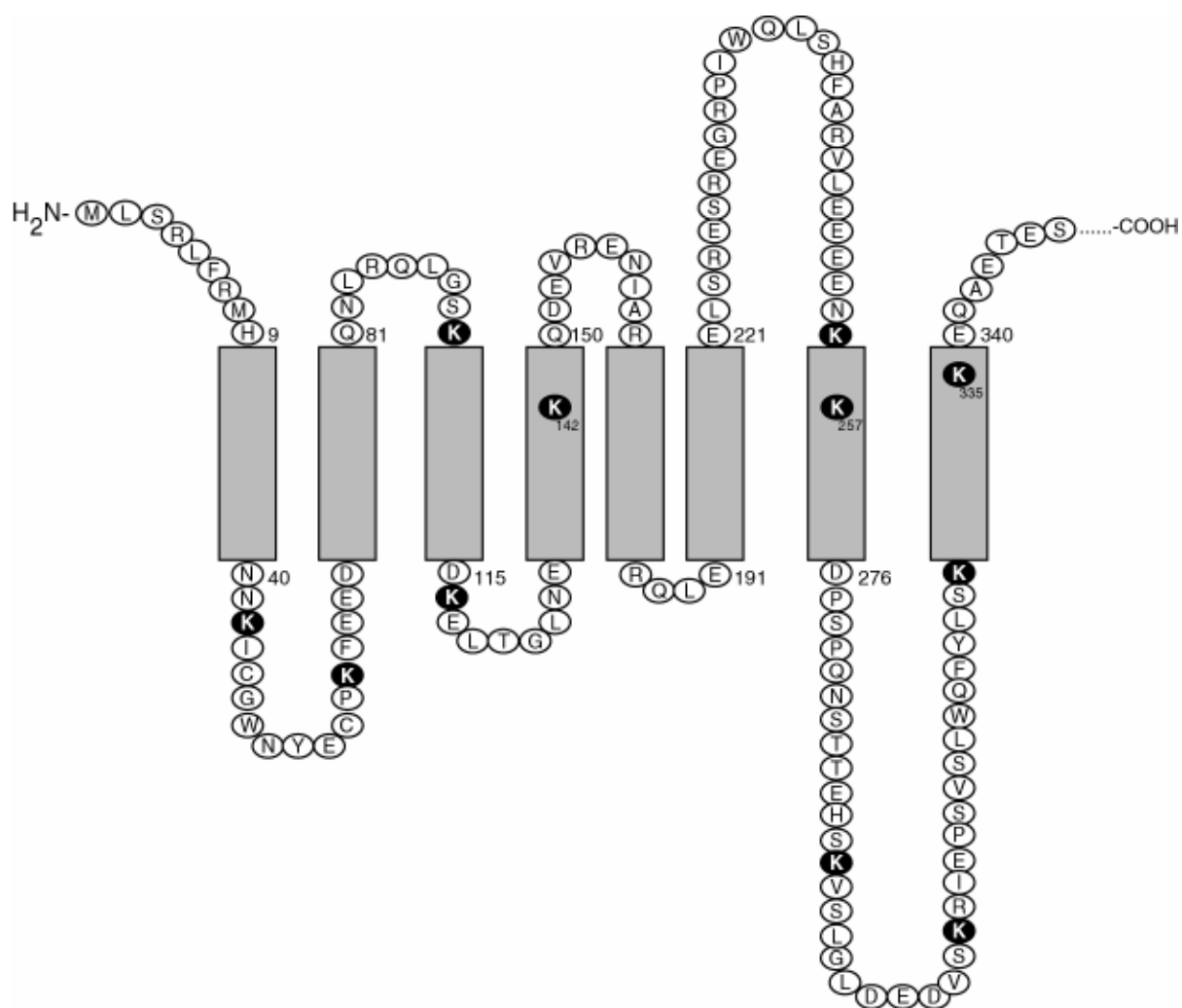
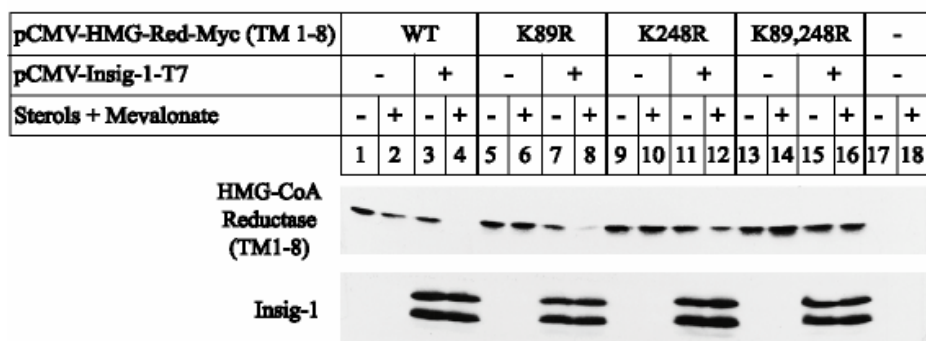


Figure 4-9. Topology of the membrane domain of hamster HMGR. Lysine residues are shown in black.

A.



B.

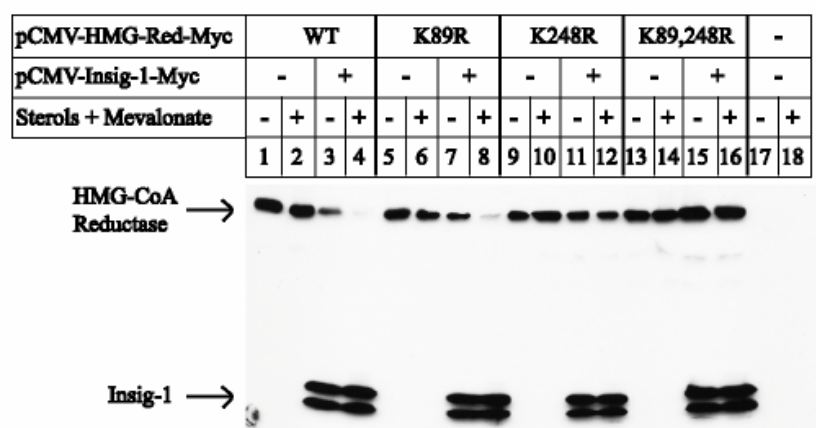


Figure 4-10. K248 is required for regulated degradation of HMGR. A. On day 1, CHO-K1 cells were transfected in 2 ml of medium B with 1 μ g of wild-type (lanes 1-4), K89R (lanes 5-8), K248R (lanes 9-12), or K89R/K248R (lanes 13-16) versions of pCMV-HMG-Red(TM1-8)-Myc in the absence or presence of 30 ng of pCMV-Insig-1-T7 as indicated. Six hours after transfection, cells received a direct addition of 2 ml of medium B containing 10 μ M compactin, and 50 μ M mevalonate (final concentrations). After 16 h at 37°C, cells were switched to medium B containing 50 μ M compactin in the absence (-) or presence (+) of sterols plus 10 mM mevalonate as indicated. After incubation for 5 h, cells were harvested, membrane fractions were prepared, and aliquots (36 μ g) were subjected to SDS-PAGE. Immunoblot analysis was carried out with anti-Myc IgG (against HMGR) and anti-T7 IgG (against Insig-1). Filters were exposed to film for 1-30s. B. On day 1, cells were transfected in medium C with 1 μ g of wild-type (lanes 1-4), K89R (lanes 5-8), K248R (lanes 9-12), or K89R/K248R (lanes 13-16) versions of pCMV-HMG-Red-Myc in the absence or presence of 100 ng of pCMV-Insig-1-Myc as indicated. Six hours after transfection, cells were switched to medium B containing 50 μ M compactin and 50 μ M mevalonate in the absence (-) or presence (+) of sterols plus 10 mM mevalonate as indicated. After incubation for 16 h, cells were harvested, membrane fractions were prepared, and aliquots (14 μ g) were subjected to SDS-PAGE. Immunoblot analysis was carried out with anti-Myc IgG. Filter was exposed to film for 30 s.

To test the effects of the lysine mutations on regulated ubiquitination, wild-type or mutant versions of pNS3 were transfected into cells with or without pCMV-Insig-1-Myc, and cells were incubated with or without sterols plus mevalonate for 16 h. To enhance sensitivity of Ub detection, cells were also transfected with pEF1a-HA-Ub, an expression plasmid encoding human Ub with an NH₂-terminal tag consisting of two copies of the HA epitope. After treatment for 4 h with MG-132, cells were harvested, transfected HMGR was immunoprecipitated from detergent lysates with anti-T7 agarose beads, and samples were subjected to SDS-PAGE. Immunoblot analysis with anti-HA revealed that ubiquitination of wild-type HMGR required MG-132 plus sterols and mevalonate (Figure 4-11, lanes 3-6). As expected, in the presence of Insig-1 sterols plus mevalonate led to an increase in the ubiquitination (lanes 7-10). However, mutating K248 to arginine eliminated the regulated ubiquitination of HMGR (lanes 11-14). Together, the results of Figures 4-10 and 4-

HA-Ub	-		+											
HMG-CoA Red	wt	-	wt								K248R			
INSIG1	+	+	-				+				+			
MG-132	+	+	-		+		-		+		-		+	
Sterols/Mevalonate	+	+	-	+	-	+	-	+	-	+	-	+	-	+
	1	2	3	4	5	6	7	8	9	10	11	12	13	14

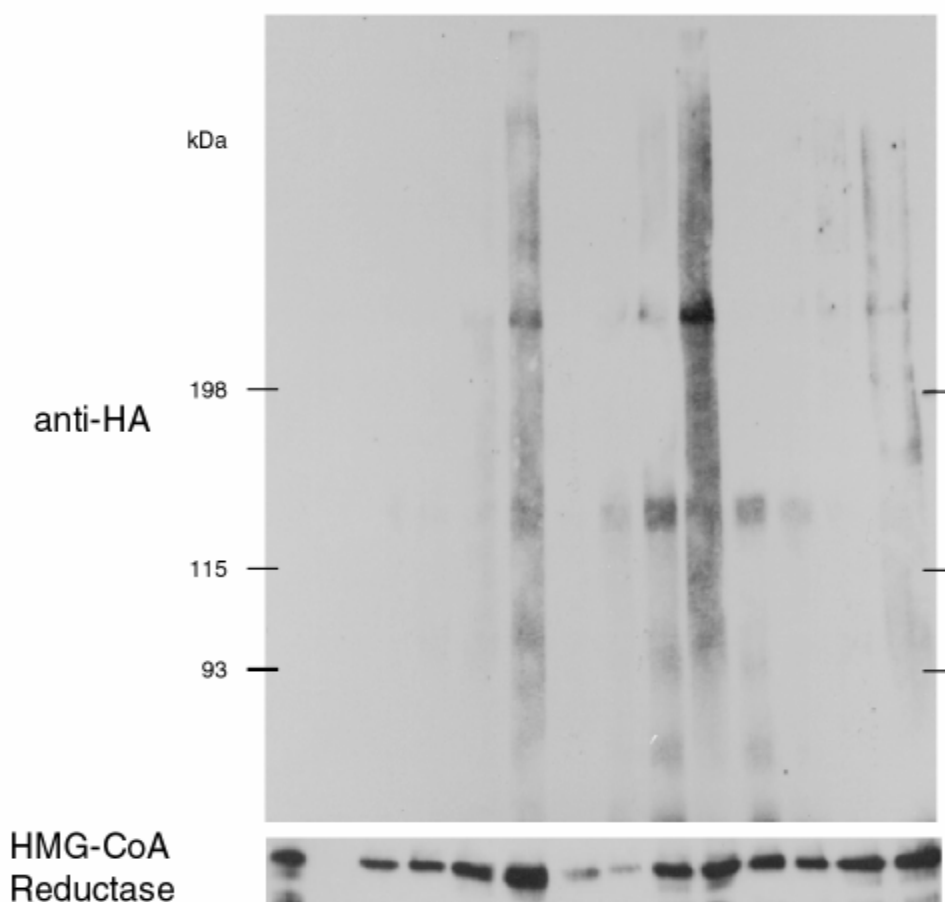


Figure 4-11. K248 is the primary site of ubiquitination. On day 1, CHO-K1 cells were transfected in medium C with 2 μ g of wild-type (lanes 1, 3-10), or K248R (lanes 11-14) versions of pNS3 and 0.5 μ g of pEF1a-HA-Ub (lanes 2-14) with or without 10 ng of pCMV-Insig-1-Myc as indicated. Six hours after transfection, cells were switched to medium B containing 50 μ M compactin, and 50 μ M mevalonate in the absence (-) or presence (+) of sterols plus 10 mM mevalonate as indicated. After 16 h, each dish received DMSO (lanes 3, 4, 7, 8, 11 and 12) or 10 μ M MG-132 (lanes 1, 2, 5, 6, 9, 10, 13 and 14). Following incubation for 4 h, cells were harvested, lysed, and subjected to IP with anti-T7 coupled agarose beads. Aliquots of IPs were subjected to SDS-PAGE and transferred to nylon membranes. Immunoblot analysis was carried out with anti-HA-IgG (against Ub) or anti-T7 IgG (against HMGR). Filters were exposed to film for 1-10 s.

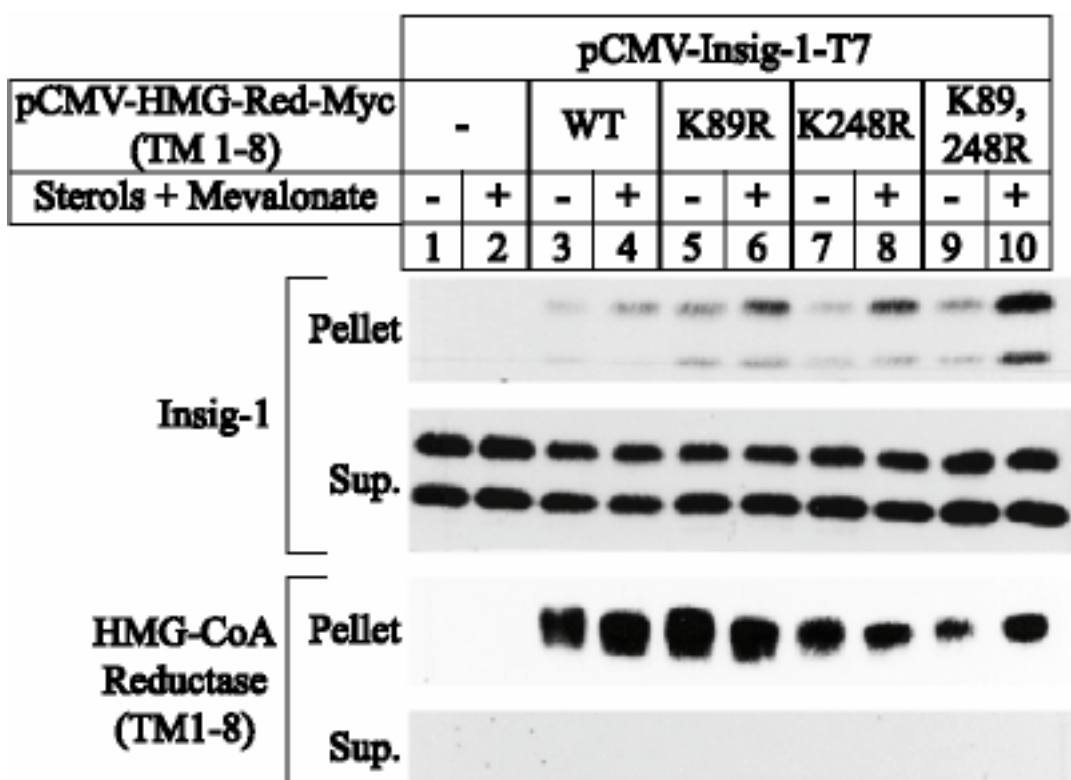


Figure 4-12. Lysine mutations preserve the binding of HMGR to Insig-1. On day 1, CHO-K1 cells were transfected in 2 ml of medium B with 30 ng of pCMV-Insig-1-T7 and/or 1 μ g of the wild-type or mutant version of pCMV-HMG-Red-Myc(TM1-8) as indicated. Six hours after transfection, cells received a direct addition of 2 ml of medium B to produce final concentrations of 10 μ M compactin, and 50 μ M mevalonate. After 16 h, cells were switched to medium B containing 50 μ M compactin, 10 μ M MG-132 in the absence (-) or presence (+) of sterols plus 10 mM mevalonate. After 5 h, cells were harvested, lysed, and subjected sequentially to IP, SDS-PAGE, and immunoblot analysis as in Figure 4-8. Filters were exposed to film for 10 s-3 min.

11 suggest that the cytosolically oriented K248 is the major site of Insig-dependent ubiquitination of HMGR. K89 may play some role when K248 is absent.

Although the data of Figure 4-11 indicate that HMGR is ubiquitinated and degraded in a sterol-dependent manner, the proportion of HMGR that was detectably polyubiquitinated at any one time was very small, even when degradation was blocked by MG-132. Thus, in the presence of MG-132 most of the HMGR that accumulated was not polyubiquitinated, as indicated by its continued migration on SDS-PAGE as a 97-kDa band (lower panel in Figure 4-11). I interpret these findings to indicate a balance between ubiquitination and de-ubiquitination reactions. According to this hypothesis, sterols stimulate the ubiquitination of HMGR. When proteasomal function is intact, most of the ubiquitinated HMGR is degraded. When proteasomal degradation is blocked, the amount of ubiquitinated HMGR at any instant reflects the equilibrium between ubiquitination and de-ubiquitination reactions. Similar conclusions have been reached by others in studies of the ubiquitination of other proteins (Mimnaugh et al., 1999).

Next, I tested whether the lysine mutations destroy the sterol-mediated interaction of HMGR and Insig-1. CHO-K1 cells were transfected with Insig-1 and wild-type or mutant versions of HMGR membrane domain and incubated with or without sterols plus mevalonate for 5 h in the presence of proteasome inhibitor. HMGR was efficiently immunoprecipitated with the anti-Myc antibody, as revealed by immunoblotting of the supernatant and pellet fractions (Figure 4-12, bottom two panels). Insig-1 was precipitated only when HMGR was transfected, and the efficiency was increased in the presence of sterols and mevalonate (lanes 1-4). None of the lysine mutations seemed to have any effect on the regulated interaction

between HMGR and Insig-1 (lanes 5-10). This result suggests that ubiquitination of HMGR is not required for binding to Insig; rather, Insig promotes the ubiquitination of HMGR in a sterol-dependent fashion.

The overexpressed SSD of SCAP blocks sterol-mediated degradation of HMGR, suggesting that the two proteins compete for the same site on Insig (Figure 4-6). Binding of SCAP to Insig is abolished upon the substitution of a cysteine for tyrosine 298 (Y298C mutant), which lies within one of the transmembrane helices in the SSD of SCAP (Yang et al., 2002; Yabe et al., 2002b). The Y298C mutant of SCAP fails to competitively inhibit sterol-mediated degradation of HMGR presumably because it fails to bind to Insig (Figure 4-6). Figure 4-13A shows an amino acid alignment between the second transmembrane helices of HMGR and SCAP. HMGR and SCAP share a tetrapeptide (YIYF) beginning at residue 75 of HMGR, which corresponds to the crucial Tyr-298 residue in SCAP. The Y75A mutant (corresponding to the Y298C mutant in SCAP) reduced only slightly the effect of sterols on degradation of HMGR (Sever et al., 2003). However, substitution of all four residues of the tetrapeptide (YIYF to AAAA) prevented sterols from exerting any effect on the degradation of HMGR (Sever et al., 2003).

The results in Figure 4-11 and Sever et al. (2003) show that K248 and the YIYF sequence are necessary for sterol-mediated HMGR ubiquitination. I utilized blue native-PAGE to test the hypothesis that mutations in the YIYF sequence of HMGR decrease the binding of protein to Insig-1, whereas substitution of K248 preserves binding but prevents ubiquitination. This technique was recently employed to identify sterol-induced complexes between Insig-1 and SCAP (Yang et al., 2002). To eliminate the potential competition

between SCAP and HMGR for Insig-1, I utilized SRD-13A cells, a CHO-derived mutant cell line that lacks SCAP (Rawson et al., 1999). In the experiment shown in Figure 4-13B, I transfected SRD13A cells with pCMV-Insig-1-Myc in the absence (lanes 1 and 2) or presence of wild-type or mutant versions of pCMV-HMG-Red-T7(TM1-8) (lanes 3-8). Following sterol depletion with hydroxypropyl- β -cyclodextrin, the cells were incubated in medium with or without sterols. The medium also contained MG-132 to prevent proteasomal degradation of the ubiquitinated HMGR membrane domain. After treatments, the cells were harvested, membranes were isolated and solubilized with digitonin. Soluble material was mixed with Coomassie Blue and 6-amino-n-hexanoic acid (to impart a negative charge and prevent precipitation of proteins) and subjected to PAGE. The fractionated proteins were transferred to membranes and blotted with various antibodies. In the absence of the HMGR membrane domain, Insig-1 appeared as a single band as revealed by immunoblotting with anti-Myc. Its migration was not altered upon sterol treatment (compare lanes 1 and 2 in the upper panel of Figure 4-13B). This band was designated as unbound Insig-1. When the cells expressed the wild-type HMGR membrane domain, some of the Insig-1 migrated more slowly (lane 3). This slower migrating band contained Insig-1 bound to the membrane domain of HMGR, as demonstrated by the fact that it was supershifted when the digitonin-solubilized material was incubated prior to PAGE with anti-T7 mAb, but not with a control antibody (compare lanes 8 and 12-14 in Figure 4-14). The anti-T7 mAb had no effect on the migration of unbound Insig-1 (Figure 4-14). Thus, we designated the slower migrating band as the HMGR-Insig complex. In the presence of sterols, unbound Insig-1 disappeared almost completely (Figure 4-13B, lane 4). The HMGR-Insig-1 complex was also diminished, but to

A

HMG-CoA Reductase 57 VLSSDIETITIRCHAILLYYYPQFQNLK 84
 SCAP 280 IGIAELPQVTEYILFPAVYSTRKID 307

B

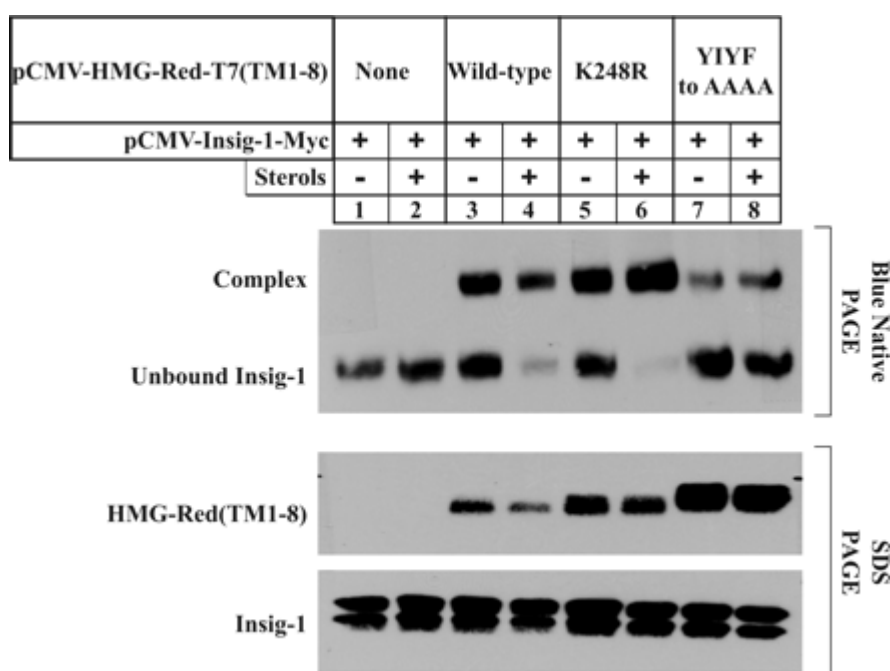


Figure 4-13. Sterols promote interaction of Insig-1 with wild-type HMGR, but not SSD mutant. A. Comparison of the amino acid sequence of the second transmembrane domain of HMGR with that of the comparable sterol-sensing region in SCAP. Sequences are from Chinese hamster HMGR (aa 57-84) and Chinese hamster SCAP (aa 280-307). GenBank accession numbers are L00165 and U67060, respectively. Identical amino acids are highlighted in black. Asterisk denotes the site of sterol-sensing mutation (Y298C) in SCAP. B. SRD-13A cells were set up for experiments as described in Chapter 3 and transfected in medium C with 60 ng of pCMV-Insig-1-Myc and/or 4 μ g of the wild-type or mutant version of pCMV-HMG-Red-T7(TM1-8) as indicated. Cells were treated with 10 μ M MG-132 in the absence or presence of sterols as indicated. After incubation for 2 h at 37°C, cells from 4 dishes were pooled. Filters were exposed to films for 30 s.

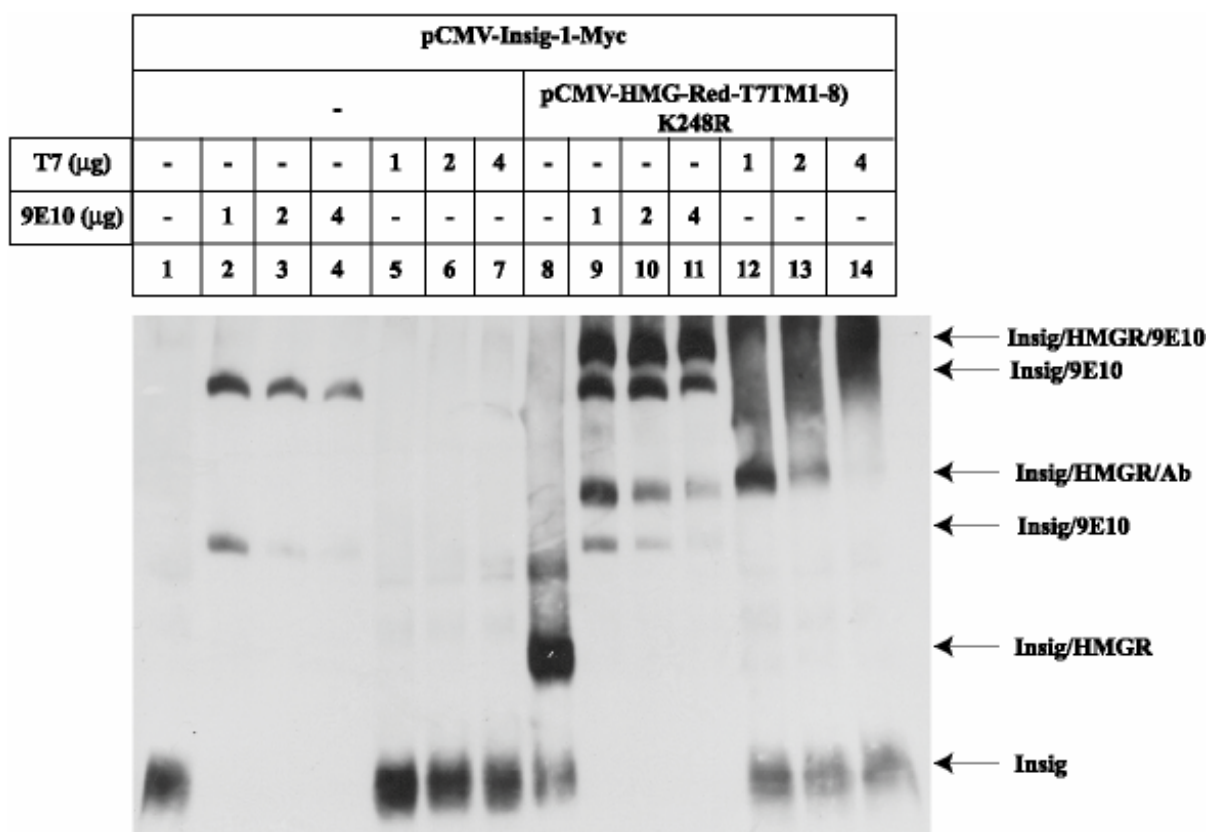


Figure 4-14. Formation of Insig-1/HMGR complex: detection by blue native-PAGE. SRD-13A cells were transfected in medium C with the indicated plasmids as described in Chapter 3: 4 μg of pCMV-HMG-Red-T7(TM1-8) K248R; and 60 ng of pCMV-Insig-1-Myc. After incubation for 2 h in the presence of sterols, cells from 3 dishes were pooled for measurement of HMGR/Insig-1 complex formation by BN-PAGE and immunoblot analysis as described in Chapter 3. Supershift assays were carried out with 4 μg control mouse monoclonal IgG-2001 (lanes 1 and 8) or the indicated amount of IgG-9E10 (lanes 2-4, 9-11) and IgG-T7 (lanes 5-7, 12-14). Filter was exposed to film for 10 s.

a lesser extent (lane 4). The decrease in the HMGR-Insig-1 complex is likely caused by incomplete inhibition of proteasomal activity, as revealed by immunoblotting of another aliquot of the same extract that was subjected to SDS-PAGE. This blot revealed a decrease in the total amount of the HMGR membrane fragment in the presence of sterols (SDS-PAGE, lower panel, lanes 3 and 4).

In cells that expressed the K248R mutant of HMGR, about half of the Insig-1 was found in the HMGR-Insig-1 complex in the absence of sterols (lane 5). Addition of sterols caused all of the Insig-1 to migrate as a complex with HMGR (lane 6), indicating that this mutation does not block the ability of sterols to enhance binding of the HMGR membrane fragment to Insig-1. Sterol addition caused only a slight decline in the total amount of the K248R HMGR membrane fragment (SDS-PAGE, lane 6), presumably because this mutant is resistant to ubiquitination and degradation. A very different result was obtained with the tetrapeptide mutant (YIYF to AAAA). In cells that expressed this mutant protein, the majority of Insig-1 was in the unbound state, and there was no increase in the complex when sterols were added (blue native-PAGE, lanes 7 and 8), nor was there a detectable decrease in the total amount of the HMGR membrane domain as revealed by SDS-PAGE (lanes 7 and 8).

To confirm the stoichiometric relationship between Insig-1 and HMGR, I performed titration experiments (Figure 4-15). SRD-13A cells were transfected with cDNAs encoding either a constant amount of HMGR K248R mutant and varying amounts of Insig-1, or a constant amount of Insig-1 and varying amounts of HMGR K248R. The cells were incubated in the absence and presence of sterols and harvested for the measurement of the amounts of bound and unbound HMGR and Insig-1. At low levels of Insig-1, the amount of unbound

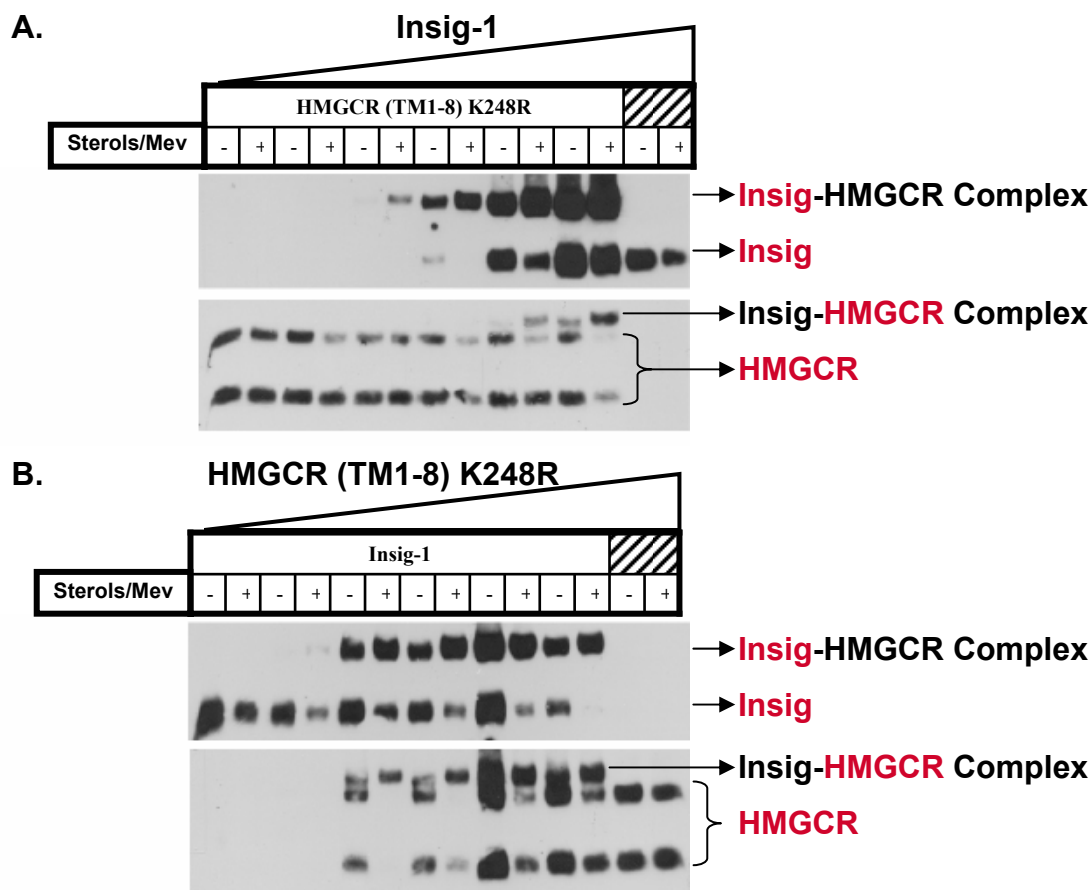


Figure 4-15. Stoichiometric relationship between Insig-1 and HMGR. SRD-13A cells were set up and transfected in medium B with (A) 4 μ g of pCMV-HMG-Red-T7(TM1-8) K248R and 1-60 ng of pCMV-Insig-1-Myc, or (B) 30 ng of pCMV-Insig-1-Myc and 0.1-4 μ g of pCMV-HMG-Red-T7(TM1-8) K248R as described in Chapter 3. After incubation for 2 h in the absence or presence of sterols and mevalonate, cells from 3 dishes were pooled. Filters were exposed to films for 1-5 min.

Insig-1 was markedly decreased by sterols as measured by BN-PAGE (A, top panel).

However, at higher Insig-1 concentrations, most of the Insig-1 remained unbound after sterol addition whereas the amount of HMGR that was found in the complex was dramatically increased (A, lanes 9-12). Conversely, at low levels of HMGR, most of the Insig-1 remained unbound after sterol addition whereas most of the HMGR was found in the complex (B, lanes 1-8). When Insig-1 is limiting, sterols cause all of the Insig-1 to bind to HMGR, leaving behind a pool of unbound HMGR (B, lanes 9-12). The slower migrating band of HMGR in the absence of Insig-1 is probably the dimeric form of HMGR, as demonstrated by the fact that HMGR runs as a single band on SDS-PAGE (see Figure 4-13 middle panel).

gp78 As A Candidate E3 Ubiquitin Ligase for HMGR

gp78 is an E3 ubiquitin ligase implicated in ERAD (Ponting et al., 2000; Fang et al., 2001). A dominant negative form of this protein extends the half-life of unassembled T cell receptor subunit CD3- δ presumably by interfering with the interaction of the wild-type counterpart with either the substrate or other components of the ubiquitination machinery, such as E2 (Fang et al., 2001). I tested whether a dominant-negative gp78 would block the Insig-mediated degradation of HMGR. As a control, I transfected HMGR alone or together with Insig-1 (Figure 4-16, lanes 1-4). HMGR was degraded by sterols and mevalonate only in the presence of Insig-1. Cotransfection of 0.1 μ g of wild-type gp78 had no effect on HMGR degradation whereas 1 μ g of wild-type gp78 led to disappearance of HMGR even in the absence of sterols or mevalonate (lanes 5-8). Interestingly, cotransfection of even 0.1 μ g of

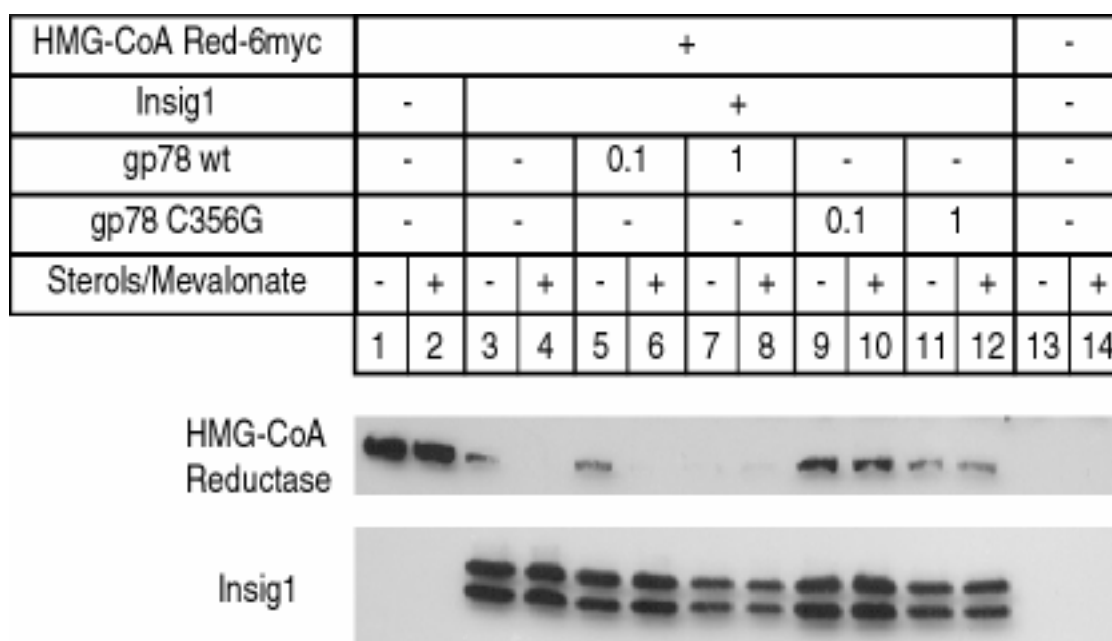


Figure 4-16. Dominant negative gp78 blocks Insig-mediated degradation of HMGR. On day 1, CHO-K1 cells were transfected in medium C with 1 μ g of pCMV-HMG-Red-Myc (lanes 1-12), 0.25 μ g of pCMV-Insig-1-Myc (lanes 3-12), and the indicated amounts of either wild-type (lanes 5-8) or C356G mutant versions (lanes 9-12) of pCIneo-gp78. Six hours after transfection, cells were switched to medium B containing 50 μ M compactin, 50 μ M mevalonate, and sterols plus 10 mM mevalonate as indicated. On day 2, cells were harvested, membrane fractions were prepared, and an aliquot (33 μ g) was subjected to immunoblot analysis with anti-Myc IgG. Filter was exposed to film for 3-60 s.

dominant-negative gp78 completely eliminated the effect of sterols and mevalonate (lanes 9-12). These results suggest the involvement of gp78 in the ubiquitination of HMGR but do not exclude the possibility that dominant-negative gp78 may saturate an E2 that is required for HMGR degradation. To rule out the latter possibility, I tested whether Myc-tagged gp78 directly interacts with HMGR. As shown in Figure 4-17, HMGR membrane domain was immunoprecipitated efficiently from the detergent extracts since all of HMGR was found in the pellet fraction. In the absence of gp78, Insig-1 caused HMGR degradation by sterols and mevalonate (lanes 1 and 2). This effect was abolished in the presence of wild-type or mutant versions of gp78, indicating that the fusion of Myc tag to the COOH-terminus of gp78 causes it to act in a dominant-negative fashion (lanes 3-6). Nevertheless, both forms of gp78 was found in the pellet fraction only in the presence of sterols and mevalonate. This was dependent on the transfection of HMGR (lanes 7 and 8). It remains to be seen whether endogenous HMGR and gp78 interact in the same way and whether this interaction requires the presence of the Insig proteins.

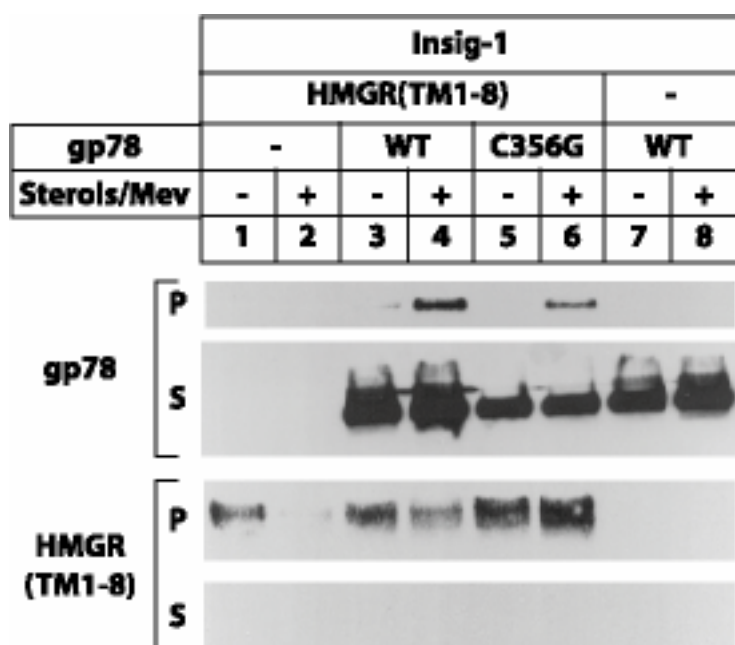


Figure 4-17. gp78 coimmunoprecipitates with HMGR. On day 1, CHO-K1 cells were transfected in 2 ml of medium B with 1 μ g of pCMV-HMG-Red-T7(TM1-8), 30 ng of pCMV-Insig-1-Myc, and 30 ng of either wild-type or C356G mutant versions of pCMV-gp78-Myc as indicated. Six hours after transfection, cells received a direct addition of 2 ml of medium B to give a final concentration of 10 μ M compactin and 50 μ M mevalonate. On day 2, cells were refed with medium B containing 50 μ M compactin in the absence (-) or presence (+) of sterols plus 10 mM mevalonate. After 5 h, cells were harvested, lysed and subjected to IP with anti-T7 coupled agarose beads as described in Chapter 3. Fractions of resuspended pellet and supernatant solutions were subjected to immunoblotting with anti-Myc IgG (against gp78) and anti-T7 IgG (against HMGR). Filters were exposed to film for 0.5-3 min.

**ISOLATION OF MUTANT CELLS THROUGH SELECTION WITH SR-12813, AN
AGENT THAT STIMULATES DEGRADATION OF HMGR**

SR-12813 As A Selecting Agent to Isolate Mutant Cells Incapable of Accelerating HMGR
Degradation

The hypocholesterolemic activity of 1,1-bisphosphonate esters such as SR-12813, and its structurally related analog, Apomine, has been well documented (Berkhout et al., 1996; 1997; Roitelman et al., 2004). In cultured cells, these drugs decrease HMGR activity by accelerating degradation of the enzyme which triggers an increase in the expression of LDL receptors, thus explaining the hypocholesterolemic activity of the drugs when administered orally to animals. The effects of SR-12813 on HMGR appear similar to those of oxysterols; however, unlike oxysterols, SR-12813 treatment does not reduce but rather enhances mRNAs for HMGR and the LDL receptor.

When overexpressed in CHO cells, I previously found that HMGR was no longer rapidly degraded in response to sterols (see Figure 4-4). Accelerated degradation of HMGR was restored by overexpressing Insig-1 or Insig-2, and by using this assay, amino acid residues in HMGR required for accelerated degradation of the enzyme were identified (see Figure 4-10 and Sever et al., 2003). Alanine substitution experiments revealed that binding of HMGR to Insigs and its subsequent ubiquitination and degradation required a tetrapeptide sequence, YIYF, in the HMGR SSD. The YIYF peptide also appears in the SSD of SCAP, where it mediates formation of the sterol-dependent SCAP-Insig complex (Yang et al., 2002;

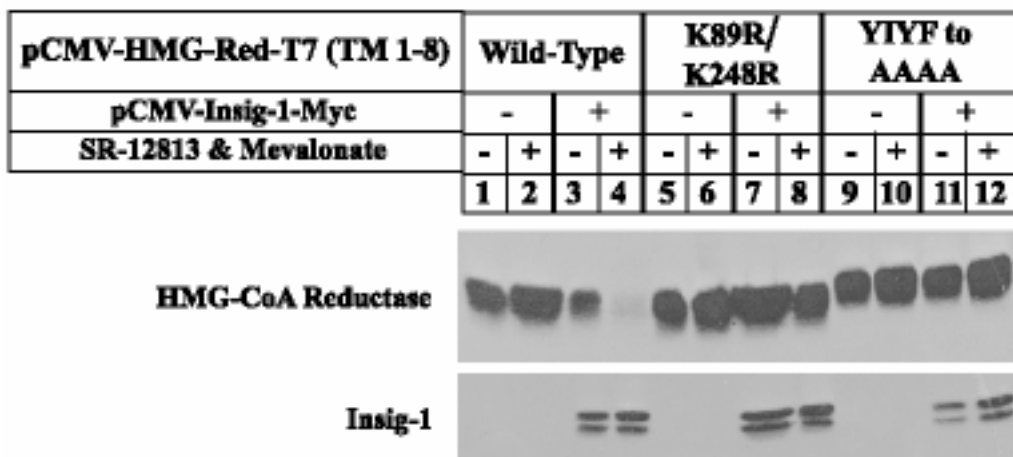


Figure 4-18. SR-12813 mimics sterols in promoting Insig-dependent degradation of wild type but not mutant forms of HMGR. CHO-7 cells were transfected on day 1 in 2 ml of medium B with 1 μ g of wild type (lanes 1-4), K89R/K248R (lanes 5-8), or ⁷⁵YIYF to AAAA (lanes 9-12) versions of pCMV-HMG-Red-T7(TM1-8) in the absence or presence of 30 ng of pCMV-Insig-1-Myc as indicated. Six hours after transfection, cells received a direct addition of 2 ml medium B containing 10 μ M compactin and 50 μ M mevalonate (final concentrations). After 16 h at 37°C, cells were switched to medium B containing 50 μ M compactin in the absence (-) or presence (+) of 10 μ M SR-12813 plus 10 mM mevalonate as indicated. After incubation for 5 h at 37°C, cells were harvested and membrane fractions prepared, and aliquots (5 μ g of protein/lane) were subjected sequentially to SDS-PAGE and immunoblot analysis with anti-T7 IgG (against HMGR) or anti-Myc IgG (against Insig-1). Filters were exposed to film for 1-10 s.

Yabe et al., 2002b). In contrast, the conservative substitution of arginine for lysines 89 and 248 of HMGR did not alter Insig binding, but HMGR was no longer ubiquitinated, and degradation was markedly slowed, implicating the lysine residues as sites for Insig-mediated, sterol-dependent ubiquitination. Thus, I next sought to determine the activity of SR-12813 toward degradation-resistant forms of HMGR (Figure 4-18). Given that the membrane domain of HMGR is not only necessary but sufficient for regulated degradation (Gil et al., 1985; Skalnik et al., 1988; see Figure 4-10A), I transfected CHO-7 cells with wild-type or mutant forms of pCMV-HMG-Red-T7(TM1-8), an expression plasmid encoding a truncated version of HMGR that contains the entire membrane domain (TM 1-8) but lacks the entire catalytic domain. The COOH terminus of this protein is composed of three tandem copies of the T7 epitope tag. Upon overexpression in CHO-7 cells, the wild type HMGR membrane domain was not subject to accelerated degradation with SR-12813 treatment (Figure 4-18, top panel, lanes 1 and 2). Likewise, both mutant forms of the HMGR membrane domain (K89R/K248R and ⁷⁵YIYF to AAAA) were not rapidly degraded when transfected alone (Figure 4-18, top panel, lanes 5, 6, 9, and 10). However, co-transfection of pCMV-Insig-1-Myc, an expression plasmid encoding full-length human Insig-1 followed by six tandem copies of the c-Myc epitope tag (Figure 4-18, bottom panel), resulted in SR-12813-dependent degradation of wild type but not mutant versions of the HMGR membrane domain (top panel, compare lanes 3 and 4 with 7, 8, 11, and 12). These results indicate that, much like the situation with sterols, SR-12813-dependent degradation of the HMGR membrane domain requires amino acids implicated in the covalent attachment of Ub (lysines 89 and 248) and binding of the HMGR to Insigs (the YIYF tetrapeptide). Additionally, the Insig requirement

for SR-12813-dependent degradation of the HMGR membrane domain is consistent with the Insig requirement for sterol-mediated degradation of HMGR.

I evaluated the utility of SR-12813 as a selecting agent in mutagenesis experiments aimed toward isolating mutant cells incapable of accelerating HMGR degradation. The experiment of Figure 4-19, which shows a series of stained Petri dishes, was designed to determine the effects of SR-12813 on the growth of CHO-7 cells. CHO-7 cells are a derivative of CHO-K1 cells that exhibit high rates of cholesterol synthesis because of their selection for growth in LPDS, a condition that renders cells dependent upon endogenous cholesterol synthesis for survival (Metherall et al., 1989). The growth of CHO-7 cells tolerated supplementation of LPDS-containing medium with as much as 3 μ M SR-12813

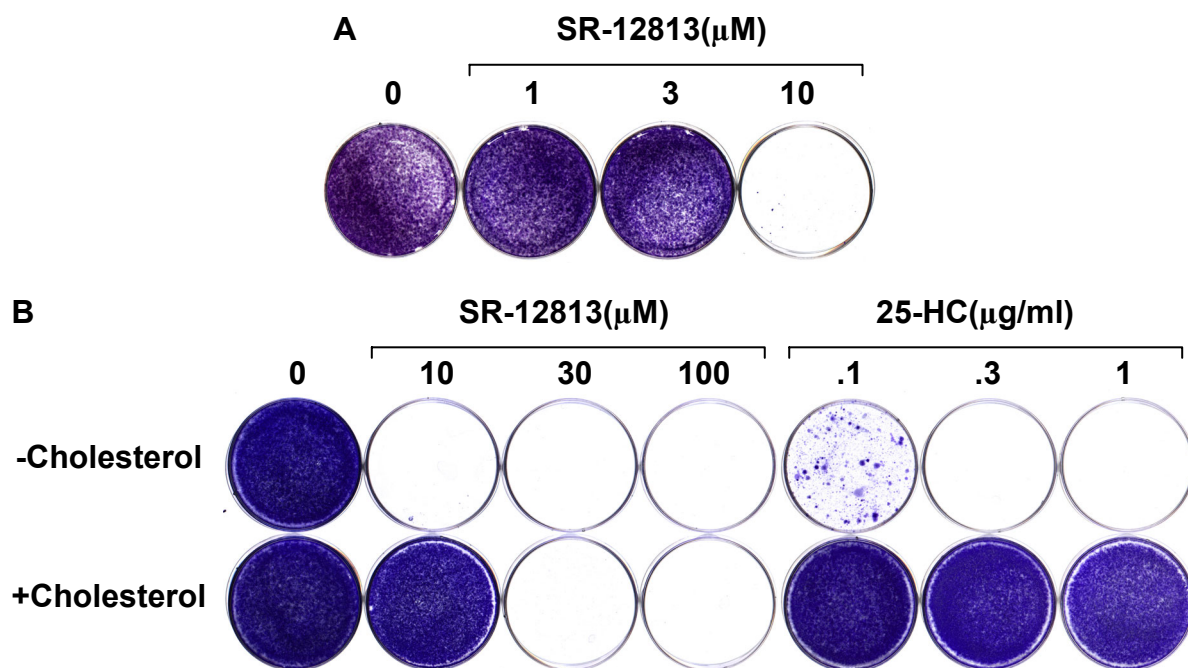


Figure 4-19. SR-12813 kills CHO-7 cells in LPDS. CHO-7 cells were set up on day 0 at 4×10^4 cells per 60-mm dish in medium B. On day 1, the cells were refed medium B supplemented with the indicated concentration of SR-12813 or 25-HC in the absence (-) or presence (+) of 5 μ g/ml cholesterol. Cells were refed every 2-3 days. On day 14, the cells were washed with PBS, fixed in 95% ethanol, and stained with crystal violet.

(Figure 4-19A). However, the cells failed to proliferate when challenged with 10 μ M SR-12813, and growth could be restored by the addition of cholesterol (5 μ g/ml) to the culture medium (Figure 4-19B). This indicates that toxicity of 10 μ M SR-12813 is attributable to its ability to accelerate degradation of HMGR, thereby inhibiting cholesterol synthesis, and ultimately leading to cell death as a result of cholesterol depletion. However, SR-12813 concentrations above 30 μ M exhibited nonspecific lethality as growth could not be restored by cholesterol. This is in contrast to 25-HC which has a wider window of specific lethality from 0.1 to 1 μ g/ml.

To demonstrate its toxic effects are due to accelerated degradation of HMGR, I assessed the ability of 10 μ M SR-12813 to kill cells expressing degradation-resistant forms of the enzyme. For this purpose, I transfected the HMGR-deficient UT-2 cells (Mosley et al., 1983) with wild type or mutant versions (K89R/K248R and ⁷⁵YIYF to AAAA) of pCMV-HMG-Red-T7, an expression plasmid encoding full-length HMGR followed by three tandem copies of the T7 epitope tag. Following transfection and selection of transformants, the cells were grown in LPDS-containing medium with or without SR-12813 supplementation. As shown in Figure 4-20, LPDS-containing medium failed to support growth of mock-transfected cells, due to the lack of HMGR activity in UT-2 cells. Growth of the cells in LPDS-containing medium was restored by the transfection of wild type and mutant forms of HMGR, but only those cells expressing the degradation-resistant forms of HMGR survived when challenged with SR-12813. Together, the results of Figures 4-19 and 4-20 demonstrate that SR-12813 efficiently kills CHO-7 cells as a result of the ability of the drug to promote HMGR degradation, which leads to the toxic depletion of cholesterol. Most importantly,

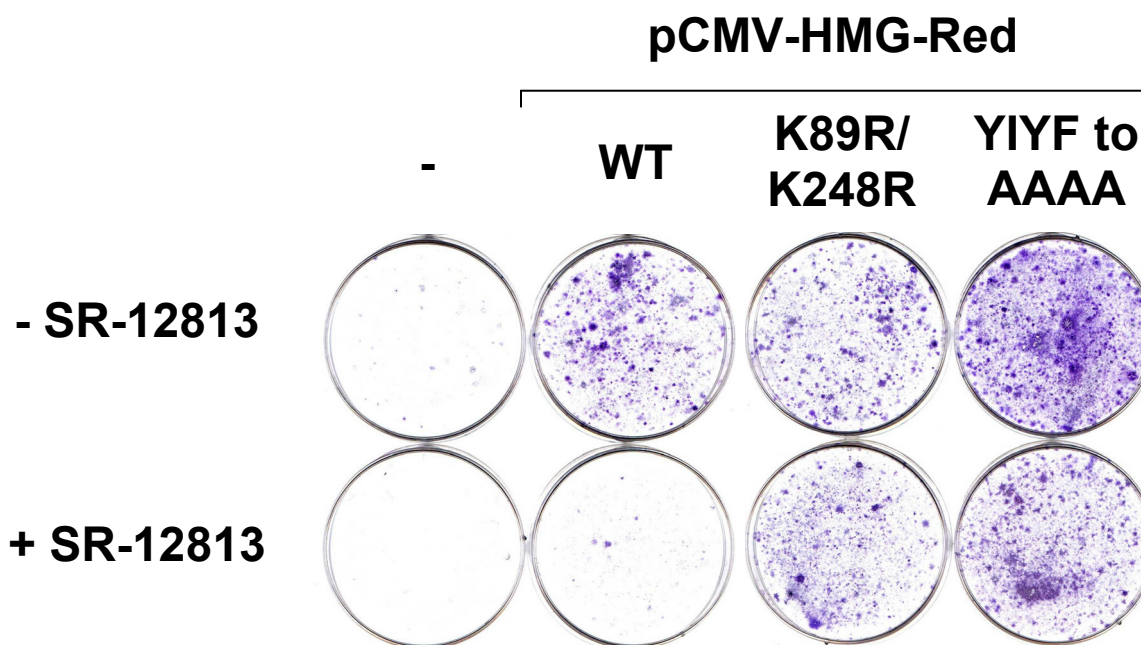


Figure 4-20. SR-12813-mediated killing of CHO cells is prevented by the expression of degradation-resistant forms of HMGR. On day 0, UT-2 cells were set up at 5×10^5 cells per 60-mm dish in medium D. On day 1, the cells were transfected with 1 μ g of pcDNA3 (mock-transfected), wild type (WT), K89R/K248R, or ⁷⁵YIYF to AAAA versions of pCMV-HMG-Red-T7. All of the plasmids contained the G418 resistance gene neo. On day 2, the cells were switched to medium E and refed every 2-3 days. On day 14, cells were switched to medium F in the absence or presence of 10 μ M SR-12813 and refed every 2-3 days. On day 24, the dishes were washed, fixed in 95% ethanol, and stained with crystal violet.

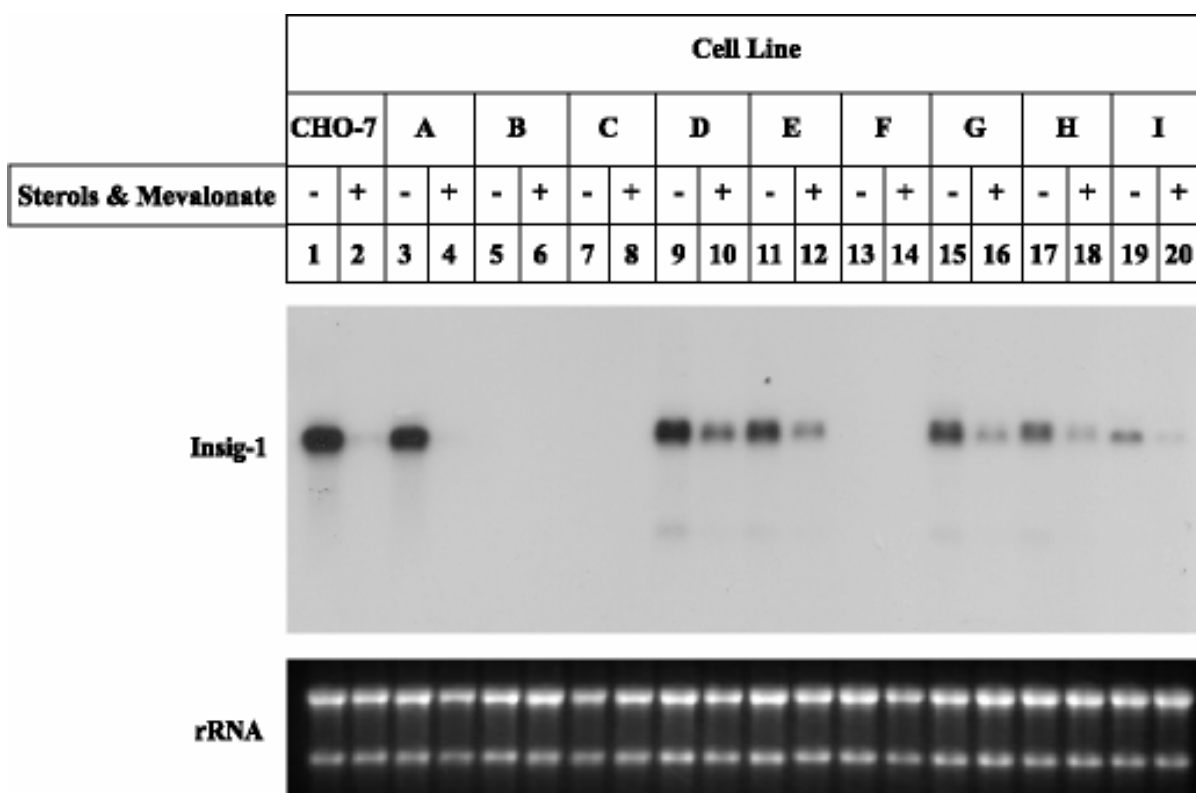


Figure 4-21. Molecular characterization of Insig-1 mRNA in parental CHO and mutant cells. Cells were set up on day 0 at 5×10^5 cells per 100-mm dish in medium B. On day 2, the cells were refed medium B supplemented with 10 μ M compactin, and 50 μ M mevalonate. After 16 h at 37°C, cells were switched to medium B containing 50 μ M compactin in the absence (-) or presence (+) of sterols and mevalonate as indicated. Following incubation at 37°C for 5 h, the cells were harvested, and total RNA was isolated as described in Chapter 3. Aliquots of total RNA (20 μ g/lane) were subjected to electrophoresis in a denaturing (formaldehyde) gel and transferred to a nylon filter by capillary blotting. The filter was hybridized with a 796-bp 32 P-labeled probe encoding the open reading frame (ORF) of Insig-1 as described in Chapter 3. The filter was exposed to film at -80°C for 16 h.

these results support my objective of isolating mutant cells that can survive chronic SR-12813 treatment because of their inability to stimulate degradation of HMGR.

Insig-1 Mutants

Approximately 2.5×10^7 CHO-7 cells were mutagenized with γ -irradiation and subjected to selection in 10 μ M SR-12813. I next conducted a series of experiments designed to assess the nature of the genetic defect that leads to the SR-12813-resistance. Figure 4-21 shows a Northern blot, comparing the amounts of Insig-1 mRNA in CHO-7 and the mutant cells. Insig-1 mRNA was present in the parental cells when they were incubated in the absence of sterols (Figure 4-21, lane 1), and it declined when the cells were treated with sterols (lane 2), a result of the sterol-dependent suppression of nuclear SREBP-2. One cell line exhibited the same pattern as the parental cell line (lanes 3 and 4). In contrast, Insig-1 mRNA failed to be detected in 8 of the colonies (lanes 5-8, 13, and 14 and data not shown). In four cell lines, Insig-1 transcripts persisted in the presence of sterols (lanes 9-12, 15-18) and reverse transcriptase-PCR (RT-PCR) of Insig-1 produced a doublet (data not shown), at least one of which must be derived from an aberrant transcript. One cell line had ~20% of normal amount of Insig-1 mRNA and was not characterized further (lanes 19 and 20).

The persistence of Insig-1 mRNA in the presence of sterols in cells expressing aberrant Insig-1 indicates that in these cells SREBP processing is refractory to suppression. I tested this hypothesis directly by comparing the effects of sterols and SR-12813 on HMGR degradation and SREBP-2 processing in CHO-7 cells and the Insig-1 mutants B and D

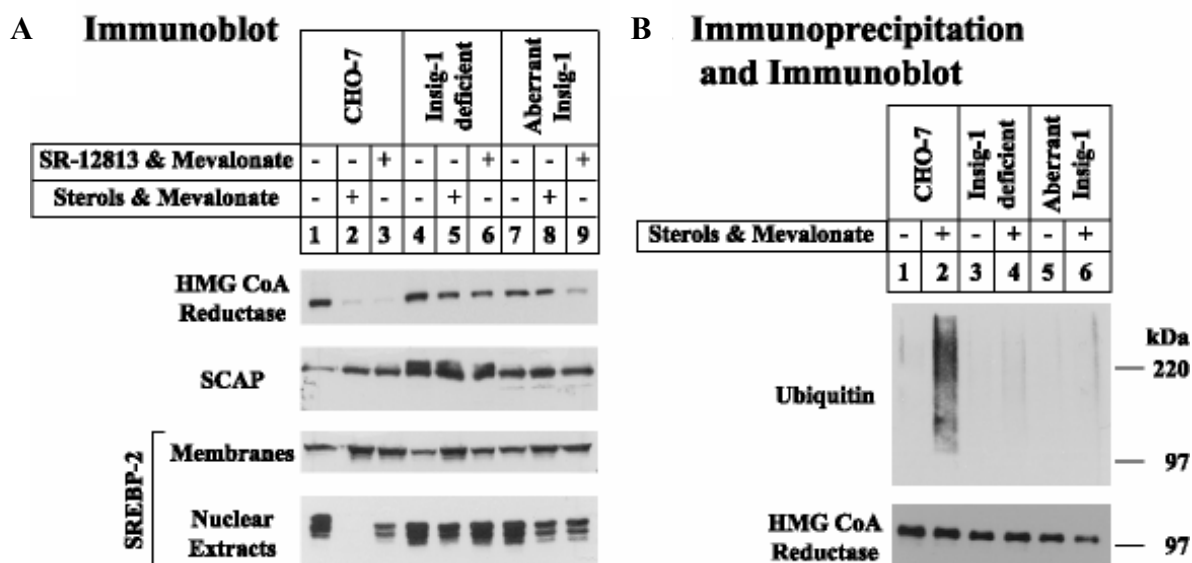


(Figure 4-22). As shown in Figure 4-22A, sterols and SR-12813 promoted the rapid degradation of HMGR in parental CHO-7 cells (top panel, lanes 2 and 3), whereas the disappearance of nuclear SREBP-2 was only observed upon sterol treatment (bottom panel, lane 2). However, both SR-12813 and sterols failed to promote degradation of HMGR, and sterols did not suppress nuclear SREBP-2 in the mutant cells (Figure 4-22A, top and bottom panels, lanes 4-9). SCAP appeared to be produced at approximately equivalent levels in the CHO-7 and Insig-1 mutant cells (Figure 4-22A, 2nd panel, lanes 1-9). Consistent with their inability to promote HMGR degradation in the mutant cells, sterols also failed to promote ubiquitination of HMGR to appreciable levels (Figure 4-22B, compare lanes 1 and 2 with 3-6). Thus, the inability of mutant cells to carry out HMGR ubiquitination and degradation explains their resistance to the growth inhibitory effects of SR-12813.

Point Mutation in Intron 3 of Insig-1

To determine whether the aberrant Insig-1 mRNA in four of the mutant cell lines (D, E, G, and H in Figure 4-21) could encode functional Insig-1 protein, I amplified the mRNA by RT-PCR, inserted the amplified fragments into a cloning vector, and sequenced 29 independent clones. 19 of the clones showed a 45-bp insertion that disrupted the reading frame at codon 215, leading to premature termination (Figure 4-23, transcript 1). 8 of the clones showed a 9-bp insertion replacing exon 3 that disrupted the reading frame at codon 162, leading to an altered sequence of amino acids that terminates at position 203 (Figure 4-23, transcript 2). If these truncated proteins were produced, they would contain only 5 or 3 of the eight membrane-spanning helices, respectively (Figure 4-23). Two other clones showed different

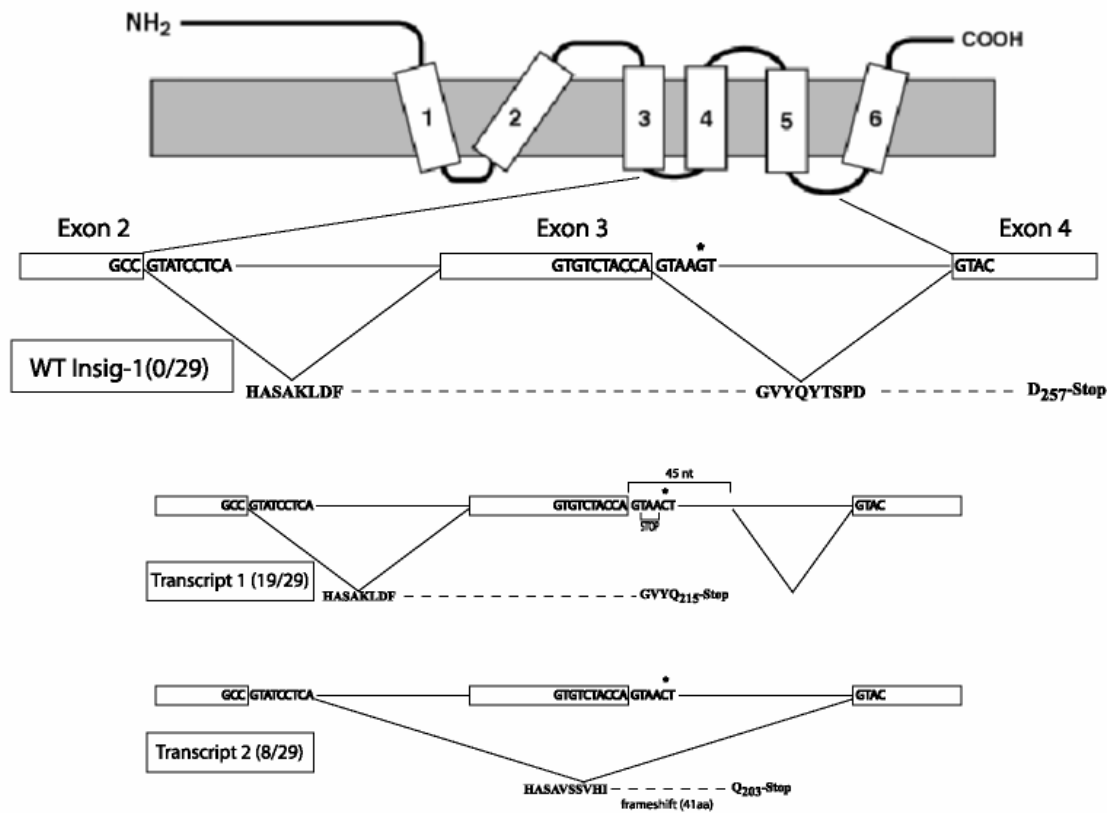


Figure 4-23. Sequence of mutant Insig-1 transcripts. The upper diagram shows a model of the membrane topology of Insig-1 (Feramisco et al., 2004). Below the model are the nucleotide and deduced amino acid sequences of the wild-type Insig-1 transcript and the mutant Insig-1 transcripts. The mutation resulting from the G to C change in intron 3 (denoted by an asterisk) disrupts the splice donor site in the mutant DNA (Patel and Steitz, 2003), which yields transcripts spliced alternatively.

deletions (not shown), all of which seemingly arising from the use of an alternative splice donor site instead of the normal site at intron 3. Such proteins could not be functional (Peter Lee and N.S., unpublished observations).

To determine the cause of the mutations in the *Insig-1* mRNA, I subjected the relevant region of genomic DNA to PCR, and I sequenced 16 clones derived from wild-type and mutant cells. All of the mutant sequences had a single point mutation that changed a G to a C. This disrupts the normal splice donor site of intron 3 (Figure 4-23). Apparently, new consensus splice donor sites are used, because all of the cellular mRNA excludes the 3'-half of intron 3. Intron 2 is a minor class intron, whose splice sites are not compatible with the major class intron 3, explaining the use of cryptic splice donor sites inside introns 2 and 3 instead of the normal site of intron 2 (not shown).

The fact that all of the genomic clones had the same point mutation suggests that the mutant cells are either homozygous for the point mutation shown in Figure 4-23, or else they have a deletion in the second copy of the gene that removes at least this region. Further, this mutation is probably preexisting since it was obtained from four independent cell lines.

Mutant Cells Lacking Insig-1

To determine whether the absence of *Insig-1* mRNA in cell line B, designated SRD-14 (sterol regulatory defective-14) cells, is due to a gross chromosomal deletion or rearrangement of the *INSIG-1* gene, I performed Southern blots with genomic DNA isolated from CHO-7 and SRD-14 cells (Figure 4-24A). *EcoRI* and *KpnI* digestions produced hybridizable fragments that had an identical size for CHO-7 and SRD-14 cells (Figure 4-

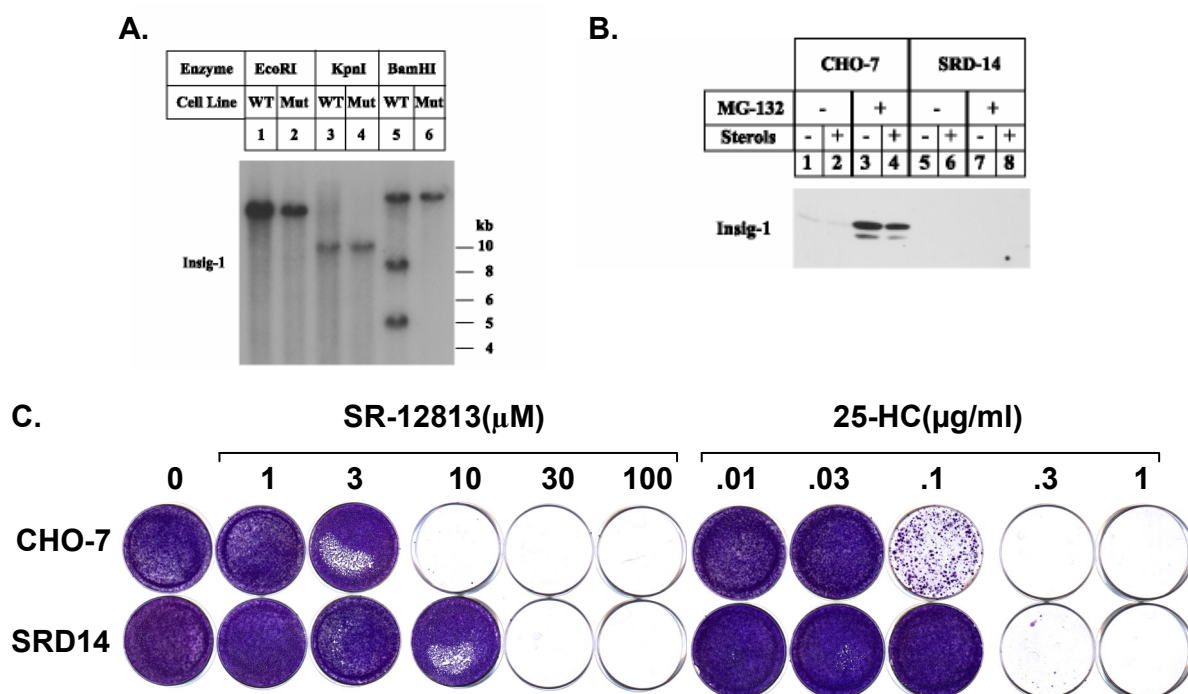


Figure 4-24. A. Southern blot of Insig-1 genomic DNA from parental CHO and mutant SRD-14 cells. Aliquots of genomic DNA (20 μ g/lane) were digested with the indicated restriction enzyme, subjected to electrophoresis on a 0.6% agarose gel, transferred to filters, and hybridized with a 796-bp 32 P-labeled probe encoding the ORF of Insig-1 as described in Chapter 3. The filter was exposed to film at -80°C for 16 h. B. Immunoblot analysis. CHO-7 and SRD-14 cells were set up and refed as in Figure 4-21. After 16 h at 37°C , cells were switched to medium B containing 50 μM compactin in the absence (-) or presence (+) of sterols and 10 μM MG-132 as indicated. After incubation at 37°C for 5 h, the cells were harvested, subjected to cell fractionation, and aliquots of the membrane fraction (30 μg of protein/lane) were subjected to SDS-PAGE, and immunoblot analysis was carried out with polyclonal anti-Insig-1. The filter was exposed to film for 30 s at room temperature. C. Comparison of growth. CHO-7 and SRD-14 cells were set up as in Figure 4-19. On day 1, the cells were refed medium B supplemented with the indicated concentration of SR-12813 or 25-HC. Cells were refed every 2-3 days. On day 14, the cells were washed, fixed in 95% ethanol, and stained with crystal violet.

24A, lanes 1-4). In contrast, the BamHI-digested SRD-14 cell DNA failed to produce the 8- and 5-kb hybridizable bands present in the corresponding digest of DNA from CHO-7 cells (Figure 4-24A, lanes 5 and 6). These results indicate that the absence of detectable Insig-1 mRNA in SRD-14 cells is caused by the partial deletion of the *INSIG-1* gene.

Membranes from CHO-7 and SRD-14 cells were isolated and subjected to immunoblot analysis with polyclonal anti-Insig-1 antibodies (Figure 4-24B). To ensure maximal expression of Insig-1, which is a target gene of SREBP-2 (Yang et al., 2002; Yabe et al., 2002a), the cells were incubated in sterol-depleting medium for 16 h and treated for an additional 5 h in the absence or presence of sterols prior to harvesting. Some of the dishes of cells also received MG-132 to inhibit the activity of proteasomes. In the absence of MG-132, Insig-1 was barely detectable in the anti-Insig-1 immunoblots, regardless of the absence or presence of sterols (Figure 4-24B, lanes 1 and 2). However, treatment of the cells with MG-132 led to the appearance of two bands at 28 and 25 kDa (Figure 4-24B, lanes 3 and 4), which likely results from the use of two start sites for translation, as has been reported for the human Insig-1 protein (Yang et al., 2002). The stabilization of Insig-1 by MG-132 indicates that the protein is rapidly degraded by proteasomes. In contrast to those from CHO-7 cells, membranes from the SRD-14 cells lacked detectable Insig-1 when incubated in the absence or presence of sterols and/or MG-132 (Figure 4-24B, lanes 5-8).

The growth assay in Figure 4-24C shows that SRD-14 cells were resistant to growth in 10 μ M SR-12813 and up to 0.1 μ g/ml 25-HC. In contrast, the parental CHO-7 cells were effectively killed by 10 μ M SR-12813, and their growth exhibited a greater sensitivity (about 3-fold) to 25-HC than that of SRD-14 cells. In mutant cell lines identified previously, the

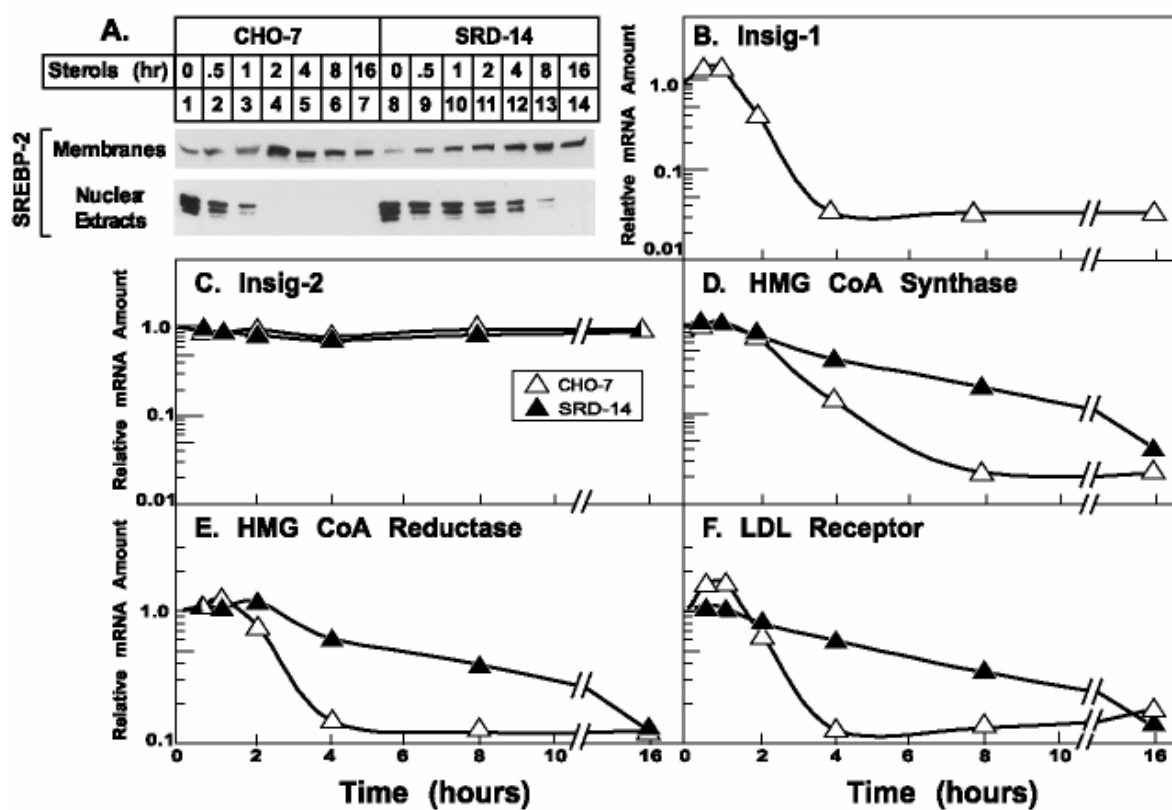


Figure 4-25. Kinetics of sterol-mediated suppression of nuclear SREBP-2 and SREBP-target gene expression in parental CHO and mutant SRD-14 cells. CHO-7 and SRD-14 cells were set up as in Figure 4-21. On day 2, the cells were refed medium B supplemented with 50 μ M compactin and 50 μ M mevalonate. Some of the cells were refed the same media supplemented with sterols for the indicated times. Sterols were added in a staggered fashion, such that all of the cells could be harvested together. A. After incubation, the cells were harvested and subjected to cell fractionation, and aliquots of the membrane (34 μ g of protein/lane) and nuclear extract (13 μ g of protein/lane) fractions were subjected to SDS-PAGE. Immunoblot analysis was subsequently carried out as described in the legend to 4-22. Filters were exposed to film for 1 s (top gel) and 1 min (bottom gel). B-F. Following incubations, the cells were harvested, and total RNA was isolated and subjected to reverse transcription as described in Chapter 3. Aliquots of reverse-transcribed total RNA were then subjected to real time PCR analysis using primers specific for the indicated SREBP-2 target gene. Each value for cells incubated with sterols for the indicated time represents the amount of target gene expression relative to that in control cells harvested at time 0. The values for Insig-2 mRNA in the cells represent its expression relative to that in wild type cells harvested at time 0.

persistence of nuclear SREBP-2 upon 25-HC treatment was indicative of the ability of the cells to survive chronic treatment with the oxysterol (Yang et al., 1994; 1995; Hua et al., 1996; Yabe et al., 2002b; Dawson et al., 1991). However, I observed that despite their resistance to sterol-mediated suppression of nuclear SREBP-2 (Figure 4-22A), SRD-14 cells were only partially resistant to growth in 25-HC (Figure 4-24C). Considering that, in Figure 4-22A, the extent to which sterols influenced SREBP-2 processing was assessed after treating cells for 5 h, I designed an experiment to compare the kinetics of sterol-dependent suppression of SREBP-2 processing in CHO-7 and SRD-14 cells (Figure 4-25A). In the wild type cells, I noticed that sterols suppressed nuclear SREBP-2 in 2 h (Figure 4-25A, bottom panel, lane 4), whereas sterol treatments for 8-16 h were required to block SREBP-2 processing in SRD-14 cells (bottom panel, lanes 13 and 14). In parallel experiments, I measured the amounts of mRNAs encoding Insig-1, Insig-2, and three SREBP-2 target genes, HMG CoA synthase, HMGR, and the LDL receptor, by quantitative real time PCR analysis; and the results are presented graphically in Figure 4-25B-F. The mRNAs encoding SREBP-2 target genes in CHO-7 cells declined with sterol treatment at rates that mirrored those of nuclear SREBP-2 suppression, and again, I found the sterol response of the SRD-14 cells was markedly delayed. As expected, Insig-1 mRNA was not detected in the mutant cells and exhibited a similar response to sterols as the other SREBP-2 target genes in wild type cells (Figure 4-25B). Insig-2 mRNA was present at similar levels in CHO-7 and SRD-14 cells and remained constant throughout the time course in both cell lines (Figure 4-25C).

To exclude the possibility that the rapid decline of nuclear SREBP-2 in wild type cells resulted from the use of high levels (1 μ g/ml) of 25-HC in the experiments of Figure 4-

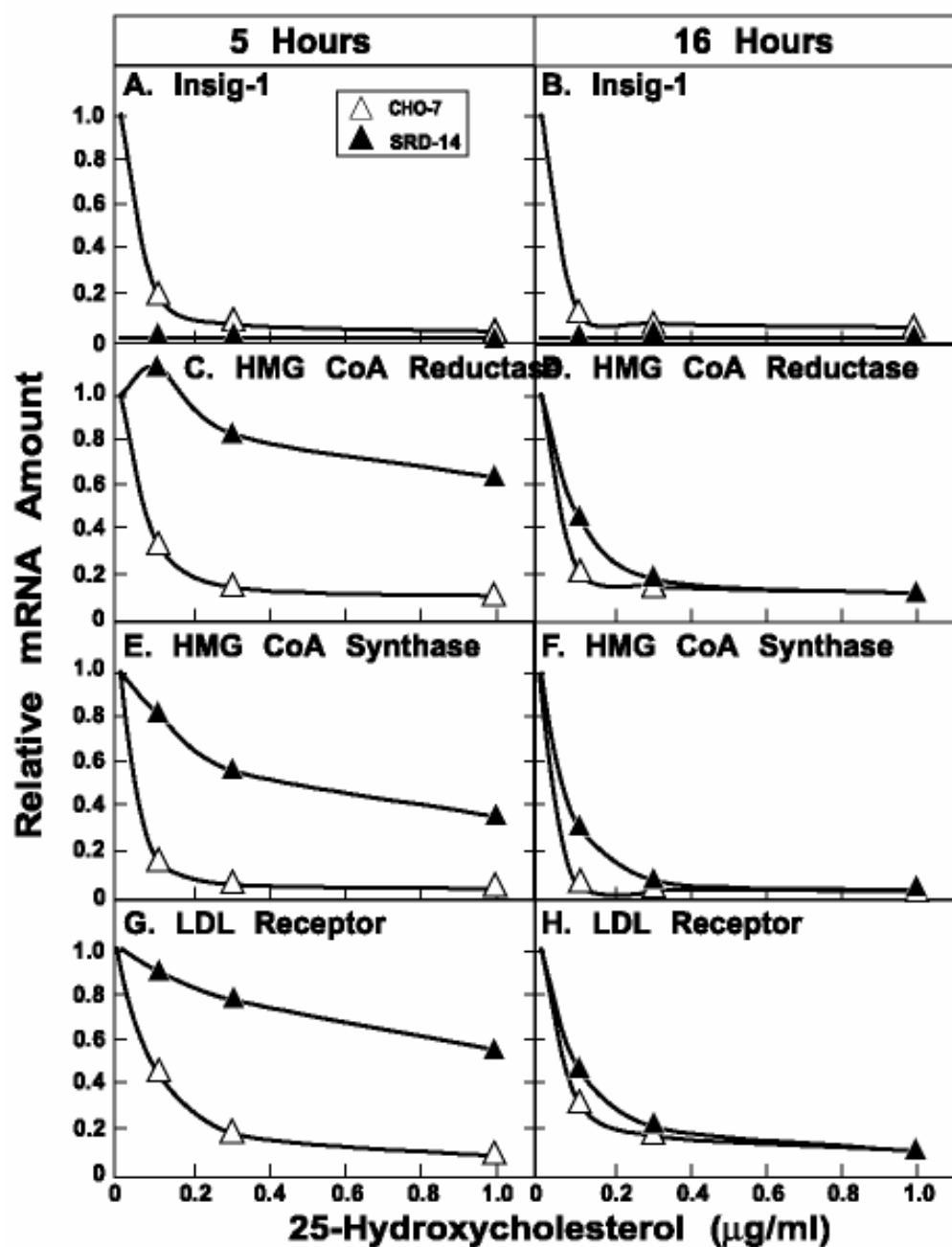


Figure 4-26. Dose-dependent effects of 25-HC on nuclear SREBP-2 and SREBP-target gene expression after 5 h and 16 h in parental CHO and mutant SRD-14 cells. CHO-7 and SRD-14 cells were set up as in Figure 4-21. On day 2, the cells were refed medium B supplemented with 50 μ M compactin and 50 μ M mevalonate. Some of the cells were refed the same media supplemented with the indicated concentrations of 25-HC and 10 μ g/ml cholesterol. Sterols were added in a staggered fashion, such that all of the cells could be harvested together after incubations for 5 or 16 h at 37°C. (*Upper panel*) After incubation, cells were harvested and subjected to cell fractionation, and aliquots of the membrane (50 μ g of protein/lane) and nuclear extract (32 μ g of protein/lane) fractions were subjected to SDS-PAGE. Immunoblot analysis was subsequently carried out as described in the legend to Figure 4-22. Filters were exposed to film for <1 (top gel) and 10 s (bottom gel). A-H. Following the incubations, the cells were harvested, and total RNA was isolated and subjected to reverse transcription as described in Chapter 3. Aliquots of reverse-transcribed total RNA were then subjected to real time PCR analysis using primers specific for the indicated SREBP-2 target gene. Each value for cells treated with 25-HC represents the amount of target gene expression relative to that in untreated control cells harvested at time 0. The values for Insig-1 mRNA in the cells represent its expression relative to that in wild type cells harvested at time 0.

25, I next performed a 25-HC dose-curve experiment at 5 and 16 h (Figure 4-26). In the nuclei of CHO-7 cells, 25-HC evoked a dose-dependent decrease in processed SREBP-2 after 5 h of treatment (Figure 4-26, bottom panel, lanes 1-4), and this sterol effect was more pronounced after 16-h treatments (bottom panel, compare lanes 1-4 with lanes 5-7). A similar response was observed for mRNAs encoding each SREBP-2 target gene (Figure 4-26A-H). A minimal reduction of nuclear SREBP-2 was found in SRD-14 cells treated with 0.3 μ g/ml 25-HC at the 5-h time point (Figure 4-26, lane 11). However, treatment of the mutant cells for 16 h with 0.1 μ g/ml 25-HC led to partial suppression of SREBP-2 processing (Figure 4-26, lane 13), and complete suppression was observed in those cells treated with 0.3 μ g/ml of the sterol (lane 14). After 5 h, target gene expression in the SRD-14 cells was somewhat more resistant to 25-HC than were their parental CHO-7 cells (Figure 4-26A, C, E, and G), yet following 16 h of treatment, target gene expression in both cell lines responded similarly to the oxysterol (Figure 4-26B, D, F, and H). Considered together, the results of Figures 4-25

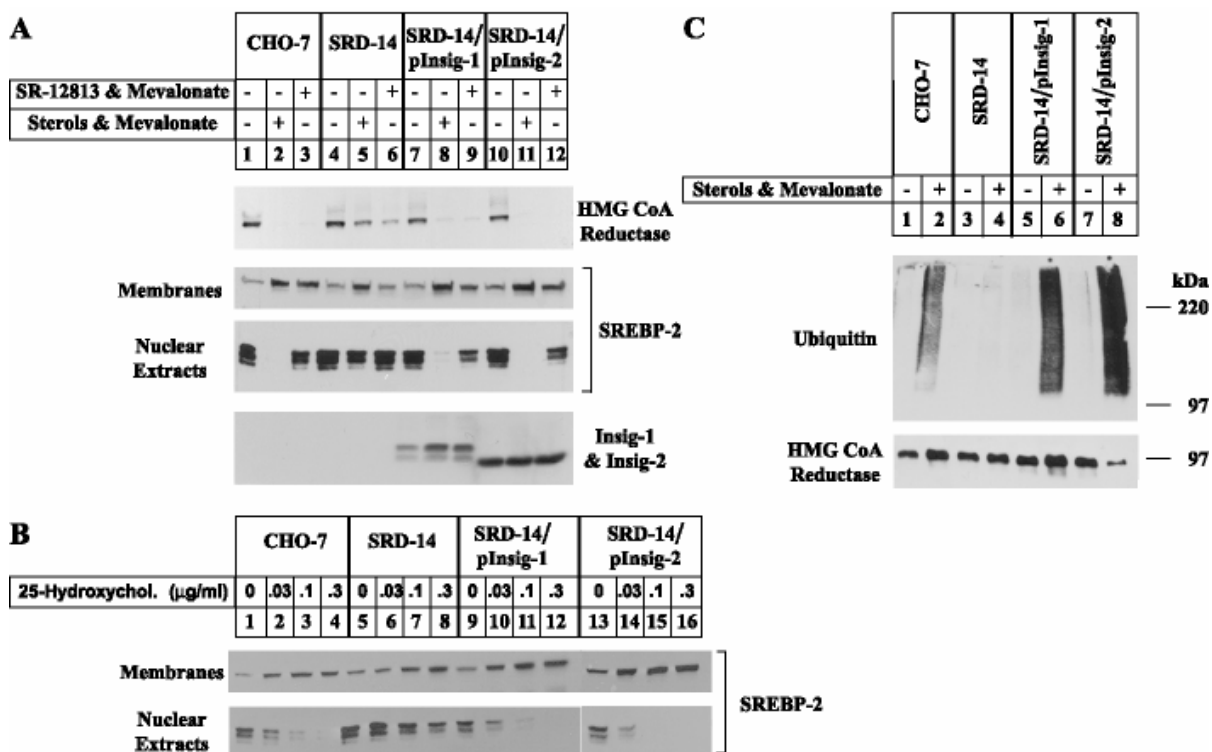


Figure 4-27. Stable transfection of SRD-14 cells with pCMV-Insig-1-Myc or pCMV-Insig-2-Myc restores regulation of HMGR degradation/ubiquitination and SREBP-2 processing mediated by sterols and SR-12813. CHO-7, SRD-14, SRD-14/pInsig-1, and SRD-14/pInsig-2 cells were set up and refed as in Figure 4-21. A and C. After 16 h at 37°C, the cells were switched to medium B containing 50 μM compactin in the absence (-) or presence (+) of sterols or 10 μM SR-12813 plus 10 mM mevalonate, as indicated. C. The medium also contained 10 μM MG-132. B. The cells were switched to medium B containing 50 μM compactin, and the indicated concentrations of 25-HC. A and B. Following incubation at 37°C for 5 h, the cells were harvested and subjected to cell fractionation, and aliquots of the membrane (4-50 μg of protein/lane) and nuclear extract (11-27 μg of protein/lane) fractions were subjected to SDS-PAGE. Immunoblot analysis was carried out with IgG-A9 (against HMGR), IgG-7D4 (against SREBP-2), and anti-Myc IgG (against Insig-1 and Insig-2). Filters were exposed to film for 1-30 s. C. After incubation for 2 h at 37°C, cells were harvested, lysed, and sequentially subjected to IP, SDS-PAGE, and immunoblot analysis as described in the legend to Figure 4-22. Filters were exposed to film for 10 s.

and 4-26 indicate that Insig-1 mediates the rapid suppression of nuclear SREBP-2 promoted by 25-HC, whereas another component of the sterol-regulatory system, likely Insig-2, orchestrates the more gradual sterol response that can be observed between 8 and 16 h in the absence of Insig-1.

Overexpressed Insig-2 Can Restore Sterol Regulation in the Absence of Insig-1

I next sought to determine whether overexpression of Insig-1 or Insig-2 would restore sterol regulation of HMGR ubiquitination/degradation and SREBP-2 processing after 5 h. SRD-14 cells were transfected with pCMV-Insig-1-Myc and pCMV-Insig-2-Myc, expression plasmids encoding full-length human Insig-1 and Insig-2 followed by six tandem copies of the c-Myc epitope, and clones that expressed equivalent levels of the Insig proteins were isolated (Figure 4-27A, bottom panel, lanes 7-12). Figure 4-27A shows that in CHO-7 cells, sterols and SR-12813 promoted complete degradation of HMGR (top panel, lanes 2 and 3), and sterols fully suppressed nuclear SREBP-2 (3rd panel, lane 2). The SRD-14 cells, as expected, were resistant to both reagents (Figure 4-27A, top and 3rd panel, lanes 4-6). In the SRD-14 cells stably overexpressing Insig-1-Myc or Insig-2-Myc, regulated degradation of HMGR and suppression of nuclear SREBP-2 was completely restored (Figure 4-27A, top three panels, lanes 7-12). Overexpression of Insig-1-Myc or Insig-2-Myc in the mutant cells also restored the sensitivity of SREBP-2 processing to low levels of 25-HC (Figure 4-27B). Finally, regulated ubiquitination of HMGR was fully restored in the SRD-14 cells upon overexpression of Insig-1 or Insig-2 (Figure 4-27C). Considered together, these results

demonstrate that the regulatory defects exhibited by SRD-14 cells can be completely restored upon stable transfection of either Insig-1-Myc or Insig-2-Myc.

A Non-Insig Mutant with Defects in HMGR Degradation but Not in SREBP Regulation

The sterol-regulation of Insig-1 mRNA levels in cell line A (see Figure 4-21) similar to CHO-7 cells indicates that in these cells SREBP cleavage is sensitive to suppression by sterols. I tested this hypothesis directly by comparing the effects of sterols and SR-12813 on HMGR degradation and SREBP-2 processing in CHO-7, SRD-14, and the non-Insig mutant cells. As shown in Figure 4-28, sterols and SR-12813 promoted the rapid degradation of HMGR in parental CHO-7 cells (top panel, lanes 2 and 3), whereas the disappearance of

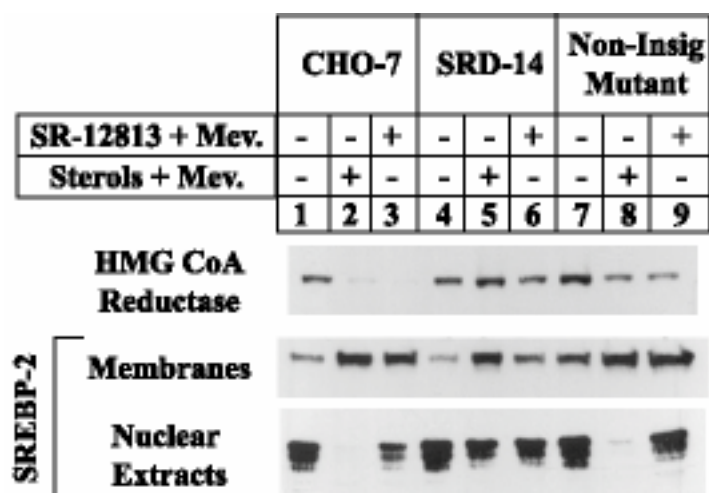


Figure 4-28. A mutant cell line with defective HMGR degradation but normal regulation of SREBP processing. Cells were set up and refed as in Figure 4-21. After 16 h at 37°C, cells were switched to medium B containing 50 μ M compactin in the absence (-) or presence (+) of either sterols or 10 μ M SR-12813 plus 10 mM mevalonate as indicated. After incubation at 37°C for 5 h, the cells were harvested and subjected to cell fractionation. Aliquots of the membrane (5-20 μ g of protein/lane) and nuclear extract fractions (14 μ g of protein/lane) were subjected to SDS-PAGE and transferred to nylon membranes, and immunoblot analysis was carried out with IgG-A9 (against HMGR) or IgG-7D4 (against SREBP-2). Filters were exposed to film for 1-60 s.

nuclear SREBP-2 was only observed upon sterol treatment (bottom panel, lane 2). However, both SR-12813 and sterols failed to promote degradation of HMGR, and sterols did not suppress nuclear SREBP-2 in the mutant SRD-14 cells (Figure 4-28, top and bottom panels, lanes 4-6). In the non-Insig mutant, both SR-12813 and sterols failed to promote degradation of HMGR as in SRD-14 cells, but sterols did suppress nuclear SREBP-2 similar to wild type CHO-7 cells (Figure 4-28, top and bottom panels, lanes 7-9). Thus, the inability of cell line A to carry out HMGR degradation explains its resistance to the growth inhibitory effects of SR-12813. The levels of Insig-1 and Insig-2 (data not shown) in these cells were similar to wild type levels. I have been unable to find any point mutations in Insig-1, Insig-2, and the membrane domains of HMGR or SCAP (data not shown).

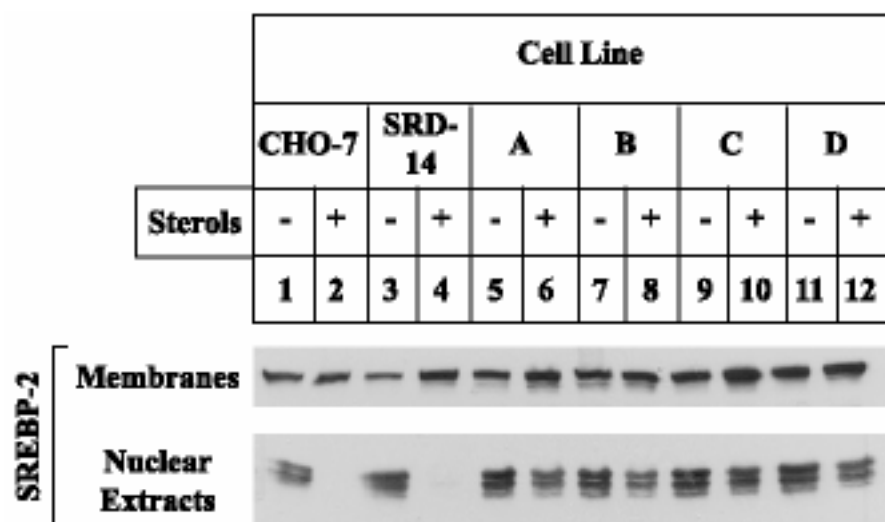


Figure 4-29. Mutant cell lines resistant to both SR-12813 and 25-HC. Cells were set up as in Figure 4-21. On day 2, cells were switched to medium B containing 50 μ M compactin and 50 μ M mevalonate in the absence (-) or presence (+) of sterols as indicated. After incubation for 16 h, the cells were harvested and subjected to cell fractionation. Aliquots of the membrane (42 μ g of protein/lane) and nuclear extract fractions (48 μ g of protein/lane) were subjected to SDS-PAGE and transferred to nylon membranes, and immunoblot analysis was carried out with IgG-7D4 (against SREBP-2). Filters were exposed to film for 1-60 s.

Mutant Cells Resistant to Both SR-12813 and 25-HC

The fact that SRD-14 cells are sensitive to 25-HC made possible the potential of isolating cells deficient in both Insig-1 and Insig-2. Approximately 2.5×10^7 SRD-14 cells were mutagenized with γ -irradiation and subjected to selection with 0.5 $\mu\text{g/ml}$ 25-HC in addition to 10 μM SR-12813. The resistance of cells to 25-HC indicates that in these cells SREBP processing is refractory to suppression even after prolonged incubation in the presence of sterols. I tested this hypothesis directly by comparing the effects of sterols on SREBP-2 processing in CHO-7 cells, SRD-14 cells and the new mutants (Figure 4-29). The disappearance of nuclear SREBP-2 was observed upon sterol treatment of CHO-7 and SRD-14 cells for 16 h (bottom panel, lanes 2 and 4). However, sterols did not suppress nuclear SREBP-2 in the new mutant cells (Figure 4-29, bottom panel, lanes 5-12). Thus, the inability of mutant cells to suppress SREBP processing explains their resistance to the growth inhibitory effects of 25-HC.

CHAPTER FIVE

Conclusions and Recommendations

CENTRAL ROLE OF INSIG-1 AND INSIG-2 IN THE CONTROL OF

CHOLESTEROL HOMEOSTASIS

Regulated Degradation of Mammalian HMGR Requires Insig Proteins

The current results confirm and extend previous observations by others that eukaryotic HMGR is degraded by a ubiquitin-proteasome mechanism that is enhanced by sterols and nonsterol mevalonate-derived products (Roitelman and Simoni, 1992; Ravid et al., 2000; Hampton, 2002a; b). The new findings demonstrate that Insig-1 and Insig-2 play an essential role in the sterol-mediated degradation of mammalian HMGR as well as in the sterol-mediated retention of SCAP in the ER. These effects are associated with sterol-activated binding of the membrane domains of SCAP and HMGR to Insigs as determined by coimmunoprecipitation and blue native-PAGE. Sterol-stimulated binding of HMGR to Insigs requires the tetrapeptide YIYF that is also present in the SSD of SCAP (Figure 4-13). Mutations within the YIYF tetrapeptide prevent sterol-mediated ubiquitination and degradation (Sever et al., 2003). The SSDs of HMGR and SCAP appear to compete for the same site on Insigs, as revealed by the ability of the overexpressed SSD of SCAP to competitively inhibit the sterol-mediated degradation of HMGR (Figure 4-6). This competition was not observed when I overexpressed the Y298C version of SCAP, which fail to bind Insigs (Yang et al., 2002; Yabe et al., 2002b).

In this study, I have not attempted to dissect the separate effects of mevalonate-derived sterols and nonsterol isoprenoids on HMGR interactions. The experiment of Figure 4-13 suggests that the major effect on HMGR degradation is mediated by sterols. In this experiment, HMGR depleted unbound Insig-1 completely when sterols were added alone. Nonsterol, mevalonate-derived products are not capable of stimulating HMGR degradation when cells are sterol-deficient, but they accelerate degradation when sterols are abundant (Nakanishi et al., 1988; Roitelman and Simoni, 1992; Correll and Edwards, 1994). GG-OH, but not farnesol, can synergize with sterols in accelerating degradation of HMGR, suggesting that a geranylgeranylated protein may be involved (Sever et al., 2003).

The conservative substitution of arginine for K248 does not interfere with sterol-stimulated binding of HMGR to Insigs (Figures 4-12 and 4-13), but it does block the subsequent ubiquitination and degradation (Figures 4-10 and 4-11). A similar replacement of K89, the only other lysine in the cytoplasmic loops of HMGR, has little effect on its own, but it further delays degradation when K248 is also replaced (Figure 4-10). These findings indicate that K248 is the primary site of HMGR ubiquitination and that K89 can become ubiquitinated to a small degree when K248 is absent. It is striking that both of these lysines are predicted to lie at the COOH-terminal ends of cytoplasmic loops where they join membrane-spanning helices (Figure 4-9). This juxtamembrane location raises the possibility that Ub is transferred to HMGR by a membrane-bound Ub transferase. Further, the ubiquitination of HMGR in permeabilized cells or isolated microsomes requires the addition of only E1 from the cytosol, suggesting that other required molecules, such as the E2 and E3, are localized to ER membranes (Song and DeBose-Boyd, 2004; Doolman et al., 2004). This

would resemble the situation in *S. cerevisiae* where, Hrd1p, a membrane-bound Ub transferase, is believed to attach Ubs to HMGR, earmarking it for degradation (Hampton et al., 2002a; b). In contrast to the mammalian system, the yeast ubiquitination reaction appears to be stimulated primarily by a nonsterol mevalonate metabolite, and not a sterol (Gardner and Hampton, 1999). Moreover, the yeast genome does not contain an easily recognizable counterpart of Insigs.

Recently, overexpression of Insig-1 in the livers of transgenic mice was shown to inhibit SREBP processing but its effect on HMGR half-life was not reported (Engelking et al., 2004). If Insigs act in the liver as it does in cultured cells, they may play a role in the buildup of HMGR in the ER that occurs when animals (and presumably humans) are treated with statins (Kita et al., 1980). By increasing the amount of active enzyme, this buildup creates a resistance to the drug, a finding that may partially explain the observation that the cholesterol-lowering effect of these drugs reaches a plateau at high doses. Part of this buildup is likely to be due to slowed degradation as a result of the partial sterol deficiency created by this drug (Nakanishi et al., 1988). Further knowledge of the mechanism for sterol-mediated HMGR degradation may point the way to agents, such as SR-12813, that accelerate this process, perhaps by increasing the binding of HMGR to Insigs. In addition, SR-12813 increases the expression of LDL receptor and LDL uptake, which can explain its hypocholesterolemic effect in vivo (Berkhout et al., 1996; 1997). SR-12813 seems to mimic sterols as they both require non-sterol mevalonate derivatives for full effect. Another class of compounds that may operate by a related mechanism is formed by tocotrienols (Parker et al., 1993). Similarly to SR-12813, γ -tocotrienol induces LDL receptor activity indicating that

both compounds are selective for HMGR versus SCAP. This raises the possibility that there may be endogenous sterols that degrade HMGR without suppressing SREBP cleavage. These could be potentially toxic intermediates in the cholesterol biosynthesis pathway that prevent their own accumulation by degrading HMGR without suppressing the more distal steps.

Compounds like SR-12813 may be acting through an unidentified protein that is involved in HMGR degradation. An intriguing possibility is that this protein is prenylated, which would explain the requirement of the nonsterol mevalonate products for complete degradation of HMGR. However, one can speculate that the SSDs of HMGR and SCAP are sufficiently different to be able to bind different ligands and the nonsterol isoprenoids may synergize with sterols for binding to HMGR. Even though there are no reports of direct binding studies using HMGR, it is important to note that oxysterols, but not cholesterol, promote HMGR ubiquitination in permeabilized cells (Song and DeBose-Boyd, 2004). This is in contrast with SCAP, which binds *in vitro* to cholesterol, but not 25-HC (Radhakrishnan et al., 2004). Inasmuch as both proteins are affected by 25-HC *in vivo*, these results together suggest that 25-HC binds to a membrane-bound receptor that subsequently transmits signals to both HMGR and SCAP. Therefore, it is likely that there are multiple mechanisms by which sterols and other compounds regulate the activities of HMGR and SCAP.

Selection of SR-12813-Resistant Cells

The data presented here describe the isolation and characterization of a new line of mutant CHO cells, designated SRD-14, resistant to chronic selection with the 1,1-bisphosphonate

ester SR-12813. I chose to select mutagenized CHO-7 cells with SR-12813 for several reasons.

- 1) SR-12813 replaced sterols in promoting Insig-dependent degradation and ubiquitination of HMGR but not ER retention of the SCAP-SREBP-2 complex (Figure 4-18; Berkhout et al., 1996).
- 2) CHO-7 cells failed to grow in the presence of SR-12813, and this was overcome by the addition of exogenous cholesterol to the growth medium (Figure 4-19).
- 3) SR-12813 did not influence the stability of degradation-resistant mutant forms of HMGR (Figure 4-18), and consequently, the drug failed to kill cells that expressed the mutant but not the wild type form of full-length HMGR (Figure 4-20).

The mutant cells that survived SR-12813 selection did so because they failed to accelerate degradation of HMGR (Figure 4-22 and 4-28). SRD-14 and 7 other lines of Insig-1-deficient cells, as well as 4 cell lines with splice site mutations in the *INSIG-1* gene, were produced from a single round of mutagenesis of $\sim 2.5 \times 10^7$ CHO-7 cells, followed by selection in SR-12813. The repeated isolation of Insig-1-deficient cells in my experiments indicates that CHO-7 cells may only have one functional copy of the *INSIG-1* gene, and thus a single mutagenic event can destroy the single copy of the *INSIG-1* gene, leading to Insig-1 deficiency. The isolation of the same splice donor site mutation from 4 cell lines indicates that this point mutation was preexisting in the parental population. The failure of SRD-14 cells to degrade HMGR in response to SR-12813 or sterols appears to result from their deficiency in total Insig. This is indicated by the restoration of regulated ubiquitination and

degradation of HMGR upon overexpression of either Insig-1-Myc or Insig-2-Myc in the SRD-14 cells (Figure 4-27).

Insig-1-deficient Cells Reveal the Role of Differential Regulation of Insig-1 and Insig-2

The growth of SRD-14 cells in SR-12813 indicates that Insig-2 alone cannot carry out HMGR degradation, whereas their inability to grow in the presence of 25-HC suggests that regulation of SREBP processing must be intact upon prolonged sterol treatment (Figure 4-24C). Thus, I compared the kinetics of sterol-dependent suppression of SREBP-2 processing in parental CHO-7 and mutant SRD-14 cells (Figures 4-25 and 4-26). In the parental cells, sterols rapidly suppressed SREBP-2 processing and mRNAs encoding Insig-1, and other SREBP-2 target genes fell accordingly. In the absence of sterols, I approximate that Insig-1 expression exceeds that of Insig-2 by 10-fold in CHO cells, thus 90% of total Insig is susceptible to sterol-dependent suppression. As expected, Insig-2 alone mediated sterol suppression of SREBP-2 processing in SRD-14 cells, although at a slower rate than wild type cells. Thus, it appears that cells require their total complement of Insigs to carry out sterol-accelerated degradation of HMGR, whereas sterol suppression of SREBP processing can occur at lower Insig levels. These results are consistent with those obtained with RNAi experiments, where transient knockdown of Insig-1 and Insig-2 blocked sterol-accelerated degradation of HMGR, but sterol-mediated suppression of SREBP processing remained intact (Sever et al., 2003; Daisuke Yabe, personal communication). This disparity may reflect differences in the affinities of HMGR and SCAP for sterols and/or Insigs. Finally, stable overexpression of Insig-1 or Insig-2 in SRD-14 cells restored the rapid suppression of

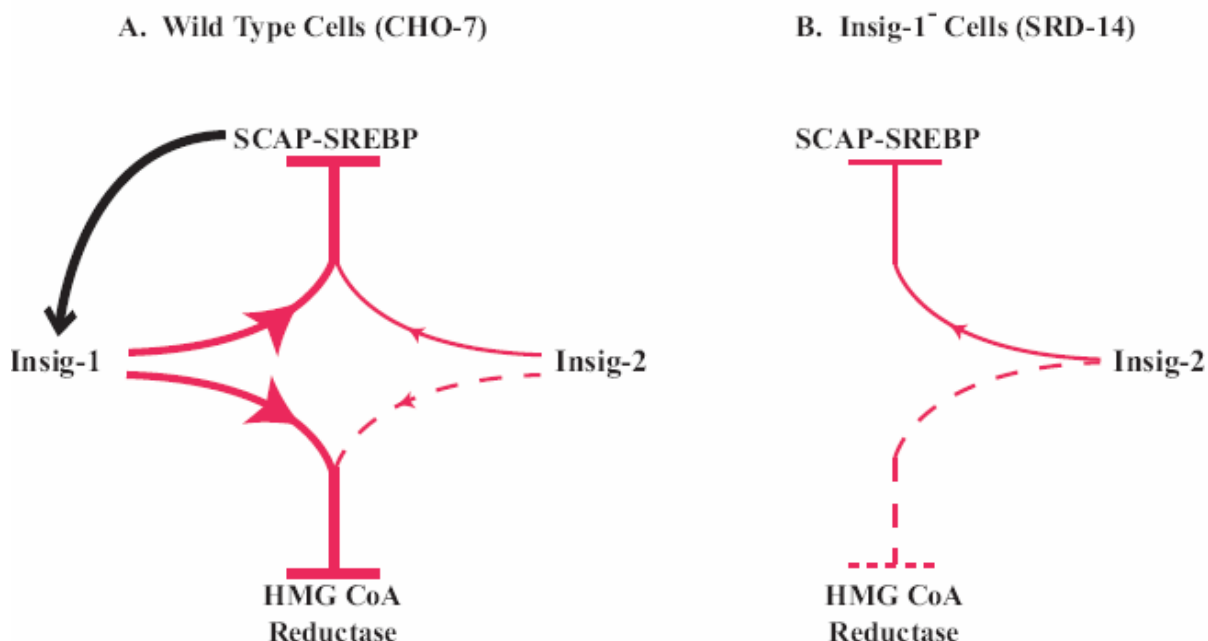


Figure 5-1. Model for Insig-mediated regulation of SREBP processing and HMGR degradation. A. When wild type CHO-7 cells are depleted of sterols, Insig-1 and Insig-2 dissociate from the SCAP-SREBP complex, allowing its entry into budding vesicles and translocation to the Golgi where SREBPs are processed. Meanwhile, HMGR is stable and produces mevalonate. In the nucleus, processed SREBPs activate transcription of genes encoding cholesterol biosynthetic enzymes and Insig-1. The resulting rise of Insig-1 protein and intracellular accumulation of sterols eventually leads to the rapid suppression of SREBP processing through the sterol-dependent binding of Insig-1 to SCAP in the ER, preventing it from escorting SREBPs to the Golgi for proteolytic activation. At the same time Insig-1 mediates sterol-accelerated degradation of HMGR. In the absence of SREBP processing, Insig-1 expression decreases, yet SREBP processing continues to be suppressed because the constitutively low level of Insig-2 is enough to retain the SCAP-SREBP complex in the ER. B. In the Insig-1-deficient SRD-14 cells, sterol-dependent suppression of SREBP processing occurs at a slower rate than in wild type cells, because of the low abundance of Insig-2. However, Insig-2 alone is not sufficient to accelerate HMGR degradation, and this renders SRD-14 cells resistant to SR-12813.

SREBP processing (Figure 4-27), thus reflecting the redundant role of the two proteins in mediating sterol regulation of SREBP as well as HMGR.

Taken together, the current results provide compelling genetic evidence for the important role Insig-1 plays in mediating two distinct sterol-regulated reactions, ER retention of SCAP and accelerated degradation of HMGR. In addition, these data substantiate previous reasoning for the existence of two Insig isoforms. Yabe et al. (2002a) hypothesized that if cells only expressed the Insig-1 isoform, it would require nuclear SREBP for expression, and sterols would only transiently block processing of SREBPs. Figure 5-1 presents a schematic model to explain the differential actions of Insig-1 and Insig-2 in regulating SREBP processing and HMGR degradation. In wild type, sterol-deprived cells, SCAP readily enters budding vesicles, en route to carrying SREBP to the Golgi for proteolytic processing, and HMGR is stable and produces mevalonate. In the nucleus, the processed SREBPs activate transcription of genes encoding cholesterol biosynthetic enzymes (including HMGR), resulting in a rise in the synthesis of sterols. The combination of sterols and Insig-1 prevents translocation of SCAP to the Golgi, resulting in the decline of SREBP processing, and promotes accelerated degradation of HMGR (Figure 5-1A). In the absence of nuclear SREBPs, Insig-1 levels diminish, and over time, the level of SCAP should eventually exceed that of Insig-1, permitting its escape from the ER to activate processing of SREBPs.

The analysis of SREBP processing in SRD-14 cells indicates that because of its constitutive, SREBP-independent expression, Insig-2 prevents the escape of SCAP from the ER in cells replete with sterols (Figure 5-1B). I reason that sterols synthesized prior to the fall of Insig-1 sensitize the system such that Insig-2 is sufficient to block SCAP transport and

maintain suppression of SREBP processing as long as intracellular sterols remain high. Considering that under conditions of sterol deprivation Insig-1 accounts for 90% of total Insigs, the ability of SREBPs to modulate levels of its inhibitor provides a reset mechanism that permits cells to rapidly modulate SREBP processing according to their demands for sterols. When cellular sterols are high, Insig-2 is the only form of Insig present, and thus the cells can respond rapidly to cholesterol depletion. On the other hand, when SREBPs are actively processed, the *INSIG-1* gene is activated, and the increase in total Insigs primes the cells for rapid suppression when sterol levels rise.

Perspectives for the Future

In conclusion, the analysis of regulated SREBP processing and accelerated degradation of HMGR in the Insig-1-deficient SRD-14 cells has revealed an interesting circuitry underlying sterol regulation; however, the complete resolution of this unique regulatory system requires the availability of Insig-2-deficient cells, as well as cells lacking both Insig-1 and Insig-2. I took advantage of the fact that Insig-1-deficient SRD-14 cells are not significantly resistant to 25-HC in order to isolate potential double Insig knockouts. These cells were mutagenized again and subjected to selection with 25-HC in addition to SR-12813. If Insig proteins are absolutely required for suppression of SREBP processing, cells lacking both Insig-1 and Insig-2 should be completely resistant to 25-HC. It is still possible that some of the resulting cell lines have mutations in SCAP, which would have the same phenotypes.

It is harder to predict whether Insig-2-deficiency alone would have an obvious phenotype because of the abundance of Insig-1 in CHO cells compared to Insig-2 and the regulation of Insig-1 itself by sterols. The latter is analogous to the role of $\text{I}\kappa\text{B}\alpha$ (inhibitor of $\text{NF-}\kappa\text{B}$) in the $\text{NF-}\kappa\text{B}$ (nuclear factor κB) signaling pathway. $\text{NF-}\kappa\text{B}$ is held inactive in the cytoplasm by three $\text{I}\kappa\text{B}$ isoforms: α , β , and ϵ . Cell stimulation by tumor necrosis factor (TNF) leads to phosphorylation and degradation of $\text{I}\kappa\text{B}$ proteins. Free $\text{NF-}\kappa\text{B}$ translocates to the nucleus, activating genes, including $\text{I}\kappa\text{B}\alpha$. In mouse knockout cells lacking $\text{I}\kappa\text{B}\beta$ and ϵ , the system produces undampened $\text{NF-}\kappa\text{B}$ oscillations in response to sustained TNF input. In wild type cells, however, $\text{I}\kappa\text{B}\beta$ and ϵ are synthesized at a steady rate and act to dampen the response of the $\text{NF-}\kappa\text{B}$ signaling pathway to TNF input. A computational model demonstrates that $\text{I}\kappa\text{B}\alpha$ is responsible for strong negative feedback that allows for a fast turn-off of the $\text{NF-}\kappa\text{B}$ response, whereas $\text{I}\kappa\text{B}\beta$ and ϵ function to reduce the system's oscillatory potential, allowing for complex temporal control (Hoffmann et al., 2002). In theory, Insig-2-deficient cells should show an oscillatory response to sterols, provided that the cells remain synchronized during the time it takes for a full period of complete SREBP suppression. Assuming the half-lives of cholesterol biosynthetic enzymes encoded by SREBP target genes are long enough, the transient expression of these genes during the peak of each oscillatory period may be enough for the cells to grow in the continual presence of 25-HC. Once double Insig knockout cell lines are isolated, Insig-1 can be introduced into these cells to mimic Insig-2-deficiency. Further, by expressing Insig-1 from its own sterol-responsive promoter, the theories speculated above could be definitively tested.

Although the sterol effects on HMGR and SCAP both appear to require binding to Insig proteins, the consequences are strikingly different (Figure 5-2). After binding to Insigs, HMGR is degraded, apparently within the ER, by a process that appears to be mediated by ubiquitination and proteasomal degradation. On the other hand, binding of SCAP to Insigs leads to ER retention of the SCAP/SREBP complex. This complex is stable and not rapidly degraded. It will be crucial to understand how binding to the same Insig proteins can have such different effects on its two ligands. This question will be answered when other members of the HMGR/Insig complex and the SCAP/Insig complex are identified. For instance, an ER-retention protein may be recruited, selectively, to SCAP/Insig complex, and an E3

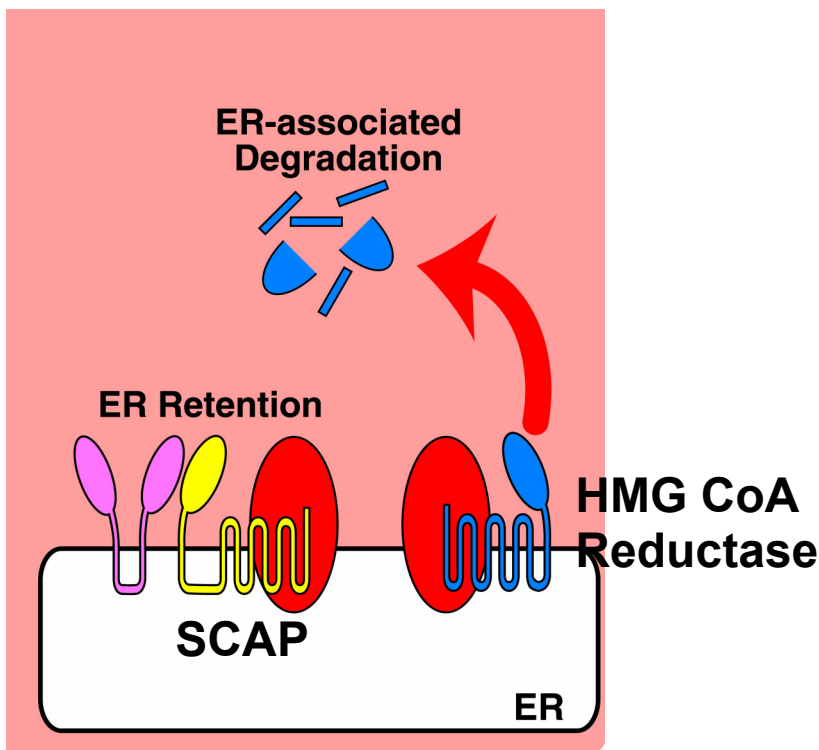


Figure 5-2. Insig-mediated regulation of HMGR and SCAP. In the presence of excess sterols, Insig-1 and Insig-2 promote the ubiquitination and the subsequent ER-associated degradation of HMGR. On the other hand, sterol-dependent Insig-SCAP interaction causes the ER retention of the SCAP-SREBP complex. Insig is in red, HMGR in blue, SCAP in yellow, and SREBP in pink.

ubiquitin ligase to HMGR/Insig complex. In this regard, gp78 seems to be recruited to HMGR in response to sterols although the endogenous requirement of it for regulation of HMGR degradation remains to be established (Figure 4-17). The isolation of a cell line with a defect in HMGR degradation but not in SREBP regulation makes possible the identification of a novel factor required specifically for HMGR degradation (Figure 4-28). Even though the cells were selected for resistance to SR-12813, HMGR in this cell line is also resistant to degradation in the presence of sterols and mevalonate, which rules out a receptor specific for SR-12813, or such potential artifacts as the exclusion of SR-12813 from the cells due to activities metabolizing or exporting the drug. The most likely possibility is a defect in an E3 ubiquitin ligase, either due to a dominant-negative mutation or a deficiency in an E3 specific for HMGR. Mutations in an E2 ubiquitin conjugating enzyme, or especially E1 ubiquitin activating enzyme, are unlikely due to lesser specificities of these enzymes and the pleiotropic effects expected of their deficiencies. Proteins involved in sensing the nonsterol mevalonate product that is required for HMGR degradation and those involved in extracting ubiquitinated HMGR from the ER membrane and presenting it to the proteasome, such as p97/VCP/Cdc48p (Doolman et al., 2004), are other possible candidates that may be mutated in this cell line. Given that these are very poorly understood aspects of HMGR degradation, and even ER-associated degradation in general, it is worth enriching for cell lines with similar phenotypes. To this end, cells transfected with multiple copies of Insig-1 (or Insig-2) should be used as the parental cell line to prevent repeated isolation of Insig-1-deficient cells since CHO-7 cells seem to have one copy of Insig-1. The defects in the resulting mutant cells could then be discovered by complementation cloning.

BIBLIOGRAPHY

- Altmann, S.W., Davis, H.R., Jr., Zhu, L.-J., Yao, X., Hoos, L.M., Tetzloff, G., Iyer, S.P.N., Maguire, M., Golovko, A., Zeng, M., et al. (2004). Niemann-Pick C1 like 1 protein is critical for intestinal cholesterol absorption. *Science* 303, 1201.
- Anderson, R.G. (1998). The caveolae membrane system. *Annu. Rev. Biochem.* 67, 199.
- Basson, M.E., Thorsness, M., and Rine, J. (1986). *Saccharomyces cerevisiae* contains two functional genes encoding 3-hydroxy-3-methylglutaryl-coenzyme A reductase. *Proc. Natl. Acad. Sci. USA* 83, 5563.
- Basson, M.E., Thorsness, M., Finer-Moore, J., Stroud, R.M., and Rine, J. (1988). Structural and functional conservation between yeast and human 3-hydroxy-3-methylglutaryl coenzyme A reductases, the rate-limiting enzyme of sterol biosynthesis. *Mol. Cell. Biol.* 8, 3797.
- Bays, N.W., Gardner, R.G., Seelig, L.P., Joazeiro, C.A., and Hampton, R.Y. (2001a). Hrd1p/Der3p is a membrane-anchored ubiquitin ligase required for ER-associated degradation. *Nature Cell Biol.* 3, 24.
- Bays, N.W., Wilhovsky, S.K., Goradia, A., Hodgkiss-Harlow, K., and Hampton, R.Y. (2001b). *HRD4/NPL4* is required for the proteasomal processing of ubiquitinated ER proteins. *Mol. Biol. Cell* 12, 4114.
- Berkhout, T.A., Simon, H.M., Jackson, B., Yates, J., Pearce, N., Groot, P.H., Bentzen, C., Niesor, E., Kerns, W.D., and Suckling, K.E. (1997). SR-12813 lowers plasma cholesterol in beagle dogs by decreasing cholesterol biosynthesis. *Atherosclerosis* 133, 203.
- Berkhout, T.A., Simon, H.M., Patel, D.D., Bentzen, C., Niesor, E., Jackson, B., and Suckling, K.E. (1996). The novel cholesterol-lowering drug SR-12813 inhibits cholesterol synthesis via an increased degradation of 3-hydroxy-3-methylglutaryl-coenzyme A reductase. *J. Biol. Chem.* 271, 14376.
- Bollag, D.M., and Edelstein, S.J. (1991). *Protein Methods* (New York: Wiley-Liss).
- Bonifacino, J.S., and Weissman, A.M. (1998). Ubiquitin and the control of protein fate in the secretory and endocytic pathways. *Annu. Rev. Cell Dev. Biol.* 14, 19.
- Brown, A.J., Sun, L., Feramisco, J.D., Brown, M.S., and Goldstein, J.L. (2002). Cholesterol addition to ER membranes alters conformation of SCAP, the SREBP escort protein that regulates cholesterol metabolism. *Mol. Cell* 10, 237.

- Brown, M.S., and Goldstein, J.L. (1996). Heart attacks: gone with the century? *Science* 272, 629.
- Brown, M.S., and Goldstein, J.L. (1997). The SREBP pathway: regulation of cholesterol metabolism by proteolysis of a membrane-bound transcription factor. *Cell* 89, 331.
- Brown, M.S., and Goldstein, J.L. (1999). A proteolytic pathway that controls the cholesterol content of membranes, cells, and blood. *Proc. Natl. Acad. Sci. USA* 96, 11041.
- Brown, M.S., Faust, J.R., Goldstein, J.L., Kaneko, I., and Endo, A. (1978). Induction of 3-hydroxy-3-methylglutaryl coenzyme A reductase activity in human fibroblasts incubated with compactin (ML-236B), a competitive inhibitor of the reductase. *J. Biol. Chem.* 253, 1121.
- Brown, M.S., Ye, J., Rawson, R.B., and Goldstein, J.L. (2000). Regulated intramembrane proteolysis: a control mechanism conserved from bacteria to humans. *Cell* 100, 391.
- Chin, D.J., Luskey, K.L., Anderson, R.G., Faust, J.R., Goldstein, J.L., and Brown, M.S. (1982). Appearance of crystalloid endoplasmic reticulum in compactin-resistant Chinese hamster cells with a 500-fold increase in 3-hydroxy-3-methylglutaryl-coenzyme A reductase. *Proc. Natl. Acad. Sci. USA* 79, 1185.
- Correll, C.C., Ng, L., and Edwards, P.A. (1994). Identification of farnesol as the non-sterol derivative of mevalonic acid required for the accelerated degradation of 3-hydroxy-3-methylglutaryl-coenzyme A reductase. *J. Biol. Chem.* 269, 17390.
- Cronin, S.R., Khoury, A., Ferry, D.K., and Hampton, R.Y. (2000). Regulation of HMG-CoA reductase degradation requires the P-type ATPase Cod1p/Spf1p. *J. Cell Biol.* 148, 915.
- Cronin, S.R., Rao, R., and Hampton, R.Y. (2002). Cod1p/Spf1p is a P-type ATPase involved in ER function and Ca^{2+} homeostasis. *J. Cell Biol.* 157, 1017.
- Dawson, P.A., Metherall, J.E., Ridgway, N.D., Brown, M.S., and Goldstein, J.L. (1991). Genetic distinction between sterol-mediated transcriptional and posttranscriptional control of 3-hydroxy-3-methylglutaryl-coenzyme A reductase. *J. Biol. Chem.* 266, 9128.
- DeMartino, G.N., and Slaughter, C.A. (1999). The proteasome, a novel protease regulated by multiple mechanisms. *J. Biol. Chem.* 274, 22123.

- Di Fiore, P.P., Polo, S., and Hofmann, K. (2003). When ubiquitin meets ubiquitin receptors: a signaling connection. *Nature Rev. Mol. Cell Biol.* 4, 491.
- Doolman, R., Leichner, G.S., Avner, R., and Roitelman, J. (2004). Ubiquitin is conjugated by membrane ubiquitin ligase to three sites, including the N terminus, in transmembrane region of mammalian 3-hydroxy-3-methylglutaryl coenzyme A reductase: implications for sterol-regulated enzyme degradation. *J. Biol. Chem.* 279, 38184.
- Edwards, P.A., Lan, S.-F., Tanaka, R.D., and Fogelman, A.M. (1983). Mevalonolactone inhibits the rate of synthesis and enhances the rate of degradation of 3-hydroxy-3-methylglutaryl coenzyme A reductase in rat hepatocytes. *J. Biol. Chem.* 258, 7272.
- Ellgaard, L., and Helenius, A. (2003). Quality control in the endoplasmic reticulum. *Nature Rev. Mol. Cell Biol.* 4, 181.
- Engelking, L.J., Kuriyama, H., Hammer, R.E., Horton, J.D., Brown, M.S., Goldstein, J.L., and Liang, G. (2004). Overexpression of Insig-1 in the livers of transgenic mice inhibits SREBP processing and reduces insulin-stimulated lipogenesis. *J. Clin. Invest.* 113, 1168.
- Espenshade, P.J., Li, W.P., and Yabe, D. (2002). Sterols block binding of COPII proteins to SCAP, thereby controlling SCAP sorting in ER. *Proc. Natl. Acad. Sci. USA* 99, 11694.
- Fang, S., Ferrone, M., Yang, C., Jensen, J.P., Tiwari, S., and Weissman, A.M. (2001). The tumor autocrine motility factor receptor, gp78, is a ubiquitin protein ligase implicated in degradation from the endoplasmic reticulum. *Proc. Natl. Acad. Sci. USA* 98, 14422.
- Faust, J.R., Luskey, K.L., Chin, D.J., Goldstein, J.L., and Brown, M.S. (1982). Regulation of synthesis and degradation of 3-hydroxy-3-methylglutaryl-coenzyme A reductase by low density lipoprotein and 25-hydroxycholesterol in UT-1 cells. *Proc. Natl. Acad. Sci. USA* 79, 5205.
- Feramisco, J.D., Goldstein, J.L., and Brown, M.S. (2004). Membrane topology of human insig-1, a protein regulator of lipid synthesis. *J. Biol. Chem.* 279, 8487.
- Friedlander, R., Jarosch, E., Urban, J., Volkwein, C., and Sommer, T. (2000). A regulatory link between ER-associated protein degradation and the unfolded-protein response. *Nat. Cell Biol.* 2, 379.

- Gardner, R.G., and Hampton, R.Y. (1999). A highly conserved signal controls degradation of 3-hydroxy-3-methylglutaryl-coenzyme A (HMG-CoA) reductase in eukaryotes. *J. Biol. Chem.* 274, 31671.
- Gardner, R.G., Shan, H., Matsuda, S.P.T., and Hampton, R.Y. (2001). An oxysterol-derived positive signal for 3-hydroxy-3-methylglutaryl-CoA reductase degradation in yeast. *J. Biol. Chem.* 276, 8681.
- Gil, G., Faust, J.R., Chin, D.J., Goldstein, J.L., and Brown, M.S. (1985). Membrane-bound domain of HMG CoA reductase is required for sterol-enhanced degradation of the enzyme. *Cell* 41, 249.
- Goldstein, J.L., and Brown, M.S. (1990). Regulation of the mevalonate pathway. *Nature* 343, 425.
- Goldstein, J.L., Basu, S.K., and Brown, M.S. (1983). Receptor-mediated endocytosis of LDL in cultured cells. *Methods Enzymol.* 98, 241.
- Goldstein, J.L., Rawson, R.B., and Brown, M.S. (2002). Mutant mammalian cells as tools to delineate the sterol regulatory element-binding protein pathway for feedback regulation of lipid synthesis. *Arch. Biochem. Biophys.* 397, 139.
- Hampton, R.Y. (2002a). ER-associated degradation in protein quality control and cellular regulation. *Curr. Opin. Cell Biol.* 14, 476.
- Hampton, R.Y. (2002b). Proteolysis and sterol regulation. *Annu. Rev. Cell Dev. Biol.* 18, 345.
- Hampton, R.Y., and Bhakta, H. (1997). Ubiquitin-mediated regulation of 3-hydroxy-3-methylglutaryl-CoA reductase. *Proc. Natl. Acad. Sci. USA* 94, 12944.
- Hampton, R.Y., Gardner, R.G., and Rine, J. (1996). Role of 26S proteasome and *HRD* genes in the degradation of 3-hydroxy-3-methylglutaryl-CoA reductase, an integral endoplasmic reticulum membrane protein. *Mol. Biol. Cell* 7, 2029.
- Hannah, V.C., Ou, J., Luong, A., Goldstein, J.L., and Brown, M.S. (2001). Unsaturated fatty acids down-regulate SREBP isoforms 1a and 1c by two mechanisms in HEK-293 cells. *J. Biol. Chem.* 276, 4365.
- Hicke, L. (2001). Protein regulation by monoubiquitin. *Nature Rev. Mol. Cell Biol.* 2, 195.

- Hoffmann, A., Levchenko, A., Scott, M.L., and Baltimore, D. (2002). The I κ B-NF- κ B signaling module: temporal control and selective gene activation. *Science* 298, 1241.
- Horton, J.D., Goldstein, J.L., and Brown, M.S. (2002). SREBPs: activators of the complete program of cholesterol and fatty acid synthesis in the liver. *J. Clin. Invest.* 109, 1125.
- Horton, J.D., Shah, N.A., Warrington, J.A., Anderson, N.N., Park, S.W., Brown, M.S., and Goldstein, J.L. (2003). Combined analysis of oligonucleotide microarray data from transgenic and knockout mice identifies direct SREBP target genes. *Proc. Natl. Acad. Sci. USA* 100, 12027.
- Hua, X., Nohturfft, A., Goldstein, J.L., and Brown, M.S. (1996). Sterol resistance in CHO cells traced to point mutation in SREBP cleavage-activating protein. *Cell* 87, 415.
- Inoue, S., Bar-Nun, S., Roitelman, J., and Simoni, R.D. (1991). Inhibition of degradation of 3-hydroxy-3-methylglutaryl-coenzyme A reductase *in vivo* by cysteine protease inhibitors. *J. Biol. Chem.* 266, 13311.
- Kaneko, M., Ishiguro, M., Niinuma, Y., Uesugi, M., and Nomura, Y. (2002). Human HRD1 protects against ER stress-induced apoptosis through ER-associated degradation. *FEBS Lett.* 532, 147.
- Kikkert, M., Doolman, R., Dai, M., Avner, R., Hassink, G., van Voorden, S., Thanedar, S., Roitelman, J., Chau, V., and Wiertz, E. (2004). Human HRD1 is an E3 ubiquitin ligase involved in degradation of proteins from the endoplasmic reticulum. *J. Biol. Chem.* 279, 3525.
- Kita, T., Brown, M.S., and Goldstein, J.L. (1980). Feedback regulation of 3-hydroxy-3-methylglutaryl coenzyme A reductase in livers of mice treated with mevinolin, a competitive inhibitor of the reductase. *J. Clin. Invest.* 66, 1094.
- Kuwabara, P.E., and Labouesse, M. (2002). The sterol-sensing domain: multiple families, a unique role? *Trends Genet.* 18, 193.
- Lecureux, L.W., and Wattenberg, B.W. (1994). The regulated degradation of 3-hydroxy-3-methylglutaryl-coenzyme A reductase reporter construct occurs in the endoplasmic reticulum. *J. Cell Sci.* 107, 2635.
- Liang, G., Yang, J., Horton, J.D., Hammer, R.E., Goldstein, J.L., and Brown, M.S. (2002). Diminished hepatic response to fasting/refeeding and liver X receptor

- agonists in mice with selective deficiency of sterol regulatory element-binding protein-1c. *J. Biol. Chem.* 277, 9520.
- Liang, J.S., Kim, T., Fang, S., Yamaguchi, J., Weissman, A.M., Fisher, E.A., and Ginsberg, H.N. (2003). Overexpression of the tumor autocrine motility factor receptor gp78, a ubiquitin protein ligase, results in increased ubiquitinylation and decreased secretion of apolipoprotein B100 in HepG2 cells. *J. Biol. Chem.* 278, 23984.
- Libby, P., Aikawa, M., and Schonbeck, U. (2000). Cholesterol and atherosclerosis. *Biochim. Biophys. Acta.* 1529, 299.
- Liscum, L., Cummings, R.D., Anderson, R.G.W., DeMartino, G.N., Goldstein, J.L., and Brown, M.S. (1983a). 3-hydroxy-3-methylglutaryl-CoA reductase: a transmembrane glycoprotein of the endoplasmic reticulum with N-linked "high-mannose" oligosaccharides. *Proc. Natl. Acad. Sci. USA* 80, 7165.
- Liscum, L., Finer-Moore, J., Stroud, R.M., Luskey, K.L., Brown, M.S., and Goldstein, J.L. (1985). Domain structure of 3-hydroxy-3-methylglutaryl coenzyme A reductase, a glycoprotein of the endoplasmic reticulum. *J. Biol. Chem.* 260, 522.
- Liscum, L., Luskey, K.L., Chin, D.J., Ho, Y.K., Goldstein, J.L., and Brown, M.S. (1983b). Regulation of 3-hydroxy-3-methylglutaryl coenzyme A reductase and its mRNA in rat liver as studied with a monoclonal antibody and a cDNA probe. *J. Biol. Chem.* 258, 8450.
- Luskey, K.L., Faust, J.R., Chin, D.J., Brown, M.S., and Goldstein, J.L. (1983). Amplification of the gene for 3-hydroxy-3-methylglutaryl coenzyme A reductase, but not for the 53-kDa protein, in UT-1 cells. *J. Biol. Chem.* 258, 8462.
- Maley, F., Trimble, R.B., Tarentino, A.L., and Plummer, T.H. Jr. (1989). Characterization of glycoproteins and their associated oligosaccharides through the use of endoglycosidases. *Anal. Biochem.* 180, 195.
- Mann, R.K., and Beachy, P.A. (2004). Novel lipid modifications of secreted protein signals. *Annu. Rev. Biochem.* 73, 891.
- Matlack, K.E., Mothes, W., and Rapoport, T.A. (1998). Protein translocation: tunnel vision. *Cell* 92, 381.
- McGee, T.P., Cheng, H.H., Kumagai, H., Omura, S., and Simoni, R.D. (1996). Degradation of 3-hydroxy-3-methylglutaryl-CoA reductase in endoplasmic reticulum membranes is accelerated as a result of increased susceptibility to proteolysis. *J. Biol. Chem.* 271, 25630.

- Meigs, T.E., and Simoni, R.D. (1997). Farnesol as a regulator of HMG-CoA reductase degradation: characterization and role of farnesyl pyrophosphatase. *Arch. Biochem. Biophys.* 345, 1.
- Meigs, T.E., Roseman, D.S., and Simoni, R.D. (1996). Regulation of 3-hydroxy-3-methylglutaryl-coenzyme A reductase degradation by the nonsterol mevalonate metabolite farnesol *in vivo*. *J. Biol. Chem.* 271, 7916.
- Metherall, J.E., Goldstein, J.L., Luskey, K.L., and Brown, M.S. (1989). Loss of transcriptional repression of three sterol-regulated genes in mutant hamster cells. *J. Biol. Chem.* 264, 15634.
- Mimnaugh, E.G., Bonvini, P., and Neckers, L. (1999). The measurement of ubiquitin and ubiquitinated proteins. *Electrophoresis* 20, 418.
- Moriyama, T., Sather, S.K., McGee, T.P., and Simoni, R.D. (1998). Degradation of HMG CoA reductase *in vitro*. Cleavage in the membrane domain by a membrane-bound cysteine protease. *J. Biol. Chem.* 273, 22037.
- Moriyama, T., Wada, M., Urade, R., Kito, M., Katunuma, N., Ogawa, T., and Simoni, R.D. (2001). 3-hydroxy-3-methylglutaryl coenzyme A reductase is sterol-dependently cleaved by cathepsin L-type cysteine protease in the isolated endoplasmic reticulum. *Arch. Biochem. Biophys.* 386, 205.
- Mosley, S.T., Brown, M.S., Anderson, R.G., and Goldstein, J.L. (1983). Mutant clone of Chinese hamster ovary cells lacking 3-hydroxy-3-methylglutaryl coenzyme A reductase. *J. Biol. Chem.* 258, 13875.
- Nadav, E., Shmueli, A., Barr, H., Gonen, H., Ciechanover, A., and Reiss, Y. (2003). A novel mammalian endoplasmic reticulum ubiquitin ligase homologous to the yeast Hrd1. *Biochem. Biophys. Res. Commun.* 303, 91.
- Nakanishi, M., Goldstein, J.L., and Brown, M.S. (1988). Multivalent control of 3-hydroxy-3-methylglutaryl coenzyme A reductase: mevalonate-derived product inhibits translation of mRNA and accelerates degradation of enzyme. *J. Biol. Chem.* 263, 8929.
- Nohturfft, A., Brown, M.S., and Goldstein, J.L. (1998a). Sterols regulate processing of carbohydrate chains of wild-type SREBP cleavage-activating protein (SCAP), but not sterol-resistant mutants Y298C and D443N. *Proc. Natl. Acad. Sci. USA* 95, 12848.

- Nohturfft, A., Brown, M.S., and Goldstein, J.L. (1998b). Topology of SREBP cleavage activating protein, a polytopic membrane protein with a sterol-sensing domain. *J. Biol. Chem.* 273, 17243.
- Nohturfft, A., DeBose-Boyd, R.A., Scheek, S., Goldstein, J.L., and Brown, M.S. (1999). Sterols regulate cycling of SREBP cleavage-activating protein (SCAP) between endoplasmic reticulum and Golgi. *Proc. Natl. Acad. Sci. USA* 96, 11235.
- Nohturfft, A., Yabe, D., Goldstein, J.L., Brown, M.S., and Espenshade, P.J. (2000). Regulated step in cholesterol feedback localized to budding of SCAP from ER membranes. *Cell* 102, 315.
- Ohgami, N., Ko, D.C., Thomas, M., Scott, M.P., Chang, C.C., and Chang, T.Y. (2004). Binding between the Niemann-Pick C1 protein and a photoactivatable cholesterol analog requires a functional sterol-sensing domain. *Proc. Natl. Acad. Sci. USA* 101, 12473.
- Ou, J., Tu, H., Shan, B., Luk, A., DeBose-Boyd, R.A., Bashmakov, Y., Goldstein, J.L., and Brown, M.S. (2001). Unsaturated fatty acids inhibit transcription of the sterol regulatory element-binding protein-1c (SREBP-1c) gene by antagonizing ligand-dependent activation of the LXR. *Proc. Natl. Acad. Sci. USA* 98, 6027.
- Parker, R.A., Pearce, B.C., Clark, R.W., Gordon, D.A., and Wright, J.J. (1993). Tocotrienols regulate cholesterol production in mammalian cells by post-transcriptional suppression of 3-hydroxy-3-methylglutaryl-coenzyme A reductase. *J. Biol. Chem.* 268, 11230.
- Patel, A.A., and Steitz, J.A. (2003). Splicing double: insights from the second spliceosome. *Nature Rev. Mol. Cell Biol.* 4, 960.
- Ponting, C.P. (2000). Proteins of the endoplasmic-reticulum-associated degradation pathway: domain detection and function prediction. *Biochem. J.* 351, 527.
- Radhakrishnan, A., Sun, L., Kwon, H.J., Brown, M.S., and Goldstein, J.L. (2004). Direct binding of cholesterol to the purified membrane region of SCAP: mechanism for a sterol-sensing domain. *Mol. Cell* 15, 259.
- Ravid, T., Avner, R., Polak-Charcon, S., Faust, J.R., and Roitelman, J. (1999). Impaired regulation of 3-hydroxy-3-methylglutaryl-coenzyme A reductase degradation in lovastatin-resistant cells. *J. Biol. Chem.* 274, 29341.
- Ravid, T., Doolman, R., Avner, R., Harats, D., and Roitelman, J. (2000). The ubiquitin-proteasome pathway mediates the regulated degradation of mammalian 3-hydroxy-3-methylglutaryl-coenzyme A reductase. *J. Biol. Chem.* 275, 35840.

- Rawson, R.B. (2003). The SREBP pathway: insights from *Insigs* and insects. *Nature Rev. Mol. Cell Biol.* 4, 631.
- Rawson, R.B., Cheng, D., Brown, M.S., and Goldstein, J.L. (1998). Isolation of cholesterol-requiring mutant Chinese hamster ovary cells with defects in cleavage of sterol regulatory element-binding proteins at site 1. *J. Biol. Chem.* 273, 28261.
- Rawson, R.B., DeBose-Boyd, R., Goldstein, J.L., and Brown, M.S. (1999). Failure to cleave sterol regulatory element-binding proteins (SREBPs) causes cholesterol auxotrophy in Chinese hamster ovary cells with genetic absence of SREBP cleavage-activating protein. *J. Biol. Chem.* 274, 28549.
- Roitelman, J., and Simoni, R.D. (1992). Distinct sterol and nonsterol signals for the regulated degradation of 3-hydroxy-3-methylglutaryl-CoA reductase. *J. Biol. Chem.* 267, 25264.
- Roitelman, J., Masson, D., Avner, R., Ammon-Zufferey, C., Perez, A., Guyon-Gellin, Y., Bentzen, C.L., and Niesor, E.J. (2004). Apomine, a novel hypocholesterolemic agent, accelerates degradation of 3-hydroxy-3-methylglutaryl-coenzyme A reductase and stimulates low density lipoprotein receptor activity. *J. Biol. Chem.* 279, 6465.
- Sakai, J., Nohturfft, A., Cheng, D., Ho, Y.K., Brown, M.S., and Goldstein, J.L. (1997). Identification of complexes between the COOH-terminal domains of sterol regulatory element binding proteins (SREBPs) and SREBP cleavage-activating protein (SCAP). *J. Biol. Chem.* 272, 20213.
- Sato, R., Goldstein, J.L., and Brown, M.S. (1993). Replacement of serine-871 of hamster 3-hydroxy-3-methylglutaryl-CoA reductase prevents phosphorylation by AMP-activated kinase and blocks inhibition of sterol synthesis induced by ATP depletion. *Proc. Natl. Acad. Sci. USA* 90, 9261.
- Schagger, H., Cramer, W.A., and von Jagow, G. (1994). Analysis of molecular masses and oligomeric states of protein complexes by blue native electrophoresis and isolation of membrane protein complexes by two-dimensional native electrophoresis. *Anal. Biochem.* 217, 220.
- Sever, N., Song, B.L., Yabe, D., Goldstein, J.L., Brown, M.S., and DeBose-Boyd, R.A. (2003). *Insig*-dependent ubiquitination and degradation of mammalian 3-hydroxy-3-methylglutaryl-CoA reductase stimulated by sterols and geranylgeraniol. *J. Biol. Chem.* 278, 5479.

- Shearer, A.G., and Hampton, R.Y. (2004). Structural control of endoplasmic-reticulum associated degradation: effect of chemical chaperones on 3-hydroxy-3-methylglutaryl-CoA reductase. *J. Biol. Chem.* 279, 188.
- Simons, K., and Ikonen, E. (1997). Functional rafts in cell membranes. *Nature* 387, 569.
- Simons, K., and Ikonen, E. (2000). How cells handle cholesterol. *Science* 290, 1721.
- Skalnik, D.G., Narita, H., Kent, C., and Simoni, R.D. (1988). The membrane domain of 3-hydroxy-3-methylglutaryl-coenzyme A reductase confers endoplasmic reticulum localization and sterol-regulated degradation onto β -galactosidase. *J. Biol. Chem.* 263, 6836.
- Song, B.L., and DeBose-Boyd, R.A. (2004). Ubiquitination of 3-hydroxy-3-methylglutaryl-CoA reductase in permeabilized cells mediated by cytosolic E1 and a putative membrane-bound ubiquitin ligase. *J. Biol. Chem.* 279, 28798.
- Sun, L., and Chen, Z.J. (2004). The novel functions of ubiquitination in signaling. *Curr. Opin. Cell Biol.* 16, 119.
- Travers, K.J., Patil, C.K., Wodicka, L., Lockhart, D.J., Weissman, J.S., and Walter, P. (2000). Functional and genomic analyses reveal an essential coordination between the unfolded protein response and ER-associated degradation. *Cell* 101, 249.
- Tsai, B., Ye, Y., and Rapoport, T.A. (2002). Retro-translocation of proteins from the endoplasmic reticulum into the cytosol. *Nature Rev. Mol. Cell Biol.* 3, 246.
- Voges, D., Zwickl, P., and Baumeister, W. (1999). The 26S proteasome: a molecular machine designed for controlled proteolysis. *Annu. Rev. Biochem.* 68, 1015.
- Weissman, A.M. (2001). Themes and variations on ubiquitylation. *Nature Rev. Mol. Cell Biol.* 2, 169.
- Yabe, D., Brown, M.S., and Goldstein, J.L. (2002a). Insig-2, a second endoplasmic reticulum protein that binds SCAP and blocks export of sterol regulatory element-binding proteins. *Proc. Natl. Acad. Sci. USA* 99, 12753.
- Yabe, D., Komuro, R., Liang, G., Goldstein, J.L., and Brown, M.S. (2003). Liver-specific mRNA for Insig-2 down-regulated by insulin: implications for fatty acid synthesis. *Proc. Natl. Acad. Sci. USA* 100, 3155.
- Yabe, D., Xia, Z.P., Adams, C.M., and Rawson, R.B. (2002b). Three mutations in sterol-sensing domain of SCAP block interaction with insig and render SREBP cleavage insensitive to sterols. *Proc. Natl. Acad. Sci. USA* 99, 16672.

- Yang, J., Brown, M.S., Ho, Y.K., and Goldstein, J.L. (1995). Three different rearrangements in a single intron truncate sterol regulatory element binding protein-2 and produce sterol-resistant phenotype in three cell lines. Role of introns in protein evolution. *J. Biol. Chem.* 270, 12152.
- Yang, J., Sato, R., Goldstein, J.L., and Brown, M.S. (1994). Sterol-resistant transcription in CHO cells caused by gene rearrangement that truncates SREBP-2. *Genes Dev.* 8, 1910.
- Yang, T., Espenshade, P.J., Wright, M.E., Yabe, D., Gong, Y., Aebersold, R., Goldstein, J.L., and Brown, M.S. (2002). Crucial step in cholesterol homeostasis: sterols promote binding of SCAP to INSIG-1, a membrane protein that facilitates retention of SREBPs in ER. *Cell* 110, 489.
- Zhang, K., and Kaufman, R.J. (2004). Signaling the unfolded protein response from the endoplasmic reticulum. *J. Biol. Chem.* 279, 25935.

VITAE

Navdar Sever was born in Mus, Turkey, on October 24, 1979, the son of Sadiye Sever and Mehmet Emin Sever. After completing his work at Ataturk Anatolian High School, Ankara, Turkey in 1996, he entered Bilkent University at Ankara, Turkey. During the summer of 1999 he worked at Purdue University. He received the degree of Bachelor of Science with a major in molecular biology and genetics from Bilkent University in June, 2000. In September, 2000 he entered the Graduate School of Biomedical Sciences at the University of Texas Southwestern Medical Center at Dallas. Since that time he has been employed as a student research assistant at the University of Texas Southwestern Medical Center at Dallas, Texas.

Permanent Address: Turan Gunes Blv. 42.Sk. 38/8 Oran
Ankara, Turkey 06450